Straight-line Drawability of Embedded Graphs

Hiroshi Nagamochi

Department of Applied Mathematics and Physics,
Kyoto University, Yoshida Honmachi, Sakyo, Kyoto 606-8501, Japan.
nag@amp.i.kyoto-u.ac.jp

Abstract: The fact that every plane embedding γ of a simple graph G admits a straight-line plane drawing D is known as Fary's theorem. The result has been extended to the class of 1-planar graphs by Thomassen by identifying two kinds of forbidden configurations, a topological characterization of all 1-plane embeddings γ that do not admit straight-line 1-plane drawings. In this paper, we first consider the classical problem setting which asks whether a given embedding γ admits a straight-line drawing D with the same planarization of γ, and show that there is a 3-plane and quasi-plane embedding that admits no straight-line drawing and cannot be characterized by a natural extension of forbidden configurations either. We next formulate a slightly relaxed problem setting which asks whether a given embedding γ of a graph G admits a straight-line drawing D under the same "frame," which is defined by a fixed biconnected plane spanning subgraph of G. We prove that a given embedding admits a straight-line drawing under the same frame if and only if it contains none of our forbidden configurations. One of our consequences is that if a given embedding is quasi-plane and its crossing-free edges induce a biconnected spanning subgraph, then its straight-line drawability (in the classical sense) can be checked by our forbidden configurations in polynomial time. Our result also implies several previously known results on straight-line drawings such as the convex-drawability of biconnected plane graphs.

Key words. Straight-line Drawing, Planar Graphs, Connectivity, Edge Crossing, Embedding, Convex Drawing, Polynomial Algorithm

1 Introduction

Graph drawing has attracted much attention due to its wide range of applications, such as VLSI design, social networks, software engineering and bioinformatics. Straight-line drawing of planar or non-planar graphs in the plane is one of the most fundamental problem issues among many kinds of two or three dimensional drawings of graphs under a variety of aesthetics and edge representations [2, 16, 18]. In this paper, we consider straight-line drawings of graphs embedded in the plane.

Throughout the paper, a graph $G = (V, E)$ stands for a simple undirected graph. A *drawing* D of a graph G is a geometric representation of the graph in the plane, such that each vertex of G is mapped to a point in the plane, and each edge of G is drawn as a curve. In this paper, we consider only the following "proper" drawings: (i) each edge contains no vertex other than its endpoints; (ii) no edge crosses itself; (iii) no two edges meet tangentially; and (iv) no three edges share a crossing. In particular, if every edge is drawn as a straight-line segment, then the drawing is called a *straight-line drawing*. A drawing is called a *k-plane* drawing (k-plane graph) if each edge has at most k crossings on it. A 0-plane drawing is called a *plane* drawing. A drawing is called *quasi-plane* if it does not contain three pairwise crossing edges.

[1]Technical report 2013-005, August 9, 2013.

It is known that every plane embedding admits a straight-line drawing [9, 21, 26]. There are algorithms for constructing straight-line drawings of planar graphs under various drawing aesthetics (e.g., [2, 16, 18]).

One direction of extending the idea of straight-line drawings is to force outer/inner facial cycles to be drawn as convex polygons, if possible. A straight-line drawing is called a *convex drawing* if every facial cycle is drawn as a convex polygon. Tutte [25] showed that every triconnected plane graph admits a convex drawing for any given boundary drawn as a convex polygon. The result has been generalized by Hong and Nagamochi [13] so that every triconnected plane graph with a fixed star-shaped polygon boundary has an *inner-convex drawing*, i.e., a drawing in which every inner face is drawn as a convex polygon (see Theorem 21 in Section 11). Also Thomassen [24] gave a necessary and sufficient condition for a biconnected plane graph with a prescribed convex boundary to have a convex drawing. The result has been extended by Hong and Nagamochi [12] who gave a necessary and sufficient condition for a biconnected plane graph with a prescribed convex boundary and a set A of corners to have a straight-line drawing with inner faces drawn by star-shaped polygons whose concave corners are allowed to be chosen only from A (see Theorem 13 in Section 7).

Another direction of extending the idea of straight-line drawings is to deal with non-planar graphs allowing edge-crossings in their straight-line drawings. More recently, the mathematical structure of "almost" planar graphs have been investigated. Ringel [20] first considered *1-planar graphs*. Subsequently, the structure of 1-planar graphs has been investigated [4, 5, 8, 15, 19, 22]. Pach and Toth [19] proved that a 1-plane graph with n vertices has at most $4n - 8$ edges as a tight bound. Korzhik and Mohar [17] proved that testing whether a given graph admits a 1-plane embedding is NP-hard. However, there is a linear time algorithm for testing *maximal* 1-planarity of a graph, if a *rotation system* (i.e., the circular ordering of edges for each vertex) is given [6]. For straight-line drawability of 1-plane graphs, Eggleton [7] conjectured and Thomassen [23] showed that a given 1-plane embedding admits a straight-line drawing if and only if it does not contain any of the two embeddings of graphs, called the B- and W-configurations, shown in Fig. 1(a) and (b). Recently, Hong *et al.* [11] gave a linear-time algorithm for testing if a given 1-plane graph contains such configurations or not and for constructing a straight-line drawing of it (if any). They also showed that the exponential lower bound on the drawing area of straight-line drawings of 1-plane embeddings.

In this paper, we first introduce a set of embeddings of some graphs as forbidden configurations so that no embedding containing one of such configurations admits a straight-line drawing. Our forbidden configurations are a natural extension of the B- and W-configurations, as shown in Fig. 1(c) and (d). We next show that there exists an example of embeddings that admits no straight-line drawing and also contains none of the forbidden configurations. We then show that any instance of straight-line drawing problem can be reduced to a 3-plane and quasi-plane instance without changing the straight-line drawability. This would suggest that assuming quasi-planarity on instances does not make the problem easy enough to solve via characterization with forbidden configurations. We then formulate a slightly relaxed problem setting which asks whether a given embedding of a graph G admits a straight-line drawing under the same "frame," which is defined by a set of crossing-free edges which induces a biconnected spanning subgraph of G. We prove that

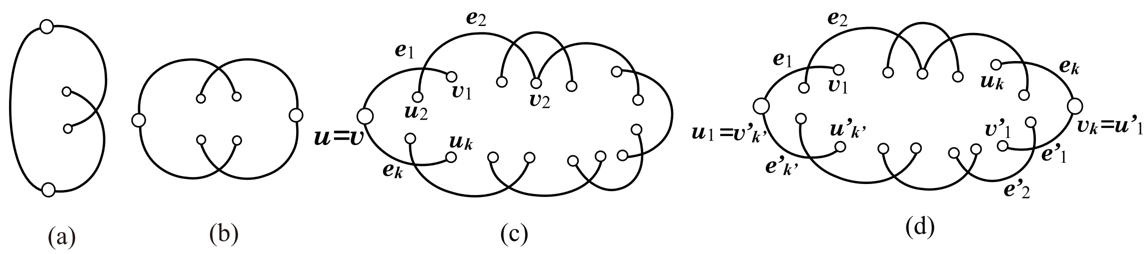

Figure 1: **(a)** B-configuration and **(b)** W-configuration, the two forbidden configurations for PSL-drawability of 1-plane graphs; **(c)** a self-closing chain; and **(d)** a zipped-chain (S, S').

a given embedding admits a straight-line drawing under the same frame if and only if it contains none of our forbidden configurations. One of our consequences is that if a given embedding is quasi-plane and its crossing-free edges induces a biconnected spanning subgraph, then its straight-line drawability (in the classical sense) can be tested by our forbidden configurations in polynomial time. This extends the characterization of straight-line-drawable 1-plane embeddings [23] to a wider class of embeddings. Another consequence is that our result also implies several previously known results on straight-line drawings such as the convex-drawability of biconnected plane graphs [12, 24]. Thus the above two directions of extending straight-line drawings of plane embeddings meet again in this paper.

This paper is organized as follows. In Section 2, we review basic terminology on plane graphs and embeddings of graphs, and extend the notion of convex polygons to "pseudo-convex" polygons. In Section 3, we define a collection of forbidden configurations, as a natural extension of the B- and W-configurations. In Section 4, we present some examples of embeddings of graphs that cannot be drawn with straight-line segments but do not contain any of our forbidden configurations, even in the case of 3-plane and quasi-plane embeddings. In Section 5, we newly formulate a problem of finding straight-line drawings from given embeddings in a slightly relaxed setting, for which the set of instances that do not have straight-line drawings are now completely characterized by our collection of forbidden configurations. Section 6 collects examples of embeddings which illustrate some of the new notions and properties on straight-line drawability. Section 7 demonstrates how our main result (Theorem 10) can imply some of the previous results on straight-line drawings. Section 8 gives some procedures of replacing some edges in polygons in a straight-line drawing with convex/concave links. In Section 9, we give a sketch of our constructive proof for the main result, which can be implemented to run in polynomial time. Section 10 collects some technical lemmas on forbidden subgraphs which will be used to establish the correctness of reductions of instances to prove Theorem 10. Section 12 designs a reduction procedure for P-nodes in the SPQR-tree. Section 13 designs a procedure for drawing the subgraphs (called cactus instances) for S-nodes without considering any edges coming from the outside. Section 14 establishes a reduction procedure for S-nodes by combining with the procedure for cactus instances. Section 15 gives a reduction procedure for R-nodes in the SPQR-tree, which completes a constructive proof for Theorem 10. In Section 16, we make some concluding remarks.

2 Preliminary

2.1 Pseudo-convex Polygons

For two distinct points p and p' in the plane, let $L[p, p']$ denote the straight-line segment (segment, for short) with endpoints p and p', and $L\langle p, p'\rangle$ denote the straight-line (with no endpoints) passing through p and p'. When we place a vertex v of a graph on a point p in the plane, the point p may be simply denoted by v for a notational convenience.

A simple polygon P is denoted by a closed sequence of points $P = (p_1, p_2, \ldots, p_n)$ in the plane, where the boundary of P has no self-intersection and is formed by a concatenation of segments $L[p_1, p_2]$, $L[p_2, p_3], \ldots$, $L[p_{n-1}, p_n]$ and $L[p_n, p_1]$. A corner at a point p_i of polygon P is called *convex* (resp., *concave* and *flat*) if its interior angle is less than π (resp., larger than π and equal to π). Every polygon has at least three convex corners. A polygon is called *convex* if each of the corners is convex or flat. A subsequence $(p_i, p_{i+1}, \ldots, p_j)$ of the closed sequence of points around a polygon is called a *concave link* (resp., *convex link*) if the corners of p_i and p_j are convex and those of $p_{i+1}, \ldots, p_{j-1}$ are concave (resp., convex). Polygon P is called *pseudo-convex* if every two distinct points $p_i, p_{i'} \in \{p_1, p_2, \ldots, p_n\}$ not on the same concave link of P are visible each other within P (i.e., all internal points of $L[p_i, p_i]$ are contained in the interior of P without intersecting the boundary of P). A polygon is called *star-shaped* if it contains an internal point p^* from which any point p on the boundary of the polygon is visible. The *kernel* $K(P)$ of a star-shaped polygon P is the set of all such internal points p^* of P. A pseudo-convex polygon is star-shaped.

Given a polygon P, we can replace some of the edges with concave or convex links so that the resulting polygon becomes pseudo-convex (if we place the new corners on the links sufficiently close to the original edges). See Section 8 for a formal procedure for converting a convex polygon into a pseudo-convex polygon by replacing edges with convex/convex links.

In Section 8, we discuss a more general problem, where we wish to convert polygons in a set of polygons in a straight-line drawing (such as a convex drawing) into polygons to keep the visibility of some two vertices in each inner face. The obtained results here will be used as a final step of our inductive proof of our main theorem.

2.2 Graphs and Plane Drawings

The set of vertices and the set of edges of a graph G are denoted by $V(G)$ and $E(G)$, respectively. A path with end vertices u and v is called a *u, v-path.* A vertex (resp., a pair of vertices) is called *a cut-vertex* (resp., a *cut-pair*) if removing it increases the number of components in the graph. For a cut-pair $\{s, t\}$ of a biconnected graph G, an *s, t-component* H is a maximal connected subgraph of G such that $st \notin E(H)$ and $H - \{s, t\}$ remains connected.

For a subset $E' \subseteq E$, let $G - E'$ denote the graph obtained from G by removing the edges in E'. For a subset $X \subseteq V$, let $E(X)$ be the set of edges $uv \in E$ with $\{u, v\} \cap X \neq \emptyset$, let $G - X$ denote the graph obtained from G by removing the vertices in X together with the edges in $E(X)$, let $G[X] = G - (V - X)$ be the graph induced from G by the vertices in X, and let G/X denote the simple graph obtained from G by contracting X into a single vertex (removing self-loops and parallel edges). *Subdividing* an edge $e = uv$ is to replace the edge with a u, v-path $u, w_1, w_2, \ldots, u_k, v$ for some $k \geq 1$. A graph H is a subdivision of G if H is obtained by subdividing some edges in G.

A plane drawing D of a graph $G = (V, E)$ divides the plane into several connected regions, called *faces*, where a face enclosed by a closed walk of the graph is called an *inner face* and the one not enclosed by any closed walk is called the *outer face.* We may mean by a face f the region enclosed by the facial cycle or the facial cycle as a subgraph interchangeably. Let $V(f)$ and $E(f)$ denote the sets of vertices and edges in a facial cycle f, respectively.

A plane drawing D *induces* an embedding γ of G, which is defined by a circular ordering of the edges around each vertex in V, called the *rotation system* (which can be represented by the set of faces) and the outer face in D. Thus a plane embedding γ of a graph $G = (V, E)$ is given by a pair (F, f^o) of a set F of faces and a face $f^o \in F$ designated as the outer face.

A straight-line drawing D of a plane embedding γ is called a *star-shaped drawing* if each face f is drawn as a star-shaped polygon P_f. A straight-line drawing D of γ is called an *inner convex drawing* if each inner face f is drawn as a convex polygon P_f, and is called a *convex drawing* if in addition the outer boudnary of D is also drawn as a convex polygon P_{out}. In some problem settings, the polygon P_{out} for the outer boundary is given as a prescribed convex/star-shaped polygon before we determine adequate positions of inner vertices to form a convex (or inner convex) drawing.

2.3 Biconnected Plane Graphs

Let $\gamma = (F, f^o)$ be a plane embedding of a biconnected graph $G = (V, E)$, and H be a connected subgraph of G. We define the embedding $\gamma|_H$ of γ induced by H to be a sub-embedding of γ obtained by removing the vertices/edges not in H keeping the same rotation around the remaining vertices and the same outer face. For a notational simplicity, we denote $\gamma|_H$, $F(\gamma|_H)$ and $f^o(\gamma|_H)$ simply by the plane graph H, $F(H)$ and $f^o(H)$, respectively. Let $V^o(H)$ denote the set $V^o(f^o(H))$ of vertices on the boundary $f^o(H)$. For two distinct vertices $s, t \in V^o(H)$, we define the *s, t-boundary walk* $f^o_{st}(H)$ to be the path obtained by traversing the outer boundary $f^o(H)$ from s to t in clockwise order. We denote $V(f^o_{st}(H))$ by $V^o_{st}(H)$. Then $f^o(H)$ is the union of walks $f^o_{st}(H)$ and $f^o_{ts}(H)$ which share s and t. We call an s, t-boundary walk an s, t-boundary *path* if it does not visit the same vertex more than once. When $\{s, t\}$ is a cut-pair which separates H from the rest of the graph $G - V(H)$, there is a face f whose boundary contains $f^o_{st}(H)$ as its subpath from t to s in clockwise order (i.e., traversing $f^o_{st}(H)$ in the opposite direction). We denote the face f by $\text{face}^{st}(H)$. Also let $\text{face}^{ts}(H)$ denote the other face containing $f^o_{ts}(H)$. Then H is surrounded by the two faces $\text{face}^{st}(H)$ and $\text{face}^{ts}(H)$. For a facial cycle f and two vertices $a, b \in V(f)$, we also define the a, b-boundary path $f^o_{ab}(f)$ by regarding f as a cycle of G.

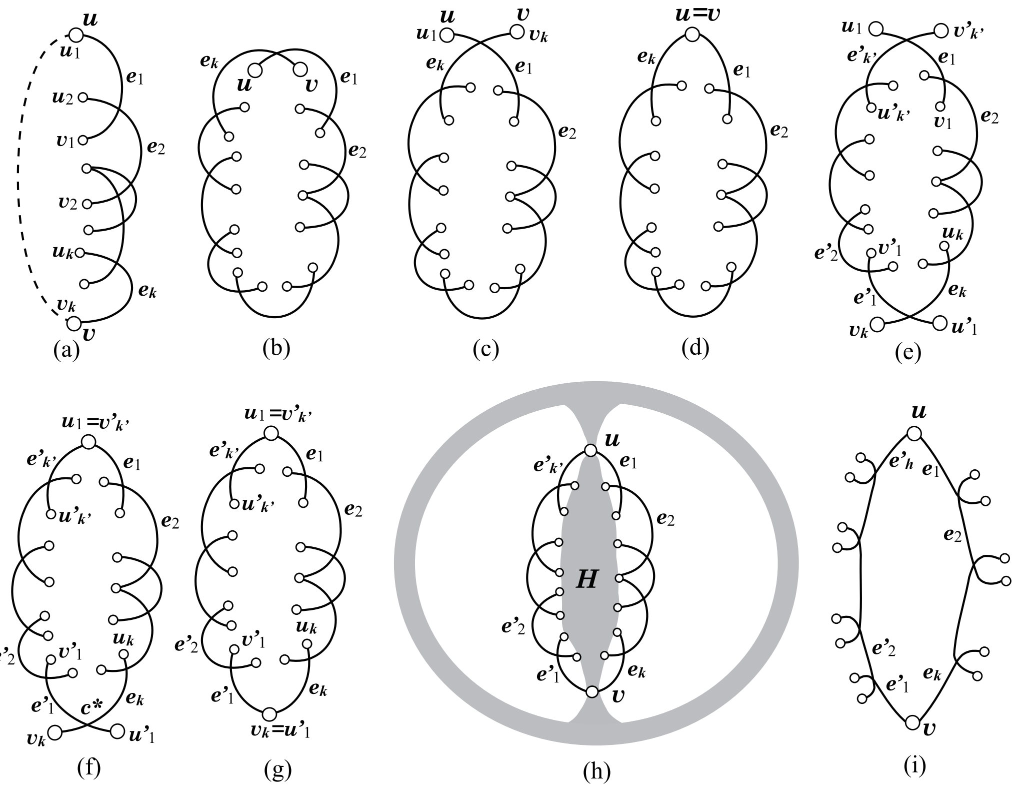

Figure 2: **(a)** A u, v-chain; **(b)** A self-closing chain with a 0-vertex-cycle; **(c)** A self-closing chain with a 0-vertex-cycle; **(d)** A self-closing chain with a 1-vertex-cycle; **(e)** A twin-chain with a 0-vertex-cycle; **(f)** A twin-chain with a 1-vertex-cycle; **(g)** A zipped-chain of length (k, k') with a 2-vertex-cycle; **(h)** A zipped-chain with terminals u and v in a standard instance where H is a u, v-component for a cut-pair $\{u, v\}$; and **(i)** A u, v-lens with length $(k = 4, h = 5)$.

2.4 Planarization of Drawings

We define embeddings possibly with edge crossings via plane embeddings. Let D be a drawing of a graph $G = (V, E)$. A crossing c made by two edges $e = uv$ and $e' = u'v'$ is represented by $(uv; u'v')$ if u' (resp., v') appears on the left hand (resp., right hand) when we traverse e from u to v; otherwise it is denoted by $c = (uv; v'u')$. We denote the set of crossings by C_D. Each edge $e \in E_D^{(k)}$ is subdivided into $k + 1$ curves, called *edge-pieces*. The *planarized* graph of G by D is the graph $\mathcal{G}_D = (\mathcal{V} = V \cup C_D, \mathcal{E}_D)$ obtained by regarding both the vertices of G and the crossings in C_D as graph vertices and the set $\mathcal{E}_D$ of edge-pieces in D as the set of edges to obtain a plane drawing. The *planarized* embedding $\mathcal{P}_D$ of D is the plane embedding of the graph $\mathcal{G}_D$ defined by the set $\mathcal{F}_D$ of faces and the outer face $f^o \in \mathcal{F}_D$ in the resulting plane drawing of $\mathcal{G}_D$. An *embedding* of G induced by D is defined to be the tuple

$$\gamma = (C_D, \mathcal{E}_D, \mathcal{F}_D, f_D^o).$$

Given an embedding $\gamma = (C, \mathcal{E}, \mathcal{F}, f^o)$ of a graph G, we say that a drawing D of G *realizes* γ if $(C_D, \mathcal{E}_D, \mathcal{F}_D, f_D^o)$ equals $(C, \mathcal{E}, \mathcal{F}, f^o)$. Given an embedding γ, let $V(\gamma)$, $E(\gamma)$, $C(\gamma)$, $\mathcal{E}(\gamma)$, $\mathcal{F}(\gamma)$, and $E^{(k)}(\gamma)$ respectively denote the sets of vertices, edges, crossings, edge-pieces, faces, and graph edges e such that there are exactly k crossings on e in γ, and let $f^o(\gamma)$ denote the outer face. An edge in $E^{(0)}(\gamma)$ is called *crossing-free*. We also say that an embedding γ of a graph *k-plane* (resp., *quasi-plane*) if a drawing D that realizes γ is *k-plane* (resp., *quasi-plane*).

If a straight-line drawing D realizes γ, then we say that γ is *planarizing-straight-line drawable* (PSL-drawable, for short). Embeddings that are not PSL-drawable are called *infeasible*.

3 Forbidden Configurations

In this section, we extend the B- and W-configurations into a collection of embeddings of some graphs as forbidden configurations which cannot be contained in any PSL-drawable embeddings.

An embedding η of a sequence $S = (e_1, e_2, \ldots, e_k)$ ($e_i = u_i v_i$) of edges is called a *chain* if the following (i) and (ii) hold:
(i) for each $i = 1, 2, \ldots, k-1$, edges e_i and e_{i+1} cross each other; and
(ii) An edge $e_0 = u_1 v_k$ can be added to η so that all other end-vertices u_i ($1 < i \le k$) and v_i ($1 \le i < k$) are enclosed by the outer facial cycle of the resulting embedding η'.

If u appears after v along the edge uv in η' in clockwise order, then S is called a u, v-chain; it is called a v, u-chain otherwise. Chain S is called *self-closing* if $u_1 = v_k$ or e_1 crosses e_k (see Fig. 1(c)).

An embedding η of a pair (S, S') of a non-self-closing u_1, v_k-chain $S = (e_1, e_2, \ldots, e_k)$ ($e_i = u_i v_i$) and a non-self-closing $u'_1, v'_{k'}$-chain $S' = (e'_1, e'_2, \ldots, e'_{k'})$ ($e'_i = u'_i v'_i$) is called a *twin-chain* of length (k, k') if the following (i) and (ii) hold:
(i) edges e_1 and $e'_{k'}$ cross (or $u_1 = u'_{k'}$) and edges e'_1 and e_k cross (or $u'_1 = u_k$); and
(ii) the end-vertices of the edges except u_1, v_k, u'_1 and $v'_{k'}$ are enclosed by the outer facial cycle $f^o(\eta)$ (where $k = 1$ or $k' = 1$, but $k + k' \ge 3$ since otherwise η does not give a proper drawing).

A twin-chain (S, S') is called a *zipped-chain* if the boundary is a simple cycle (i.e., $u_1 = u'_{k'}$ and $u'_1 = u_k$), where we call the vertices $u_1 = u'_{k'}$ and $u'_1 = u_k$ the *terminals* of the zipped-chain. See Fig. 1(d) for a zipped-chain and Section 10 for more illustrations. We define a *forbidden configuration* to be a self-closing chain or a twin-chain.

Lemma 1 *Let γ be an embedding of a graph $G = (V, E)$. If G contains an edge subset E' which induces a forbidden configuration η, then γ it is not PSL-drawable.*

Proof: Consider the case where η is a twin-chain of a u_1, v_k-chain $S = (e_1, e_2, \ldots, e_k)$ ($e_i = u_i v_i$) and a $u'_1, v'_{k'}$-chain $S' = (e'_1, e'_2, \ldots, e'_{k'})$ ($e'_i = u'_i v'_i$) such that $u_1 = u'_{k'}$ and edges e'_1 and e_k have a crossing c^* (the other cases can be treated analogously). See Fig. 2(f). Assume without loss of generality that S and S' are minimal in the sense that no edge e_i ($1 < i < k$) or e'_i ($1 < i < k'$) can be removed without keeping S and S' as a twin-chain. In this case, each e_i ($1 \le i < k$) does not cross with any edge e_{i+2}. Similarly for the edges e'_i in S'. Hence the crossing $c_{i,i+1}$ ($1 \le i < k$) made by two edges e_i and e_{i+1} appears on the boundary $f^o(\eta)$. Analogously with the crossing $c'_{i,i+1}$ ($1 \le i < k'$) made by edges e'_i and e'_{i+1}. Hence $f^o(\eta)$ is a simple cycle formed by $Q = (u_1 = u'_{k'}, c_{1,2}, c_{2,3}, \ldots, c_{k-1,k}, c^*, c'_{1,2}, c'_{2,3}, \ldots, c'_{k'-1,k'})$ plus edge-pieces $c^* u_k$ and $c^* u'_1$. In any straight-line drawing D that realizes γ, the cycle Q is drawn as a $(k + k')$-gon P_Q (recall that $k + k' \ge 3$). However, the interior angle at any corner of Q except for those at the two points $u_1 = u'_{k'}$ and c^* needs to be larger than π since the corner is made by two line-segments each of which has an end-point inside P_Q. Note that there are $(k + k' - 2)$ such concave corners in P_Q. Since the total of interior angles over all corners of any $(k + k')$-gon is exactly $(k + k' - 2)\pi$, the sum of interior angles at corners for $u_1 = u'_{k'}$ and c^* must be negative, a contradiction. This shows that γ cannot admit a straight-line drawing D. ∎

Here we observe one more property on chains.

Lemma 2 *Let γ be an embedding of a graph $G = (V, E)$ such that the boundary $f^o(\gamma)$ consists of edges in $E^{(0)}(\gamma)$ and the edges in $E^{(0)}$ induces from γ a biconnected spanning plane graph $(V, E^{(0)}(\gamma))$ from γ. Then any forbidden configuration η is a zipped-chain (S, S') with terminals $u, v \in V$ such that $\{u, v\}$ is a cut-pair of G, and the edges in (S, S') surround a u, v-component H of G. See Fig.* 2(h).

Proof: Let η be a forbidden configuration η in γ, where η is a self-closing chain S or a twin-chain (S, S'). In any case, the interior of $f^o(\eta)$ strictly contains an end-vertex u_{in} of some edge of S or S' (note that a self-closing chain S consists of at least two edges, since otherwise γ would not give proper drawings). By assumption, the boundary $f^o(\gamma)$ of γ contains a vertex v_{out} of G. Since $(V, E^{(0)}(\gamma))$ in γ is a biconnected spanning graph, $(V, E^{(0)}(\gamma))$ must contain at least two internally disjoint paths between vertices $u_{\rm in}$ and $v_{\rm out}$. Such two paths cannot exist except when η is a zipped-chain (S, S'), since for the other case, graph $\mathcal{G}(\eta) = (V(\eta) \cup C(\eta), \mathcal{E}(\eta))$ has a cycle that passes through at most one graph vertex and separates the region containing $u_{\rm in}$ from the outer region. Note that the cycle $f^o(\eta)$ of a zipped-chain $\eta = (S, S')$ has only two graph-vertices, which is a cut-pair in G that separates $u_{\rm in}$ and the vertices in $f^o(\gamma)$. Again by the biconnectivity, v and u and v are connected within $f^o(\eta)$. ∎

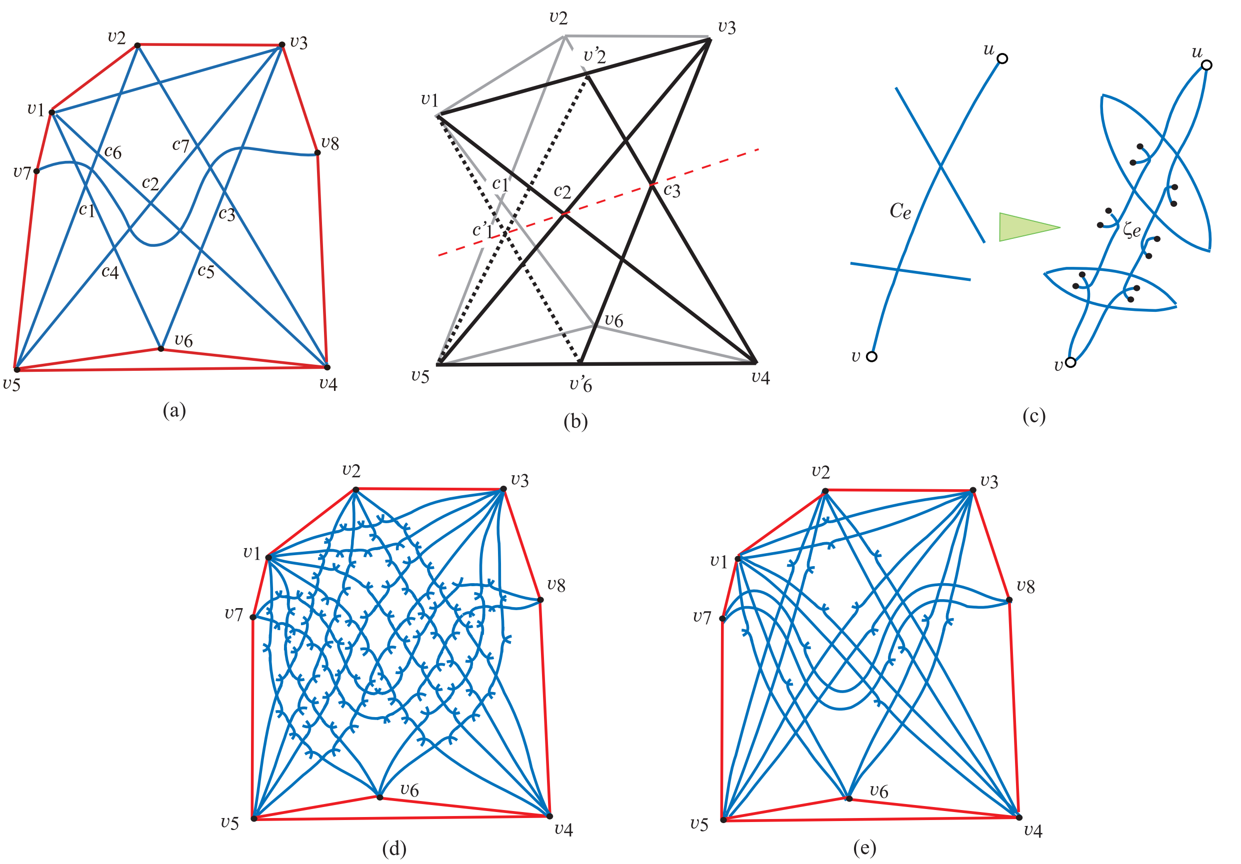

Figure 3: **(a)** Pappus' kite, an embedding that has neither a straight-line drawing nor self-closing chains/twin-chains; **(b)** A geometric configuration with thick lines, where c_1', c_2 and c_3 are co-linear by Pappus' theorem; **(c)** Replacing a curve C_e drawn for a crossing edge $uv \in E^{(k)}(\gamma)$ with a u, v-lens ζ_e of length (k, k); **(d)** The embedding Γ obtained from Pappus' kite by replacing crossing edges with lenses; and **(e)** The embedding γ_{i-1} for $i = |E - E^{(0)}(\gamma)|$ constructed in the proof of Lemma 4.

4 PSL-Drawablity

4.1 Counterexample

In this section, we observe that there is an embedding that contains no forbidden configuration but admits no PSL-drawing either. We call the embedding of a graph in Fig 3(a) the *Pappus kite*.

Let $G = (V, E)$ be a graph with eight vertices v_i, $i = 1, 2, \ldots, 8$ and 15 edges v_iv_j with (i) $1 \leq i < j \leq 3$; (ii) $4 \leq i < j \leq 6$; (iii) $1 \leq i \leq 3 < j \leq 6$ with $(i, j) \notin \{(1, 5), (2, 6), (3, 4)\}$; and (iv) $(i, j) \in \{(1, 7), (5, 7), (3, 8), (4, 8), (7, 8)\}$. See Fig 3(a).

An embedding γ of G is constructed as follows. First draw the graph $G - \{v_7v_8\}$ except edge v_7v_8 as a straight-line drawing $D(G - \{v_7v_8\})$, where we denote by $c(v_iv_j; v_kv_h)$ the crossing made by two edges $v_iv_j, v_kv_h \in E$. For this, place five vertices v_i, $i = 1, 2, \ldots, 5$ to form a convex 7-gon $v_7v_1v_2v_3v_8v_4v_5$, and place v_6 strictly inside triangle $v_4v_5c_2$ for $c_2 = c(v_1v_4; v_3v_5)$. This determines a straight-line drawing $D(G - \{v_7v_8\})$ of $G - \{v_7v_8\}$, as shown in Fig 3(a). Let $c_1 = c(v_1v_6; v_2v_5)$, $c_3 = c(v_2v_4; v_3v_6)$, $c_4 = c(v_1v_6; v_3v_5)$, $c_5 = c(v_1v_4; v_3v_6)$, $c_6 = c(v_1v_4; v_2v_5)$, and $c_7 = c(v_2v_4; v_3v_5)$. Finally we draw edge v_7v_8 within the convex 7-gon so that it intersects six edge-pieces v_1c_1, c_1c_6, c_2c_4, c_2c_5, c_3c_7 and c_3v_3 of $D(G-\{v_7v_8\})$. Let γ be the resulting embedding of G with 14 crossings induced by the drawing of G. We call the resulting embedding the *Pappus kite*.

Lemma 3 *The Pappus kite is not PSL-drawable and contains no forbidden configuration either.*

Proof: We know that γ admits a straight-line drawing D if we ignore the edge v_7v_8. See Fig 3(a). Thus, it suffices to show that c_2 will always be placed under the straight line L passing c_1 and c_3 in D when we take v_2 on the top level and v_4v_5 on the bottom level. To see this, we take three new points in D: (i) $v_2' = c(v_1v_3; v_2v_4)$, (ii) the crossing point v_6' of $L[v_4, v_5]$ and the straight line $L\langle v_6, v_3\rangle$ passing through v_6 and v_3, and (iii) $c_1' = c(v_1v_6'; v_2'v_5)$. See Fig. 3(b). Now v_1, v_2' and v_3 (resp., v_5, v_6' and v_4) are co-linear in D, for which we can apply Pappus' hexagon theorem (A.D. 320) to know that c_1', c_2 and c_3 are also co-linear. This means that c_2 is under the straight line $L\langle c_1, c_3\rangle$ passing c_1 and c_3 in D, as required.

We next show that there is no forbidden configuration in γ. Since the current embedding γ satisfies the condition of Lemma 2, any forbidden configuration η is a zipped-chain such that the two vertex $u, v \in V$ on $f^o(\eta)$ is a cut-pair of G, and u and v are connected within the region $f^o(\eta)$. Hence η is enclosed by the boundary $f^o(\gamma)$ of edges in $E^{(0)}(\gamma)$ whereas $f^o(\eta)$ encloses a u, v-path of edges in $E^{(0)}(\gamma)$. Clearly we see that such a pair $\{u, v\}$ cannot exist in γ. Hence γ has no forbidden configurations. ∎

The Pappus kite has a straight-line drawing if we draw edge v_7v_8 so that it intersects edge-pieces c_2c_6 and c_2c_7 instead of c_2c_4 and c_2c_5. Of course this is not allowed in finding a drawing of the same planarization in the PSL-drawability problem. However the above example may imply that keeping the configuration of pairwise crossing edges in PSL-drawability is a direct reason why our collection of forbidden configurations cannot completely characterize the infeasibility of instances. In other words, can we always find our forbidden configurations in quasi-plane infeasible instances? The answer is no, as we see below that the above example can be converted into a quasi-plane infeasible instance. We define a *u, v-lens* to be the reversal of a zipped-chain with terminals u and v. Given an embedding γ, we replace each crossing edge uv is a u, v-lens (as shown in Fig 3(c)) so that each of the new edges has exactly one crossing with an edge in some other lens. Let Γ be the resulting embedding, which is 3-plane and quasi-plane. Fig. 3(d) illustrates the embedding Γ of the Pappus' kite. We can prove that the original embedding admits a straight-line drawing (resp., contains a forbidden configuration) if and only if so does Γ (see Lemma 4 in the next subsection). Hence Γ in Fig. 3(d) is a 3-plane and quasi-plane embedding that has neither a straight-line drawing nor self-closing chains/twin-chains.

4.2 Quasi-plane Instances of PSL-drawability

In this section we then show that a problem instance γ can be reduced a 3-plane and quasi-plane instance Γ without changing both the PSL-drawability and the existence of forbidden configurations.

Let $\eta = (S, S')$ be a zipped-chain with vertices u and v on its boundary $f^o(\eta)$ such that
(i) $S = (e_1, e_2, \ldots, e_k)$ ($e_i = u_iv_i$), $S' = (e_1', e_2', \ldots, e_h')$ ($e_i' = u_i'v_i'$) for $k + h \geq 3$, and $u = u_1 = v_h'$ and $v = v_1' = u_k$;
(ii) no two edges in S and S' share the same common end-vertices (except $u_1 = v_h'$ and $v_1' = u_k$); and
(iii) two edges a and b in S and S' cross only when $a = e_i$ and $b = e_{i+1}$ with $1 \leq i < k$ (or $a = e_i'$ and $b = e_{i+1}'$ with $1 \leq i < h$).

Let ζ be the embedding obtained by reversing the above zipped-chain η (i.e., exchanging the inner and outer faces). Now all the end-vertices of edges in S and S' appear on the outer closed walk $f^o(\zeta)$. Such an embedding ζ is called a *u, v-lens* of length (k, h). Note that any straight-line drawing D_ζ that realizes ζ encloses its interior with a convex polygon, which provides a space for drawing a segment $L[u, v]$ inside D_ζ.

We are ready to show how to convert a given embedding γ into a quasi-plane one. Let D be a drawing that realizes γ. In D, we take a simple connected region R_e that strictly contains the curve C_e of each edge $e \in E - E^{(0)}(\gamma)$ except for the end-points and that does not contain any other vertices or crossings not on the curve C_e. For each edge $e = uv \in E^{(k)}(\gamma)$ $(k \geq 1)$, we replace the curve C_e with a drawing of u, v-lens ζ_e with length (k, k) within the region R_e so that each edge in ζ_e receives exactly one new crossing (which is made by an edge in some other lens $\zeta_{e'}$, $e' \neq e$). See Fig. 3(c). Let Γ denote the embedding of the resulting drawing. See Fig. 3(d) for an example. We easily see that Γ is a 3-plane and quasi-plane embedding.

Lemma 4 *For an embedding γ of a graph G, let Γ be the above 3-plane and quasi-plane embedding. Then γ is PSL-drawable if and only if Γ is PSL-drawable. Moreover γ contains a forbidden configuration if and only if so does Γ.*

Proof: It is easy to see that PSL-drawability is preserved since in a straight-line drawing D_γ of γ, we can take a simple connected region R_e around the segment L_e for each edge $e = uv \in E^{(k)}(\gamma)$ so that R_e can house a straight-line drawing of u, v-lens ζ_e of length (k, k) instead of L_e in a similar manner of construction of Γ. Conversely, in a straight-line drawing D_Γ of Γ, we can replace the straight-line drawing of lens ζ_e for each edge $e = uv \in E - E^{(0)}(\gamma)$ with a segment $L[u, v]$.

We next show that the existence of forbidden configurations is also preserved. Each edge $e = uv \in E - E^{(0)}(\gamma)$ in γ is now drawn as a u, v-lens $\zeta_e = (S_e, S'_e)$ in Γ. There are $|E - E^{(0)}(\gamma)|$ such lenses in Γ.

Assume that γ contains a self-closing chain $\eta = S$ or a twin-chain $\eta = (S, S')$. For each edge $e = uv$ in η, we see that when e is replaced with one of v, u-chain S_e and u, v-chain S'_e, say S_e, the end-vertices of all edges in S_e will appear on the outer boundary of the modified embedding of η. In this case, we use the other chain S'_e (otherwise use S_e) as a building block B_e for the edge e. Now we replace each edge $e = uv$ in η with the chain B_e to obtain a drawing η', where if u (resp., v) is inside $f^o(\eta)$ then u (resp., v) still is inside the resulting drawing η'. From each chain $B_e = S_e$ (or S'_e), we discard any edge $e_i = u_i v_i$ (or $e'_i = u'_i v'_i$) if the both of end-vertices are outside η' so that if u (resp., v) of an edge $e = uv$ is outside $f^o(\eta)$, then B_e will be shorten to have an edge $e_j = u_j v_j$ (or $e'_j = u'_j v'_j$) with exactly one of the end-vertices inside the drawing η'.

Conversely assume that Γ contains a self-closing chain $\eta = S$ or a twin-chain $\eta = (S, S')$. To see that γ also contains a forbidden configuration, we consider a sequence of embeddings γ_i, $i = 1, 2, \ldots, K$ such that
(i) $\gamma_1 = \gamma$ and $\gamma_K = \gamma$;
(ii) γ_{i-1} $(i > |E - E^{(0)}(\gamma)|)$ is obtained from γ_i by replacing two crossing edges $e_j = u_j v_j$ and $e_{j+1} = u_{j+1} v_{j+1}$ in a lens with a single edge $u_j v_{j+1}$; and
(iii) γ_{i-1} $(1 < i \leq |E - E^{(0)}(\gamma)|)$ is obtained from γ_i by replacing a u, v-lens of length $(1, 2)$ with a single edge uv.

See Fig. 3(e) for an example of embeddings γ_{i-1} for $i = |E - E^{(0)}(\gamma)|$.

Hence K is the number of edges in all lenses in Γ minus $2|E - E^{(0)}(\gamma)|$. In other words, Γ is constructed from γ first by replacing each edge $e = uv \in E - E^{(0)}(\gamma)$ with a u, v-lens with length $(1, 2)$ and then by splitting an edge in a lens with two crossing edges so that each edge in a lens receives exactly one crossing with some other lens.

It suffices to show that if γ_i contains a forbidden configuration η, then so does γ_{i-1}.

In the case of $i \leq |E - E^{(0)}(\gamma)|$, an edge $e = uv \in E - E^{(0)}(\gamma)$ is replaced with a u, v-lens $(S = (e_1 = u_1 v_1), S' = (e'_1 = u'_1 v'_1, e'_2 = u'_2 v'_2))$ of length $(1, 2)$, where $u = u_1 = v'_2$ and $v = v_1 = u'_1$. In the other case of $i > |E - E^{(0)}(\gamma)|$, $e = uv \in E - E^{(0)}(\gamma)$ is replaced with two crossing edges $e'_1 = u'_1 v'_1$ and $e'_2 = u'_2 v'_2$ (where $u = v'_2$ and $v = u'_1$).

We consider the case of $i \leq |E - E^{(0)}(\gamma)|$ (the other case can be treated in a similar and easier way).

Let c_e be the crossing of e'_1 and e'_2 in γ_i, where e'_1 (resp., e'_2) is split into edge-pieces $u'_1 c_e$ and $c_e v'_1$ (resp., $u'_2 c_e$ and $c_e v'_2$). By the way of replacing edges with lenses, we see that no edge intersects any of edge-pieces $u'_2 c_e$ and $c_e v'_1$; no edge intersects two edge-pieces $u'_1 c_e$ and $c_e v'_2$ at the same time; and three edges e_1, e'_1 and e'_2 enclose none of vertices and crossings in γ_i. Hence an edge intersects e'_1 or e'_2 if and only if it intersects e_1. We consider the case where γ_i contains a twin-chain $\eta = (S_a, S_b)$ as a forbidden configuration (the case where η is a self-closing chain can be treated analogously). Recall that η has at most four vertices on its boundary $f^o(\eta)$. Assume that e'_1 or e'_2 (say e'_1) is contained in S_a or S_b (say S_a), since otherwise η also appears in γ_{i-1}.

Let $c_e t$ be the first edge-piece in $c_e v'_2$ starting c_e (i.e., $t = v'_2$ or t is the first crossing along $c_e v'_2$).

Now consider the embedding Q of a sequence of edge-pieces $v_1 c_e$ and $c_e v'_2$ in γ_i.

We distinguish two cases:

(1) $c_e t$ is inside $f^o(\eta)$ (for example when v'_1 is within $f^o(\eta)$): If Q does not cross any edge in $S_a \cup S_b - \{e'_1\}$, then the embedding obtained from η by replacing e'_1 and e'_2 with $e = uv$ is a forbidden configuration in γ_{i-1}, since Q and e_1 (hence $e = uv$) intersect the same set of edges in γ_i. If Q intersects an edge in $S_a - \{e'_1\}$, then we choose the edge $e_a \in S_a - \{e'_1\}$ closest to e'_1 among such edges, and we see that the union of $e = uv$ and the subsequence of S_a between e'_1 and e_a gives a forbidden configuration in γ_{i-1}. Finally consider the case where Q intersects an edge $e_b \in S_b$ without intersecting any edges in $S_a - \{e'_1\}$. If a subsequence S'_b of S_b and Q enclose the end-vertices of the edges in S'_b, then the union of S'_b and $e = uv$ gives a forbidden configuration in γ_{i-1}. Assume that no such subsequence S'_b exists. Then Q intersects S_b at most twice, and Q splits the region $f^o(\eta)$ into two regions R_1 and R_2, where we assume that R_1 contains the other end-vertex u'_1 of e'_1 (possibly on the boundary of R_1). The set of edges forming the boundary of R_1 and $e = uv$ give a forbidden configuration in γ_{i-1}.

(2) $c_e t$ is outside $f^o(\eta)$: In this case, v'_1 is on the boundary $f^o(\eta)$ or strictly outside $f^o(\eta)$. If Q does not cross any edge in $S_a \cup S_b - \{e'_1\}$, then the embedding obtained from η by replacing e'_1 and e'_2 with $e = uv$ is a forbidden configuration in γ_{i-1}. If a subsequence S'_a of S_a and Q enclose the end-vertices of the edges in S'_a, then the union of S'_a and $e = uv$ gives a forbidden configuration in γ_{i-1}. Assume that no such subsequence S'_a exists. Then Q intersects S_a at most twice. If a subsequence S'_b of S_b and Q enclose the end-vertices of the edges in S'_b, then the union S'_b and $e = uv$ gives a forbidden configuration in γ_{i-1}. Assume that no such subsequence S'_b exists. Then Q intersects S_b at most once. Assume that t is a crossing on an edge in S_a (the other case where t is a crossing on an edge in S_b can be treated analogously). When Q and S_a enclose the end-vertices of edges in S_b, the union of $e = uv$ and the edges of S_a in the boundary of the enclosed region gives a forbidden configuration in γ_{i-1}. On the other hand, Q and the region $f^o(\eta)$ enclose e'_1. In this case, if Q does not intersect S_b (i.e., v'_2 is within $f^o(\eta)$), then the union of $e = uv$ and the edges of S_a in the boundary of the enclosed region gives a forbidden configuration in γ_{i-1}. Otherwise (Q intersects S_b), we see that Q does not intersect with S_b twice, since otherwise we would have the above subsequence S'_b. In this case, Q splits the region $f^o(\eta)$ into two regions R_1 and R_2, where we assume that R_1 contains the other end-vertex u'_1 of e'_1. The set of edges forming the boundary of R_1 and $e = uv$ gives a forbidden configuration in γ_{i-1}. ∎

By Lemma 3 and Lemma 4, we have the next.

Lemma 5 *The above embedding Γ obtained from the Pappus kite γ by replacing crossing edges with lenses is a 3-planar and quasi-plane embedding that is not PSL-drawable and has no forbidden configurations either.*

With only quasi-planarity, we cannot characterize infeasible instances by our forbidden configurations. How can we extend the result for straight-line drawability of 1-plane embeddings? Observe that the set of crossing-free edges in the Pappus kite γ induces a biconnected spanning subgraph while introducing lenses lowers the connectivity of spanning subgraph of crossing-free edges in the quasi-plane embedding Γ.

In this paper, the next result will be implied by our main result (Theorem 8) on a new concept of drawability of embeddings.

Theorem 6 *Let γ be an embedding is quasi-plane and its crossing-free edges induces a biconnected plane spanning subgraph. Then γ is PSL-drawable if and only if it has no forbidden configurations.*

4.3 Star Augmentation

We here investigate how much we can increase the connectivity of spanning subgraphs of crossing-free edges by adding some new crossing-free edges (without changing straight-line drawability).

Let γ be an embedding of a graph $G = (V, E)$. A simple cycle $\mathcal{E}' \subseteq \mathcal{E}(\gamma)$ is called *separating* if a vertex $u \in V$ and a vertex $v \in V$ respectively are strictly inside and outside the region enclosed by $\mathcal{E}'$. A simple cycle $\mathcal{E}' \subseteq \mathcal{E}$ is called a k-vertex-cycle if there are exactly k vertices on it (i.e., it contains $|\mathcal{E}'| - k$ crossings in $C(\gamma)$).

A *star augmentation* γ_A of γ is an embedding of an augmented graph $G_A = (V \cup V_A, E \cup E_A)$ obtained by introducing new edges/vertices as follows: for each facial cycle $f \in \mathcal{F}(\gamma)$ with $|V(f)| \geq 2$ (at least two vertices in V in $C(\gamma)$), we place a new vertex u_f together with new edges $u_f v$ ($v \in V(f)$) within the region f. Let V_A and E_A be the sets of newly introduced vertices and edges, respectively. Note that all edges in E_A are crossing-free in the resulting embedding γ_A of the graph $G_A = (V \cup V_A, E \cup E_A)$. (See Fig. 6 in Section 6.)

Lemma 7 *Let γ be an embedding of a graph $G = (V, E)$ such that the graph $\mathcal{G}(\gamma) = (V \cup C(\gamma), \mathcal{E}(\gamma))$ is connected. Then*
- any forbidden configuration in the star augmentation γ_A is a forbidden configuration in γ; and
- the set of crossing-free edges induces a connected (resp., biconnected) spanning subgraph in γ_A if and only if $\mathcal{G}(\gamma)$ has no separating 0-vertex-cycles (resp., 0- or 1-vertex-cycle), not necessarily facial.

Proof: The set of crossing free-edges in γ_A is $E^{(0)}(\gamma) \cup E_A$. In γ_A, any newly added edge $e \in E_A$ is crossing-free and has an end-vertex u_f to which no crossing edge is incident. This means that no new edge is contained in any self-closing chains or twin-chains in γ_A, and hence any forbidden configuration in the star augmentation γ_A is a forbidden configuration in γ.

We next show that the spanning subgraph $G_A^{(0)} = (V \cup V_A, E^{(0)}(\gamma) \cup E_A)$ of crossing-free edges is connected if and only if $\mathcal{G}(\gamma)$ has no separating 0-vertex-cycles. We easily see that if $\mathcal{G}(\gamma)$ has a separating 0-vertex-cycle, then no newly introduced crossing-free edges in E_A can connect two vertices $u, v \in V$ that are separated by the separating 0-vertex-cycle. We show the converse. Assume that $G_A^{(0)}$ is not connected. Then $(V \cup V_A, E^{(0)}(\gamma) \cup E_A)$ contains a component H which has no vertices in $V(f^o(\gamma))$, since all outer vertices in $V(f^o(\gamma))$ will be joined to the same vertex $u_{f^o(\gamma)}$ (when $|V(f^o(\gamma))| \geq 2$). Consider the set of faces $f \in \mathcal{F}(\gamma)$ that contain at least one vertex in H. The outer boundary of the union of these faces will be a closed walk W which passes through only crossings in $C(\gamma)$. Hence W contains a separating 0-vertex-cycle of $\mathcal{P}(\gamma)$.

We finally show that $G_A^{(0)}$ is biconnected if and only if $\mathcal{G}(\gamma)$ has no separating 0- or 1-vertex-cycles. If there is a separating 1-cycle containing a vertex $w \in V$, then two vertices $u, v \in V$ separated by the cycle cannot be connected by two internally disjoint paths in $E^{(0)}(\gamma) \cup E_A$ due to w which will be a cut-vertex in G_A. We show the converse. Assume that $G_A^{(0)}$ is connected, but not biconnected (since we have shown that if $G_A^{(0)}$ is not connected, then $\mathcal{G}(\gamma)$ contains a separating 0-vertex-cycle). Then $(V \cup V_A, E^{(0)}(\gamma) \cup E_A)$ contains a biconnected component H which is disjoint with $V(f^o(\gamma))$. We choose a minimal subgraph H among such components. Since $G_A^{(0)}$ is connected, it contains a path P that connects a vertex $u_{\text{out}} \in V(f^o(\gamma))$ and a vertex $u_{\text{in}} \in V(H)$, where u_{in} is chosen so that P is maximal subject to the condition. Hence the first vertex w that appears along P starting from u_{out} is a vertex in V (not a new vertex in V_A), and that $H - \{w\}$ contains another vertex in V (since a new vertex in V_A is placed in a face with at least two vertices in V along its boundary). Consider the set of faces $f \in \mathcal{F}(\gamma)$ that contain at least one vertex in H. We then discard the faces which contain only w from the vertices in H. Then the outer boundary of the union of the collected faces will be a closed walk W which passes through only crossings in $C(\gamma)$ except w. Hence W contains a separating 1-vertex-cycle of $\mathcal{G}(\gamma)$. ∎

In the next section, we formulate a problem of finding straight-line drawings allowing pairwise crossing edges to have arbitrary orders of crossings along edges (see Fig. 5 in Section 6), while a certain connectivity of spanning subgraph induced by crossing-free edges is required.

5 FSL-Drawablity

For a biconnected graph $G = (V, E)$, we take a subset $M \subseteq E$ of edges such that $G_M = (V, M)$ is a biconnected spanning subgraph of G, and $\gamma_M = (M, F_M, f_M^o)$ is a plane embedding of $G_M = (V, M)$.

Consider a drawing D of G such that all edges in M are crossing-free and the drawing induced from D by (V, M) realizes γ_M (some edges in $E - M$ may be crossing-free). In other words, D is obtained from a drawing D_M that realizes γ_M by drawing each edge $e = uv \in E - M$ within the region of a face $f \in F_M$ such that $V(f) \subseteq \{u, v\}$. When $\{u, v\}$ is a cut-pair of $G_M = (V, M)$, there are two or more facial cycles f in F_M that contain both u and v. Let $F_M(e)$ be the set of faces $f \in F_M$ with $V(f) \subseteq \{u, v\}$. The *assignment* α_D of D specifies a face $\alpha(e) \in F_M(e)$ in which e is drawn. A *frame* of G is define to be a tuple

$$\psi = (M, F_M, f^o_M, \alpha_D).$$

(See Fig. 7 in Section 6 for an example.)

Given a frame $\psi = (M, F_M, f^o_M, \alpha)$ of a graph G, we say that a drawing D of G *realizes* ψ if M induces the embedding (M, F_M, f^o_M) from D and α_D equals the given α. If a straight-line drawing D realizes $\psi = (M, F_M, f^o_M, \alpha)$, then we say that the frame ψ is *frame-straight-line drawable* (FSL-drawable, for short) or D is an FSL-drawing of ψ.

If a drawing D of G realizing ψ induces γ, then we say that an embedding γ of G *realizes* ψ (possibly different drawings D and D' realizing the same frame ψ may induce distinct embeddings).

Note that, for two embeddings γ_1 and γ_2 that realize the same frame ψ of a graph G, the set of crossings and the set of edges with k crossings are same. Only the ordering of crossings on an edge can be different, and this occurs for embeddings with pairwise crossing edges. Notice that if γ_1 contains a forbidden configuration η, then γ_2 also contains a forbidden configuration, since the ordering of crossing along each edge is not required to be fixed in the definition of forbidden configurations. In fact, if η is minimal, then it is minimal in any embedding that realizes the same frame. Thus, forbidden configurations in a frame ψ are defined to be those in any embedding γ that realizes ψ.

In this paper, we prove that our collection of forbidden configurations can characterize the FSL-drawability.

Theorem 8 *Let $\psi = (M, F_M, f^o_M, \alpha)$ be a frame of a graph $G = (V, E)$. Then (G, ψ) is FSL-drawable if and only if it has no forbidden configurations.*

Theorem 6 follows from the theorem. Also it is not difficult to see that Theorem 8 implies the characterization of infeasible 1-plane embeddings by the B-configuration or the W-configuration (see Section 7 for the detail).

Outer Boundaries

Lemma 9 *Let $(G = (V, E), M, F_M, f^o_M, \alpha)$ denote a given instance, and $\psi = (M, F_M, f^o_M)$ denote the plane embedding (frame) of the biconnected graph $G_M = (V, M)$. Let γ be an embedding of G that realizes frame $\psi = (M, F_M, f^o_M)$. If the number r of vertices in V that appear on the outer boundary $f^o(\gamma)$ is at most two, then ψ has a forbidden configuration.*

Proof: Let $E' \subseteq E$ be the set of edges whose edge-pieces appear on the boundary $f^o(\gamma)$. If $r \leq 1$, then E' gives a self-closing chain. If $r = 2$, then E' gives a twin-chain of a uv-chain and a vu-chain for the two vertices $u, v \in V$ on $f^o(\gamma)$. ∎

Assume that for any embedding γ of G that realizes a given frame $\psi = (M, F_M, f^o_M)$, the outer facial cycle $f^o(\gamma)$ consists of crossing-free edges in M; if necessary, we place three new vertices v_a, v_b and v_c in the outer face and join them with the vertices in V on $f^o(\gamma)$ to from a biconnected plane embedding on these vertices. This clearly does not create a new forbidden configuration. Thus we can assume that the facial cycle f^o_M is simple and no edge in $E - M$ is assigned witin f^o_M to examine the FSL-drawability of an instance.

We call an instance $(G, M, F_M, f^o_M, \alpha)$ *standard* if the facial cycle f^o_M is simple and no edge in $E - M$ is assigned witin f^o_M (i.e., the outer boundary of the embedding contains only edges in M).

To prove Theorem 8, we show the next slightly stronger result, where the outer boundary is drawn as a prescribed convex polygon P_{out} possibly with flat corners. Let $Q_1, Q_2, \ldots, Q_k$ be the subpaths of f_o, each corresponding to a segment of P_{out}. A u,v-chain S of inner edges (possibly

$|S| = 1$) is called *squashed* if u and v are contained in the same subpath Q_i, where Q_i contains a v,u-path S' of outer edges with no convex corners on it, and we also call (S, S') a squashed chain.

Theorem 10 *Let $(G, M, F_M, f_M^o, \alpha)$ be a standard instance. Then a precribed convex polygon $P_{\rm out}$ drawn for f_o can be extended to an FSL-drawing D of (M, F_M, f_M^o, α) if and only if there is no zipped-chain or squashed chain.*

Theorem 8 follows from the theorem, because no squashed chain appears when $P_{\rm out}$ is chosen as a convex polygon with no flat corners. In the rest of the paper, we focus on establishing a constructive proof of Theorem 10.

6 Some Examples

This section gives a collection of examples which illustrates some of the new notions and definitions introduced in this paper.

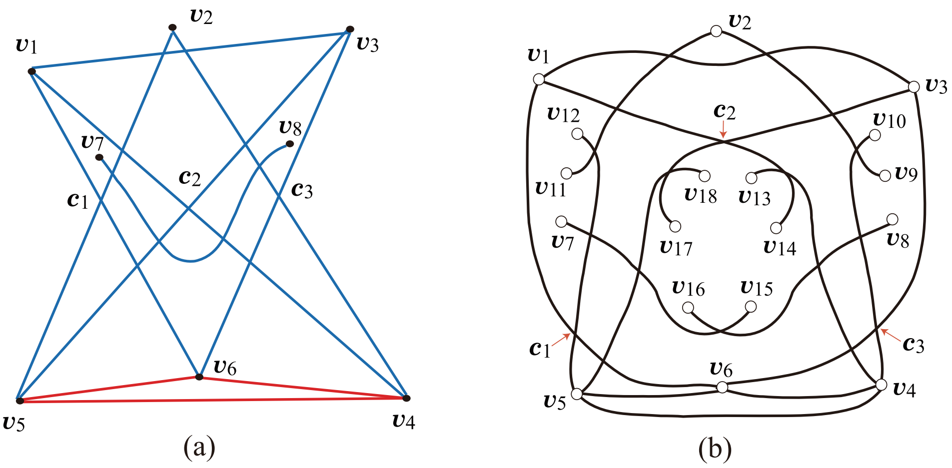

Figure 4: Infeasible instances minimal subject to edge sets: **(a)** An infeasible embedding which has only one set of pairwise crossing edges v_1v_4, v_3v_5 and v_7v_8; and **(b)** A 3-plane and quasi-plane infeasible embedding which contains no forbidden configurations.

Fig. 4 illustrates two minimal instances that do not admit PSL-drawings but contain none of our forbidden configurations either, where these two instance are "minimal" in the sense that they admit straight-line drawings if we drop arbitrary one of the edges. The infeasible embedding in Fig. 4(a) has only one set of pairwise crossing edges v_1v_4, v_3v_5 and v_7v_8 and contains no forbidden configurations, where crossing c_2 will be above the line $L\langle c_1, c_3\rangle$ passing through crossings c_1 and c_3 in any straight-line drawing without using edge v_7v_8. Fig. 4(b) shows a 3-plane and quasi-plane infeasible embedding which contains no forbidden configurations, which is obtained from the embedding in Fig. 4(a) by replacing each edge with a chain keeping c_2 above the line passing $L\langle c_1, c_3\rangle$ through c_1 and c_3. It is not difficult to see that the embedding in Fig. 4(b) admits no straight-line drawing.

Fig. 5 illustrates an example of a proper embedding γ_1 of a graph and its straight-line drawing D_1. Note that γ_1 has only one set of pairwise crossing edges v_2v_{12}, v_1v_{21} and $v_{22}v_{26}$ with three crossings $c_1 = (v_1v_{21}; v_2v_{12})$, $c_2 = (v_1v_{21}; v_{22}v_{26})$ and $c_3 = (v_2v_{12}; v_{22}v_{26})$. In D_1, the ordering of these crossings on the pairwise crossing edges are different from that in γ_1, and D_1 is not a PSL-drawing of γ_1. When such a change of orderings is allowed, our method in the paper can find such a drawing since crossing-free edges can be added to γ_1 so that they form a biconnected spanning graph, as will be shown Fig. 6 and Fig. 7(b).

Fig. 6 illustrates an embedding γ of a graph $G = (V, E)$ and its star-augmentation $G_A = (V \cup V_A, E \cup E_A)$. In this case, the crossing-free edges in G_A induce a biconnected spanning graph,

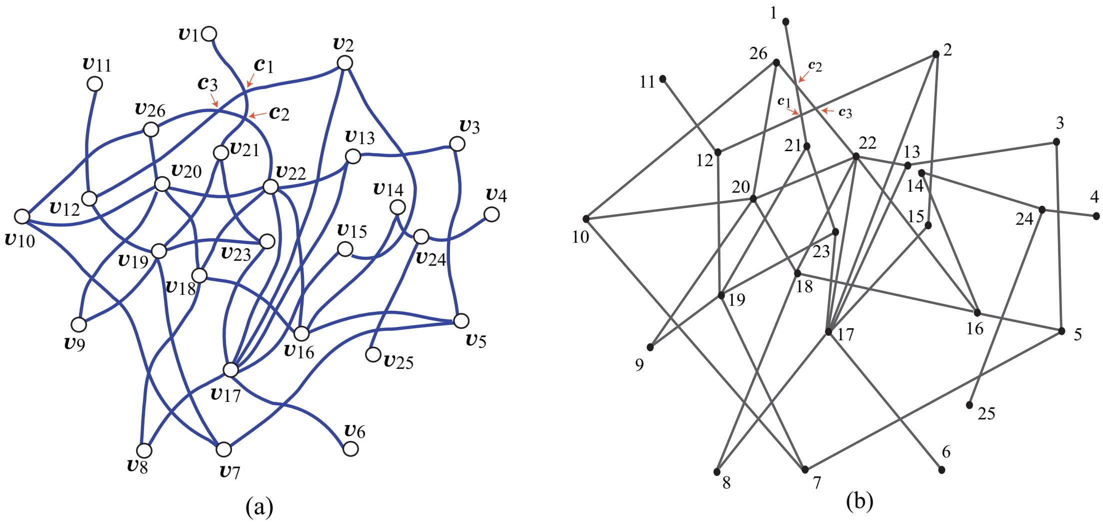

Figure 5: **(a)** An embedding γ_1, which has only one set of pairwise crossing edges v_2v_{12}, v_1v_{21} and $v_{22}v_{26}$; and **(b)** A straight-line drawing D_1 that realizes γ_1 in (a), where the crossings on the pairwise crossing edges appear in a different order from that in γ_1.

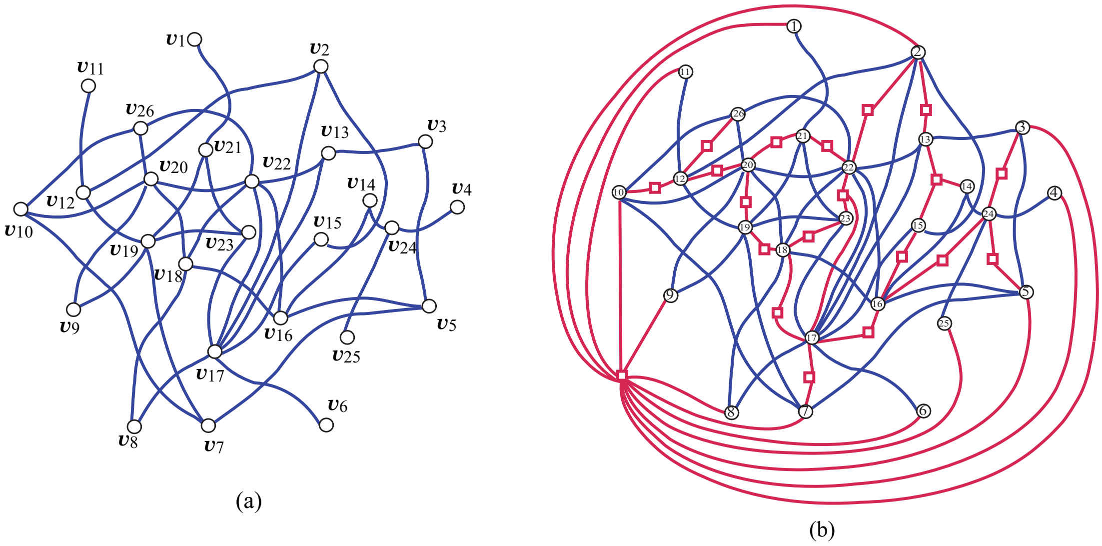

Figure 6: **(a)** An embedding γ of a graph $G = (V, E)$; and **(b)** The star-augmentation $G_A = (V \cup V_A, E \cup E_A)$ of γ in (a).

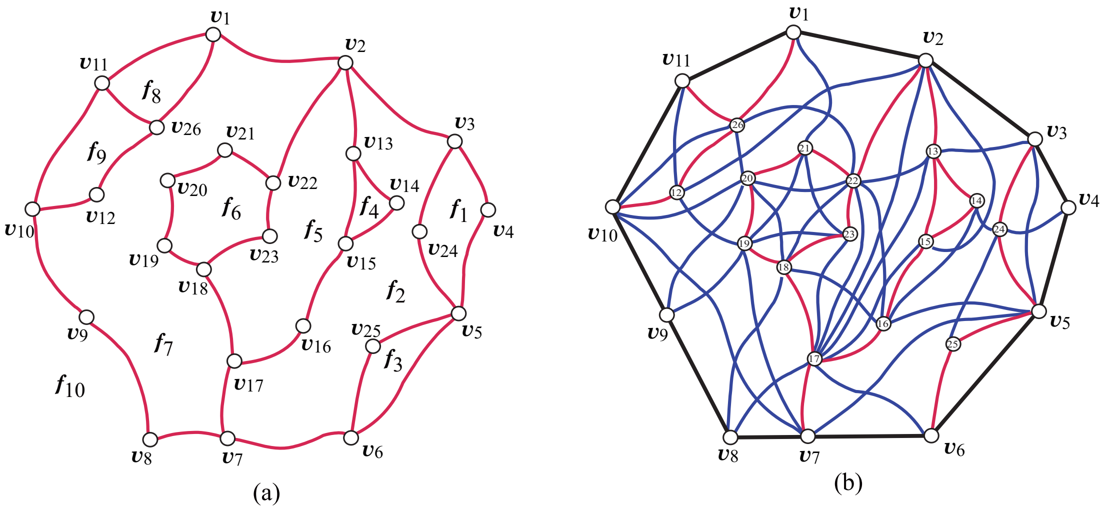

Figure 7: **(a)** A biconnected plane graph $G_M = (V, M)$ with a set $F_M = \{f_1, f_2, \ldots, f_{10}\}$ and an outer face $f^o_M = f_{10}$; and **(b)** A standard instance $(G, M, F_M, f^o_M, \alpha, P_{\text{out}})$ on the graph G_M in (a), where the set of blue edges in each inner face f are those assigned to f by α, and the black lines on the outer boundary indicate a prescribed convex polygon P_{out}.

and our method in the paper can test whether the original embedding γ admits a straight-line drawing D wherein the ordering of crossings on pairwise crossing edges may not be preserved.

Fig. 7 illustrates examples of frames. The embedding in Fig. 7(a) is a biconnected plane graph $G_M = (V, M)$ with a set $F_M = \{f_1, f_2, \ldots, f_{10}\}$ of faces and an outer face $f^o_M = f_{10}$. The embedding in Fig. 7(b) is obtained from (G_M, F_M) by assigning some more edges to inner faces in F_M. In particular, the six edges assigned to inner face $f_6 \in F_M$ makes the polygon P_{f_6} to be drawn for f_6 convex. Also facial cycle f_5 will be drawn as a star-shaped polygon whose kernel contains the point for v_{17} due to the five edges incident to v_{17} within region f_5. The outer boundary f^o_M is now fixed to a prescribed polygon P_{out}.

7 Implications by the Main Theorem

In this section, we show that several previously known results on straight-line drawings can be derived from our main result.

7.1 Implication to Straight-line Drawability of 1-plane Embeddings

Let us first observe that Theorem 8 implies the characterization of infeasible 1-plane embeddings by the B- or W-configuration shown in Fig. 1(a) and (b).

Let γ be a 1-plane embedding of a graph such that its planarization $\mathcal{G}(\gamma)$ is connected. Then we easily see that $\mathcal{G}(\gamma)$ cannot have a separating 0- or 1-vertex-cycle since γ is 1-plane and no two crossings are adjacent in $\mathcal{G}(\gamma)$. Hence by Lemma 7, the star-augmentation γ_A of γ has a biconnected spanning graph of crossing-free edges. Since 1-plane embeddings are quasi-plane, γ_A is PSL-drawable if and only if it is FSL-drawable, where we choose the set of all crossing-free edges as M, the embedding induced from γ_A by M as (M, F_M, f^o_M) and the assignment of the rest of edges in the faces in F_M as α. Hence by Theorem 8, if γ_A is not PSL-drawable, then γ has a forbidden configuration, which is a 1-plane zipped-chain, i.e., the B- or W-configuration.

7.2 Implication to Convex Drawability of Biconnected Plane Embeddings

As an application of FSL-drawings, we introduce new edges within several inner faces in a given plane embedding of a graph so that selected inner faces will be drawn as convex polygons or star-shaped polygons, as shown in Fig. 7 (in fact such technique will be frequently used in our constructive proof of Theorem 10). For example, given a plane embedding $\gamma = (F, f^o)$ of a biconnected graph $G = (V, E)$, suppose that we wish to make several pairs of vertices u and v visible in the interior of an inner face $f \in F$ in a straight-line drawing D of γ, i.e., $L[u, v]$ will be contained in the polygon P_f for f without intersecting P_f except the common points u and v in D. Finding such a constrained drawing D is reduced to a problem instance of finding an FSL-drawing. More formally, when we select a set E_f^{visible} of some pairs of vertices $u, v \in V(f)$ along each inner face $f \in F - \{f^o\}$ (possibly $E_f^{\text{visible}} = \emptyset$ for some faces f), we let $G' = (V, E')$ with $E' = E \cup (\cup_{f \in F} E_f^{\text{visible}})$, and frame (M, F_M, f_M^o) of G' be (E, F, f^o). Obviously G has a straight-line drawing D of $\gamma = (F, f^o)$ in which the vertices in each pair $(u, v) \in E_f^{\text{visible}}$, $f \in F$ is visible within f if and only if G' has an FSL-drawing D'.

In particular, when we select a subset $F' \subseteq F$ of inner faces of length ≥ 4 to be drawn as convex polygons with no flat corners, we prepare E_f^{visible} as the set of every pairs $u, v \in V(f)$ with distance 2 along f, which automatically makes every corner of the polygon for f in D' convex. The following statement is immediate from Theorem 10.

Corollary 11 *Let (F, f^o) be a plane embedding of a biconnected graph $G = (V, E)$, and F' be a subset of inner faces. Then a convex polygon P_{out} possibly with flat corners drawn for f_o can be extended to a convex drawing D of G if and only if the following conditions* (i)-(ii) *hold:*
(i) *For each cut-pair $\{u, v\}$, no u, v-component is enclosed by a pair of two inner faces $f, f' \in F'$; and*
(ii) *Let $Q_1, Q_2, \ldots, Q_k$ be the subpaths of f_o, each corresponding to a segment of P_{out}. Then for each $i = 1, 2, \ldots, k$, there is no edge uv whose end-vertices are contained in Q_i, and for each cut-pair $\{u, v\}$ with $u, v \in V(Q_i)$, no u, v-component is enclosed by a pair of an inner face $f \in F'$ and the outer face f^o.*

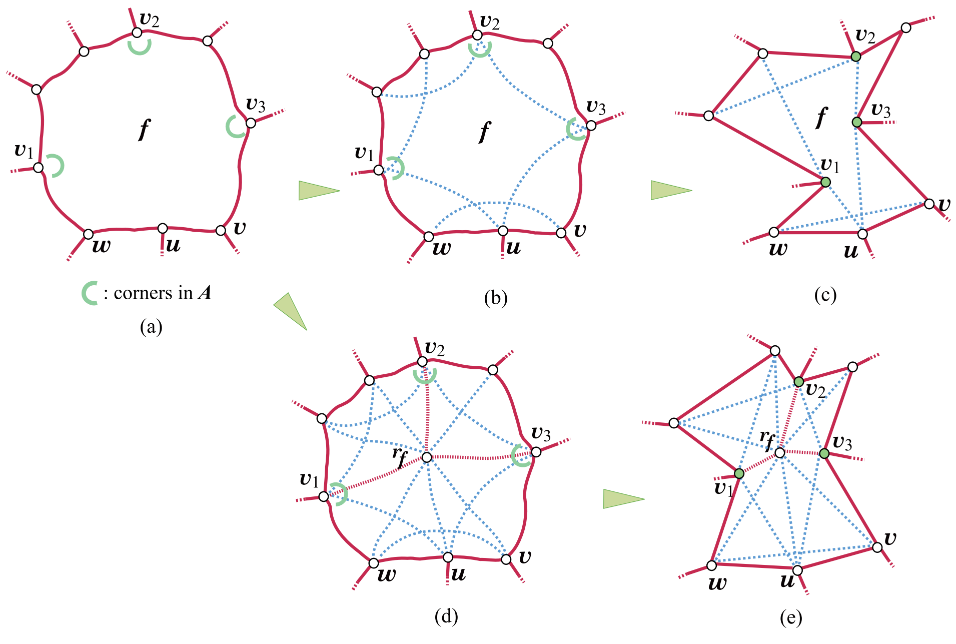

Figure 8: **(a)** An inner face f in a plane embedding, where $(v_1, f), (v_2, f), (v_3, f) \in A$ are required to be realized as concave corners in a polygon P_f for f; **(b)** face f assigned new edges vw covering vertex u.; **(c)** Polygon P_f in an FSL-drawing for the augmented embedding in (b); **(d)** A new vertex r_f which is joined to all vertices $v \in V(f)$; and **(e)** Polygon P_f in an FSL-drawing for the augmented embedding in (d).

We now observe that Corollary 11 implies the next necessary and sufficient condition for a biconnected plane graph with the outer face fixed as a convex polygon to admit a convex drawing.

Theorem 12 [24] *Let (F, f^o) be a plane embedding of a biconnected graph $G = (V, E)$. Then a convex polygon $P_{\rm out}$ possibly with flat corners drawn for f_o can be extended to a convex drawing D of G if and only if the following conditions* (i)-(iii) *hold:*
(i) *For each inner vertex v of degree ≥ 3, there exist three paths disjoint except v, each connecting v and an outer vertex;*
(ii) *Every cycle of G which has no outer edge has at least three vertices v degree ≥ 3; and*
(iii) *Let $Q_1, Q_2, \ldots, Q_k$ be the subpaths of f_o, each corresponding to a segment of $P_{\rm out}$. Then for each $i = 1, 2, \ldots, k$, there is no inner edge uv whose end-vertices are contained in Q_i, and the graph $G - V(f_o)$ has no component H such that all the outer vertices adjacent to vertices in H are contained in Q_i.*

For each inner vertex v of degree 2 and each outer vertex v of degree 2 placed on $P_{\rm out}$ as a flat apex, we replace the two edges uv and vw incident to v with a single edge uw, since such vertices v will be only flat corners in the adjacent faces in a convex drawing. If this creates multiple edges, then we see that the given instance admits no convex drawing, and that it violates the necessary condition (ii). Now we assume that any vertex of degree 2 appears as a convex corner of $P_{\rm out}$ and consider if a given instance has a convex drawing in which every inner face is drawn as a convex polygon with no flat corners. By Menger's theorem, an inner vertex v of degree at least 3 is separated from the outer vertices by a cut-pair $\{u, u'\}$ in a biconnected plane graph if and only if there is no three disjoint paths between v and the outer vertices. Hence it is not difficult to see that Corollary 11 with $F' = F - \{f^o\}$ the conditions (i)-(ii) are equivalent with those in Theorem 12. This proves that Theorem 12 follows from Corollary 11.

7.3 Implication to Straight-line Drawability of Biconnected Plane Embeddings under Concave Corner Constraints

We first review related notations in the problem of finding straight-line drawings under concave corner constraints [12].

Let $\gamma = (F, f^o)$ be a plane embedding of a biconnected graph $G = (V, E)$, A *corner* λ around a vertex v is defined to be a pair (v, f) of the vertex v and the facial cycle $f \in F$ whose interior contains the corner. See Fig. 8(a). Let $\Lambda(v)$ denote the set of all corners around a vertex v in γ, and $\Lambda(\gamma)$ denote the set of all corners in γ. A corner (v, f^o) of a vertex v in the outer facial cycle f^o of γ is an *outer corner* of f^o. We let $\Lambda^o(\gamma)$ denote the set of the outer corners of the outer facial cycle f^o. We call a simple cycle C in G a *cut-cycle* if a cut-pair $\{u, v\} \subseteq V(C)$ separates the vertices outside C from those along C (including those inside C). A corner (v, f) of a vertex v in a cut-cycle C is an *outer corner* of C if v is not in the cut-pair of C, and f is one of the two facial cycles outside C that share the cut-pair of C. We denote by $\Lambda^o(C)$ the set of the outer corners of a cut-cycle (or the outer facial cycle) C.

Let D be a straight-line planar drawing that realizes γ. A corner of γ is called *concave* in D if its angle in D is greater than π (note that along the outer boundaryf^o a concave corner means a convex apex of the polygon drawn for f^o). A vertex v in a straight-line drawing D is called *concave* if one of the corners around v is concave in D. Let $\Lambda^c(D)$ denote the set of all concave corners in D.

The following result is known [12].

Theorem 13 *Let $\gamma = (F, f^o)$ be a plane embedding of a biconnected graph $G' = (V, E')$, and A be a subset of $\Lambda(\gamma)$. Then:*

(a) *There exists a straight-line drawing D' of γ such that $\Lambda^c(D') \subseteq A$ if and only if $|A \cap \Lambda^o(f^o)| \geq 3$ and $|A \cap \Lambda^o(C)| \geq 1$ for all cut-cycles C in γ.*

(b) *Let A satisfies the condition in* (a), *and f^o be drawn as a convex polygon $P_{\rm out}$ with $\Lambda^o(P_{\rm out}) = A \cap \Lambda^o(f^o)$. Then $P_{\rm out}$ can be extended to a star-shaped drawing D^* of G' with $\Lambda^c(D^*) \subseteq A$.*

First we show that Theorem 13(a) can be derived from Theorem 8. The only-if-part is easy to observe independently. We show that the if-part can be derived from Theorem 10. The if-part means that a straight-line drawing D' of γ such that $\Lambda^c(D') \subseteq A$ exists if $|A \cap \Lambda^o(f^o)| \geq 3$ and $|A \cap \Lambda^o(C)| \geq 1$ for all cut-cycles C in γ.

Denote the given plane graph by $(M = E', F_M = F, f^o_M = f^o)$. We next assign news edges as follows:
(i) For each inner face $f \in F(\gamma)$ of length at least four, assign a new edge vw inside the region f for every two adjacent edges $vu, uw \in E(f)$ such that $(u, f) \notin A$, as shown in Fig. 8(b); and
(ii) For the outer face f^o, assign a new edge vw in the outer region of γ for every two adjacent edges $vu, uw \in E(f)$ such that $(u, f) \notin A$.

Let $E - M$ be the set of all new edges, and α be the assignment of edges in $E - M$ to faces in F defined in the above. This defines an instance I of the FSL-drawing problem.

Since $|A \cap \Lambda^o(f^o)| \leq 3$, f^o_M cannot be surrounded by at most two chains. Hence any forbidden configuration to I is a zipped-chain, since $G_M = (V, M)$ is biconnected. Assume that I has a zipped-chain (S, S') with terminals a and b, where we choose a zipped-chain so that the a, b-component H has the minimum number of vertices among all such components surrounded by zipped-chains in I. Then we see that the boundary $f^o(H)$ is a simply cycle, since otherwise a subgraph H' of H would be surrounded by another zipped-chain by the way of introducing new edges. This, however, contradicts that a given set $A \subseteq \Lambda(\gamma)$ satisfies $|A \cap \Lambda^o(f^o(H))| \geq 1$. Therefore by Theorem 8, I has an FSL-drawing D. Let D' be the straight-line drawing induced from D by the set of original edges in $M = E$. Then clearly every other corner (u, f) not in A is realized as a convex corner due to the augmenting edges vw in D, as shown in Fig. 8(c). Thus, D' is a straight-line drawing of γ such that $\Lambda^c(D') \subseteq A$. This proves the if-part of Theorem 8.

Next we show that Theorem 13(b) can be derived from Theorem 10. Given a plane embedding γ, a subset $A \subseteq \Lambda(\gamma)$. a convex polygon P_{out} drawn for f^o in Theorem 13(b), we construct a fame as follows.
(i) For each inner face $f \in F(\gamma)$ of length at least four, assign a new edge vw inside the region f for every two adjacent edges $vu, uw \in E(f)$ such that $(u, f) \notin A$; and
(ii) For each inner face $f \in F(\gamma)$ which has at least two corners from A, create a new vertex r_f, add a crossing-free edge $r_j v$ for each vertex $v \in V(f)$ with $(v, f) \in A$ and an edge $r_j v'$ for the other vertices in $V(f)$, as shown in Fig. 8(d). (Hence the region f is split into $|\{v \in V(f) :\ (v, f) \in A\}|$ regions.)

Let M be the union of E' and the edges $r_f v$ with $(v, f) \in A$ introduced in (ii), F_M be the set of outer face f^o and the resulting inner faces, and $f^o_M := f^o$. Let $E - M$ be the set of all new edges introduced in (i) and the edges $r_f v'$ with $(v', f) \notin A$ introduced in (ii). We regard that each edge in $E - M$ is assigned one of the split region when the corresponding region f is split in (ii). This determines an assignment α of all edges in $E - M$ to some faces in F_M. This defines an instance I of the FSL-drawing problem. Analogously with case (a), we see that introducing new edges in (i) creates no zipped-chain or squashed chain. If some new edge $r_f v$ in (ii) is used in a zipped-chain or squashed chain, then I must have an a, b-component H containing r_f but is disjoint with the outer boundary. However, by construction in (ii) on a biconnected graph G', there cannot be such a cut-pair $\{a, b\}$. Hence I admits an FSL-drawing D by Theorem 10. Let D' be the straight-line drawing induced from D by the original vertices/edges in G'. Then every other corner (u, f) not in A is realized as a convex corner due to the augmenting edges vw in D, and the face f to which a new vertex r_f was created is drawn as a star-shaped polygon P_f, as shown in Fig. 8(e). Note that the polygons P_f in D' for the other inner faces are always star-shape, because P_f has at most one concave corner along it. Thus, D' is a star-shaped drawing of γ such that the outer boundary is P_{out} and $\Lambda^c(D') \subseteq A$ holds. This proves Theorem 13(b).

7.4 Application to Straight-line Drawability of SEFE with Biconnected Intersection Graph

Theorem 6 allows us to check the straight-line drawability of the following simultaneous embeddings.

Given two planar graphs $G_1 = (V, E_1)$ and $G_2 = (V, E_2)$ with a common vertex set V as input, *Simultaneous Embedding with Fixed Edges* (SEFE) asks whether G_i, $i = 1, 2$ admits a plane drawing γ_i such that: (i) each vertex $v \in V$ is mapped to the same point in γ_1 and in γ_2; and (ii) every edge

$e \in E_1 \cap E_2$ is mapped to the same curve in γ_1 and γ_2. The intersection graph $G_{1\cap 2}$ is defined to be the spanning subgraph $(V, E_1 \cap E_2)$.

Angelini et al. [1] proved that the SEFE problem for two graphs with a biconnected intersection graph can be solved in linear time.

By Theorem 6, the straight-line drawability of simultaneous embeddings in such a case.

Corollary 14 *Let γ be a simultaneous embedding of $G_1 = (V, E_1)$ and $G_2 = (V, E_2)$ such that $(V, E_1 \cap E_2)$ is biconnected. Then γ is PSL-drawable if and only if it has no forbidden configurations.*

8 Converting Convex Polygons into Pseudo-convex Polygons

In this section, we show how to convert a convex polygon into a pseudo-convex polygon by replacing its side with convex/convex links. For a convex k-gon $P = (p_1, p_2, \ldots, p_k)$, the segment between two adjacent apices p_i and p_{i+1} is called a *side* of P, which is denoted by p_ip_{i+1} such that p_i and p_{i+1} appear in this order when we traverse the boundary of P in the clockwise order. When we place a vertex v of a graph on a point p in the plane, the point p may be denoted by v for a notational convenience. For two distinct points p and p', let $L[p, p'\rangle$ denote the half-line (with exactly one endpoint p) passing through p and p'. The distance between two points p and p' is denoted by $|L[p, p']|$. For three distinct points p, p' and p'', let $\delta(p; p', p'')$ be the distance from a point p to the straight-line $L\langle p', p''\rangle$ for two points p' and p'' (i.e., $\delta(p; p', p'')$ is the length of altitude from p to $L\langle p', p''\rangle$).

Given a convex polygon P, we can replace the line-segment drawn for each side on the boundary of P with a convex or concave line so that the resulting polygon remains pseudo-convex if each convex or concave line is drawn sufficiently near the original position of the corresponding segment.

More formally, assume that we replace the segment $L[u, v]$ for each side uv on P with a convex or concave link Q with h new points, say $Q = (u, u_1, u_2, \ldots, u_h, v)$, where h may be different for each side uv (possibly $h = 0$, which means that we keep the segment $L[u, v]$ without introducing new vertices on it). Let S_P^- (resp., S_P^+) be denote the set of sides uv which are required to be replaced with concave links (resp., convex links). Assume that
(A1) for each side uv, the new vertices are initially placed along the current segment $L[u, v]$ as distinct flat corners as their positions (keeping the clockwise order that they appear along P);
(A2) An upper bound $\epsilon > 0$ on the movement is given so that a final position of each new vertex is required to be within distance ϵ from its initial position in (A1).

We replace the sides of P with concave/convex links as follows.

1. Define $\delta(P)$ to be the minimum of the following:

$$\min\{|L[p, p']| : \text{ for every two distinct points } p \text{ and } p' \text{ along } P\}$$

   and

$$\min\{\delta(p; p', p'') : \text{ for every three non-co-linear points } p, p' \text{ and } p'' \text{ along } P\ \}.$$

2. For each new vertex w, take a circle zone Z_w with radius $\min\{\epsilon, \delta(P)/4\}$ with the current initial position of w as its center.

3. For each side $uv \in S_P^-$ (resp., $uv \in S_P^+$), move the new vertices $u_1, u_2, \ldots, u_h$ within their circle zones to form a concave link (resp., a convex link).

In Step 2, we see that every two vertices w and w' not on the same link are still visible with no interference by any other segments, after changing the position of a new vertex w to any new position within Z_w. Hence a desired pseudo-convex polygon can be obtained after Step 3.

The construction can be applied to a set of convex polygons in straight-line drawings. In a plane embedding, each side uv is shared by two inner faces, denoted by $f(uv)$ and $f(vu)$, where u and v appear in this order along $f(uv)$ in the clockwise order (or along $f(vu)$ in the anti-clockwise order).

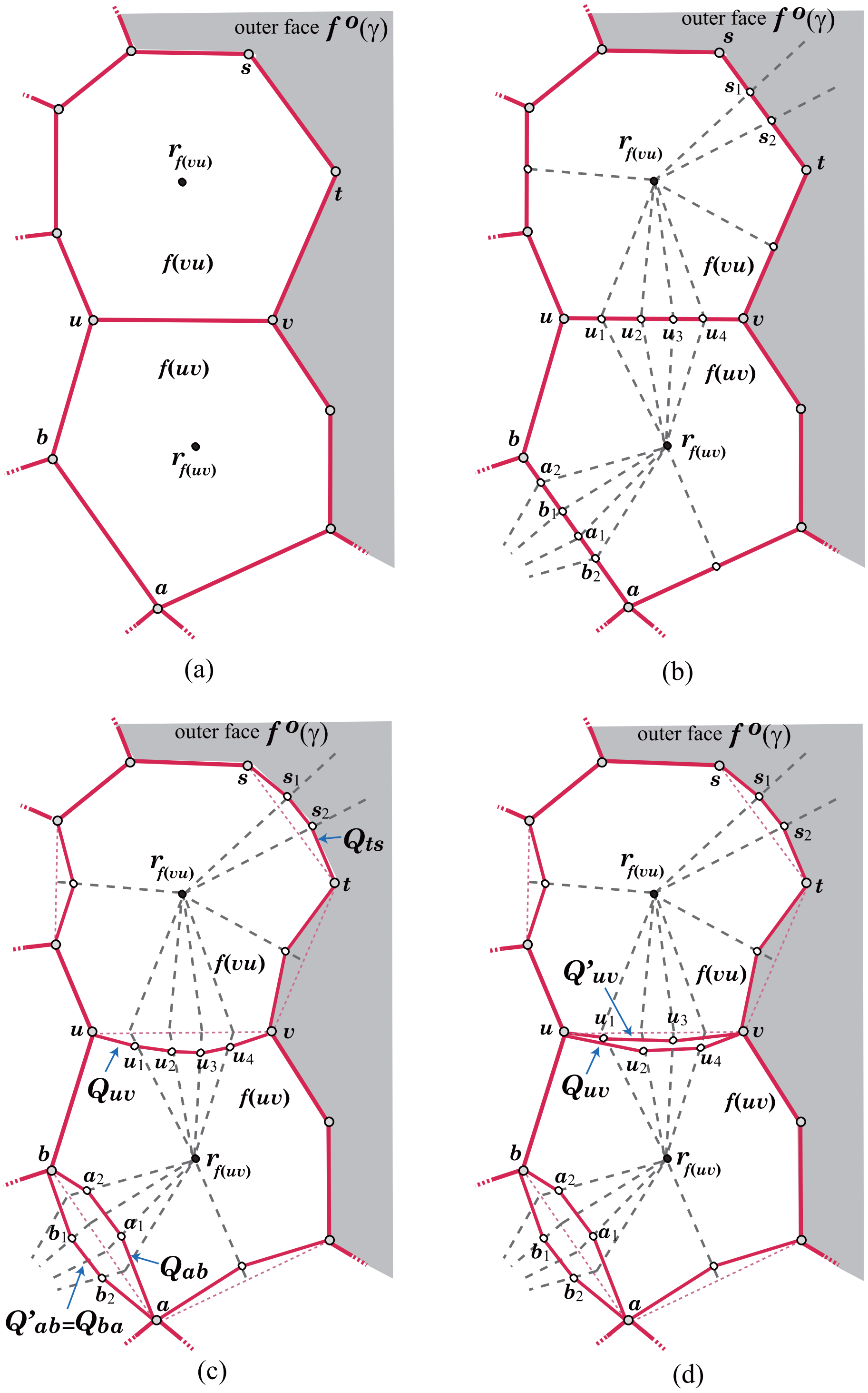

Figure 9: Illustration for converting convex polygons in inner convex drawings into pseudo-convex polygons by replacing some sides with concave/convex links: **(a)** Some convex polygons drawn for inner faces in an inner convex drawing D, where black circles indicate the reference points r_f for inner faces f; **(b)** New vertices with initial positions on the segments of the corresponding sides of polygons, where dashed lines indicate the tracks around each reference point r_f; **(c)** The new vertices are moved to form concave links Q_{uv}, Q_{ts}, Q_{ab} and Q_{ba}; and **(d)** A convex link Q'_{ab} is realized as a concave link Q_{ba}, and a concave link Q'_{uv} is generated from a combined concave link Q_{uv}.

Lemma 15 *Let D be a straight-line drawing of a plane embedding γ such that each inner face $f \in F(\gamma) - f^o(\gamma)$ is drawn as a convex polygon P_f. For specified $S^-(P_f)$ and $S^+(P_f)$, $f \in F(\gamma) - f^o(\gamma)$, and $\epsilon > 0$, given initial positions of new vertices on the current sides can be changed within distance ϵ so that*
- each side $uv \in S^-(P_f)$ (resp., $uv \in S^+(P_f)$) will be replaced with a concave (resp., convex) link of P_f and
- the polygon P_f for each inner face $f \in F(\gamma) - f^o(\gamma)$ remains pseudo-convex.

Proof: I. Now for each side uv, $uv \in S^-(P_{f(uv)})$ of $uv \in S^+(P_{f(vu)})$, and if $uv \in S^-(P_{f(uv)}) \cup S^+(P_{f(vu)})$, then $vu \in S^-(P_{f(vu)}) \cup S^+(P_{f(vu)})$. For each new vertex w, we take a circle zone Z_w with radius

$$\min[\epsilon, (1/4)\min\{\delta(P_f) : \ f \in F(\gamma) - f^o(\gamma)\}]$$

with the initial position of w as its center. Then we see that the above construction can be applied independently to the set of new vertices $u_1, u_2, \ldots, u_h$ for each side $uv \in S^-(P_{f(uv)}) \cup S^+(P_{f(vu)})$ to obtain a desired set of pseudo-convex polygons P_f, $f \in F(\gamma) - f^o(\gamma)$.

II. We here show some systematical way of moving new vertices w from their initial positions to adequate positions within Z_w. Before we move the new vertices, we select a reference point r_f from the interior of P_f of each inner face $f \in F(\gamma) - f^o(\gamma)$, as shown in Fig. 9(a). For each new vertex w on $L[u,v]$ for a side and the initial position p_w, use the segments $L[p_w, r_{f(uv)}]$ and $L[p_w, r_{f(vu)}]$ as tracks only along which the vertex w is allowed to move; when $f(vu) = f^o(\gamma)$, we use the half-line $L[r_{f(uv)}, p\rangle$ as a track for w on $L[u,v]$, as shown in Fig. 9(b), where the face $f(st)$ is equal to $f^o(\gamma)$. Now we move the new vertices w along their tracks so that each side $uv \in S_P^-$ (resp., $uv \in S_P^+$), form a concave link (resp., a convex link), as shown in an example of a concave link Q_{uv} for side uv in Fig. 9(c). ∎

Now we consider the case where the segment of a side uv of a polygon is replaced not only with a single concave/convex link but also with a pair of concave/convex links Q_{uv} and Q'_{uv}. Thus, we allow a side uv of a polygon to satisfy one of the following:

(i) $uv \in S^-(P_{f(uv)})$ and $vu \in S^-(P_{f(vu)})$;

(ii) $uv \in S^-(P_{f(uv)})$ and $vu \in S^+(P_{f(vu)})$; and

(iii) $uv \in S^+(P_{f(vu)})$ and $vu \in S^-(P_{f(vu)})$.

A new polygon P_{uv} to be created between Q_{uv} and Q'_{uv} also needs to be pseudo-convex. In other words,

(i) Q_{uv} is a concave link to the polygon $P_{f(uv)}$, Q'_{uv} is a concave link to the polygon $P_{f(vu)}$, and Q_{uv} and Q'_{uv} form a pseudo-convex polygon P_{uv};

(ii) Q_{uv} is a concave link to the polygon $P_{f(uv)}$, Q'_{uv} is a convex link to the polygon $P_{f(vu)}$, and Q_{uv} and Q'_{uv} form a pseudo-convex polygon P_{uv}; and

(iii) Q_{uv} is a convex link to the polygon $P_{f(uv)}$, Q'_{uv} is a concave link to the polygon $P_{f(vu)}$, and Q_{uv} and Q'_{uv} form a pseudo-convex polygon $P_{f(uv)}$.

Note that a pseudo-convex polygon P_{uv} in (i) is always convex. Even for the case where the segment of some side of a polygon is replaced with a pair of concave/convex links, we obtain an analogous result.

Lemma 16 *Let D be a straight-line drawing of a plane embedding γ such that each inner face $f \in F(\gamma) - f^o(\gamma)$ is drawn as a convex polygon P_f. For specified $S^-(P_f)$ and $S^+(P_f)$, $f \in F(\gamma) - f^o(\gamma)$, and $\epsilon > 0$, given initial distinct positions of new vertices on the current sides can be changed within distance ϵ so that*
- each side $uv \in S^-(P_f)$ (resp., $uv \in S^+(P_f)$) will be replaced with a concave (resp., convex) link of P_f and
- the polygon P_f for each inner face $f \in F(\gamma) - f^o(\gamma)$ and the polygon newly created between a pair of two links will be pseudo-convex.

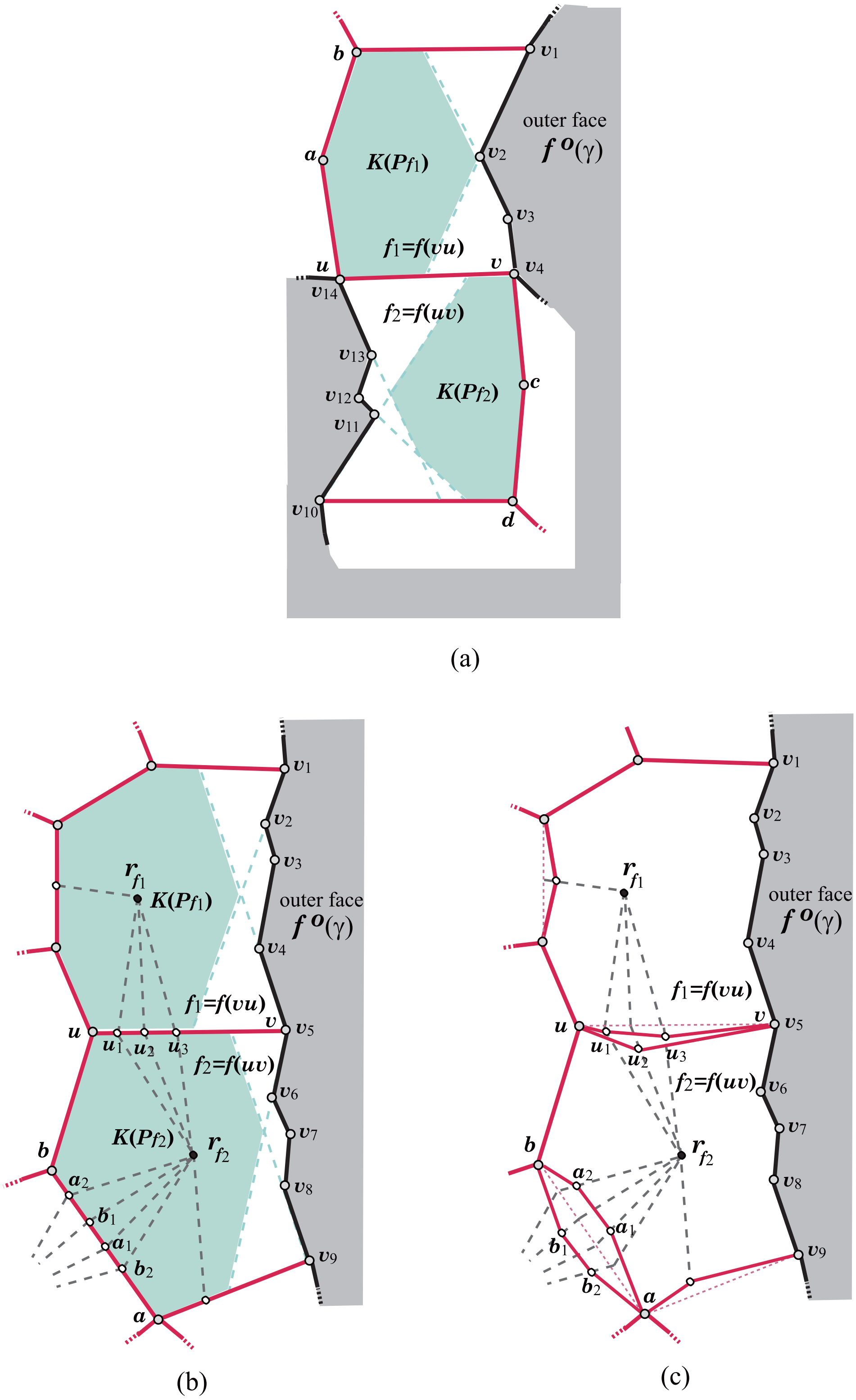

Figure 10: Illustration for replacing sides of polygons with single concave links with convex/concave links: **(a)** An inner edge uv in a straight-line drawing D for a biconnected plane graph, where the kernels $K(P_{f(uv)})$ and $K(P_{f(vu)})$ of the polygons of the inner faces adjacent to uv have no intersection along the segment $L[u, v]$; **(b)** New vertices for each side uv are initially placed on the visible area $K(P_{f(uv)}) \cap K(P_{f(vu)})$ along segment $L[u, v]$, and the reference point r_f for each inner face f is taken from the interior of the kernel $K(P_f)$ of the initial polygon P_f; and **(c)** Required concave/convex links are realized in the same manner with the proof of Lemma 16.

Proof: All new vertices are placed on given initial positions on the segments $L[u,v]$ of the corresponding sides uv, where the two set of new vertices, one for Q_{uv} and Q'_{uv} are all on the same segment $L[u,v]$, keeping their clockwise order along $P_{f(uv)}$. By assumption, no two vertices are placed on the same initial position. We prepare reference points and tracks as in the proof II of Lemma 15.

We first consider the case where none of types (ii) and (iii) of pairs of links are given. In this case, we can move the new vertices for a sinlge concave/convex link Q_{uv} and a pair of a concave link Q_{uv} and a convex link Q'_{uv} in the same manner with the proof II of Lemma 15, since a convex link Q'_{uv} will be served as a concave link Q_{vu}. See an example of a concave link Q_{ab} and a convex link Q'_{ab} for side ab in Fig. 9(c). Thus we can construct each concave link independently by moving the new vertices w along their tracks within zone Z_w to obtain a desired set of pseudo-convex polygons. Note that the polygon P_{uv} between Q_{uv} and Q'_{uv} will automatically become convex since we move the new vertices along their tracks which always ensure the convexity of polygon P_{uv}.

Next we consider how to handle types (ii) and (iii) of pairs of links. For a side uv, assume that we are supposed to construct type (ii) of links, i.e., a concave link Q_{uv} to the polygon $P_{f(uv)}$, a convex link Q'_{uv} to the polygon $P_{f(vu)}$ (type (iii) can be treated symmetrically). Then let W_{uv} and W'_{uv} be the set of new vertices on Q_{uv} and Q'_{uv}, where both W_{uv} and W'_{uv} are initially on $L[u,v]$. We first construct two links Q_{uv} and Q'_{uv} as a single combined concave link with the new vertices in $W_{uv} \cup W'_{uv}$ to $P_{f(uv)}$. We do this for each single concave link in the above case and each combined concave link independently by moving the new vertices w along their tracks within zone Z_w. With the resulting concave links, each polygon is a required pseudo-convex polygon.

The remaining task is to split each of the combined concave links. This can be done for each concave link independently as follows. Let Q_{uv} be a combined concave link, which is a convex link to the other polygon $P_{f(vu)}$. Then we leave the vertices in W_{uv} as they are on the link Q_{uv} while we move the vertices in W'_{uv} toward their initial positions along their tracks, letting $W'_{uv} \cup \{u,v\}$ keep to form a convex link to $P_{f(vu)}$ until the polygon P_{uv} between W_{uv} and W'_{uv} becomes pseudo-convex. Note that every new vertex $W_{uv} \cup W'_{uv}$ in the combined link Q_{uv} was visible from any vertex along $P_{f(vu)}$. Hence the visibility of vertices in W'_{uv} will be preserved as long as they move toward the reference point $r_{f(vu)}$ within $P_{f(vu)}$. Hence when P_{uv} becomes pseudo-convex (i.e., every two vertices $w \in W_{uv}$ and $w' \in W'_{uv}$ are visible), we obtain a desired pair of links Q_{uv} and Q'_{uv}. Fig. 9(d) illustrates how Q'_{uv} is constructed from the combined link Q_{uv} in Fig. 9(c).

From the above, we see that all specified links can be realized to form a desired set of pseudo-convex polygons P_f, $f \in F(\gamma) - f^o(\gamma)$. ∎

Let D be a straight-line drawing that realizes a biconnected plane graph with the outer face f^o, and let P_f denote the polygon in D drawn for an inner face f. We call a polygon P_f *convex-interior* if it satisfies the followings:

(i) There is no inner vertex of degree 2;

(ii) Each inner edge $uv \in E(f) - E(f^o)$ is drawn as a single segment $L[u,v]$ along P_f;

(iii) P_f is star-shaped (where an outer edge $uv \in E(f) \cap E(f^o)$ is allowed to be drawn as any sequence of segments (not necessarily convex or concave one to P_f); and

(iv) For each inner edge $uv \in E(f) - E(f^o)$ and the two inner faces $f(uv)$ and $f(vu)$ containing edge uv, the intersection of $L[u,v]$, kernels $K(P_{f(uv)})$ and $K(P_{f(vu)})$ has a positive length.

We call D a *convex-interior* drawing if all polygons P_f in D are convex-interior. We can replace each "inner" edge in a convex-interior drawing with a single concave/convex link or a pair of concave/convex links keeping the visibility of two vertices u and v within each inner face as long as there are not on the same link or the sequence of segments for an outer edge (where we do not change the sequence of segments for each outer edge).

Fig. 10(a) illustrates part of a straight-line drawing D that realizes a biconnected plane graph with the outer face f^o, where the polygon P_{f_1} is not convex-interior in D, because for the inner edge $uv \in E(f_1)$, the kernels $K(f_1)$ and $K(f_2)$ of the polygons of the inner faces f_1 and f_2 adjacent to uv have no intersection along the segment $L[u,v]$. Note that $\{u,v\}$ is a cut-pair of the graph.

Fig. 10(b) illustrates convex-interior polygons P_{f_1} and P_{f_2}, where for the inner edge $uv \in E(f_1) \cap E(f_2)$, the intersection of the kernels $K(P_{f_1})$ and $K(P_{f_2})$ and $L[u,v]$ has a positive length.

In the next lemma, no initial positions of new vertices on links are specified.

Lemma 17 *Let D be a convex-interior drawing of a plane embedding γ of a biconnected graph $G = (V, E)$. Let $S^-(P_f)$ and $S^+(P_f)$ be sets of sides of polygon P_f in D for each inner face $f \in F(\gamma) - f^o(\gamma)$ such that $S^-(P_f) \cup S^+(P_f)$ contains no sides for outer edges on $f^o(\gamma)$. Then the segment for each inner edge can be replaced with specified links so that*

- each side $uv \in S^-(P_f)$ (resp., $uv \in S^+(P_f)$) will be replaced with a concave (resp., convex) link of P_f,

- the polygon newly created between a pair of two links will be pseudo-convex; and

- for each inner face $f \in F(\gamma) - f^o(\gamma)$, two vertices $u, v \in V(f)$ are visible within the polygon P_f unless u and v are on the same link or the sequence of segments for an outer edge.

Proof: By definition (iv) of convex-interior polygons, for an inner edge $uv \in E(f) - E(f^o)$ and the two inner faces $f(uv)$ and $f(vu)$, the intersection of $L[u,v]$, kernels $K(P_{f(uv)})$ and $K(P_{f(vu)})$ has a positive length. Hence each of kernels $K(P_{f(uv)})$ and $K(P_{f(vu)})$ has a positive area, and their intersection $K(P_{f(uv)}) \cap K(P_{f(vu)})$ does so. Since no initial positions of new vertices on each link are specified, we place them on the corresponding segment $L[u,v]$ within the region $K(P_{f(uv)}) \cap K(P_{f(vu)})$. Then we choose a reference point r_f from kernels $K(P_f)$, and set up tracks as in the proof of Lemma 16. Since the positions of outer vertices along an inner face f remain unchanged, the other inner or newly introduced vertices in along f are always visible from these outer vertices as long as they stay inside $K(P_f)$. Hence we see that the new vertices can be moved along their tracks so that all specified links are realized to form a desired set of polygons P_f, $f \in F(\gamma) - f^o(\gamma)$ after selecting $\epsilon = (1/4)\min\{\delta(P_f) : f \in F(\gamma) - f^o(\gamma)\}$, as in the proof of Lemma 16. ∎

9 A Constructive Proof for the Main Result

We prove Theorem 10 by an induction on the number of edges in $M - E(f^o_M)$. In what follows, we denote a given instance without zipped-chains/squashed chains by a tuple

$$I = (G, M, F_M, f^o_M, \alpha, P_{\text{out}}).$$

For a straight-line drawing D of a standard instance I, we call two vertices u and v (or edge $e = uv \in E$) *M-visible* in D if the segment $L[u,v]$ does not intersect the segment $L[a,b]$ (except at end-points a and b) of any edge $ab \in M$ in D. When $G_M = (V, M)$ is drawn as a straight-line plane drawing, every edge in M is M-visible. Then a straight-line drawing D of I that realizes the frame (M, F_M, f^o_M) is an FSL-drawing of I if and only if every edge in E is M-visible in D.

When $M - E(f^o_M) = \emptyset$, i.e., M forms a prescribed convex polygon P_{out}, clearly the instance I is FSL-drawable since there is no squashed chain. Assume that $M - E(f^o_M) \neq \emptyset$. Our idea is to construct an instance $I' = (G', M', F_{M'}, f^o_{M'}, \alpha', P'_{\text{out}})$ with $|M' - E(f^o_{M'})| < |M - E(f^o_M)|$ by simplifying a subgraph H of G such that

(i) no new zipped-chains/squashed chains will be created in I'; and

(ii) any FSL-drawing D' for I' (which exists by induction hypothesis) can be modified into an FSL-drawing D of the original instance I.

Exposed Vertices We here introduce a notion of "exposed vertices" along a subgraph of G_M. Let H be an s,t-component for a cut-pair $\{s,t\}$ in G_M, and let $(v_1 = t, v_2, \ldots, v_k = s)$ denote the t,s-boundary path of $f^o_{ts}(H)$. Let $v_iv_j \in E - M$ be an edge assigned to face$^{ts}(H)$ such that $v_iv_j \in V^o_{ts}(H)$. We say that edge v_iv_j *covers* a vertex $v_h \in V^o_{ts}(H) - \{s,t\}$ if $v_i, v_j \neq v_h$ and edge v_iv_j together with $f^o_{ts}(H)$ encloses v_h (i.e., v_i, v_h and v_j appear along $f^o_{ts}(H)$ in this order). When face$^{ts}(H)$ is an inner face of F_M, a vertex $v_h \in V^o_{ts}(H) - \{t,s\}$ is called *exposed* along $f^o_{ts}(H)$ if no edge v_iv_j ($v_i, v_j \in V^o_{ts}(H)$) assigned to face$^{ts}(H)$ covers v_h. When face$^{ts}(H) = f^o_M$, a vertex

$v_h \in V^o_{ts}(H) - \{t, s\}$ is called *exposed* along $f^o_{ts}(H)$ if the corner at vertex v_h in polygon $P_{\rm out}$ is not a flat corner (note that no edge is assigned to face$^{ts}(H) = f^o_M$). We say that H is *exposed* along $f^o_{ts}(H)$ if a vertex $u \in V^o_{ts}(H) - \{s, t\}$ is exposed along $f^o_{ts}(H)$, and that H is *fully exposed* along $f^o_{ts}(H)$ if all vertices $u \in V^o_{ts}(H) - \{s, t\}$ are exposed along $f^o_{ts}(H)$.

A set of edges $v_i v_{i+2}$ $(1 \le i \le k-2)$ and $v_1 v_{k-1}$ and $v_2 v_k$ assigned to face$^{ts}(H)$ is called a *convex-support* along $f^o_{ts}(H)$. Symmetrically we define exposition along $f^o_{st}(H)$. In our reductions for instances, we sometime introduce a convex-support along a newly constructed path so that the path is drawn as a convex polygon (minus one side) in an FSL-drawing of the reduced instance.

To find adequate subgraphs H, we use the decomposition of a graph $G_M = (V, M)$ into triconnected components, which can be represented by a rooted SPQR tree (see Section 11 for details). For a simple graph G_M, there are three types of nodes, P-, R- and S-nodes. A node ν provides a graph, called the skeleton $\mathrm{skn}(\nu)$ which is an abstract structure of a subgraph, denoted by $G^-(\nu)$, of the entire graph G_M. Based on $\mathrm{skn}(\nu)$, we design a procedure for simplifying the subgraph $H = G^-(\nu)$ to obtain a smaller instance I'. However, if we simplify $H = G^-(\nu)$ too much, say to a single edge, then it would be impossible to construct a necessary straight-line drawing by extending any FSL-drawing D' of the reduced instance I'. Although removing vertices/edges from I never creates a new forbidden configuration (zipped-chain or squashed chain), this again may leave an instance I' whose FSL-drawing cannot be modified into that for I. To keep some area in a drawing D' of a reduced instance I' so that a necessary straight-line drawing of $H = G^-(\nu)$ can be constructed there, we sometimes introduce new edges in our reduction process. However, we need to be careful in introducing new edges or contracting vertices, because such kind of operations could easily introduce a new forbidden configuration.

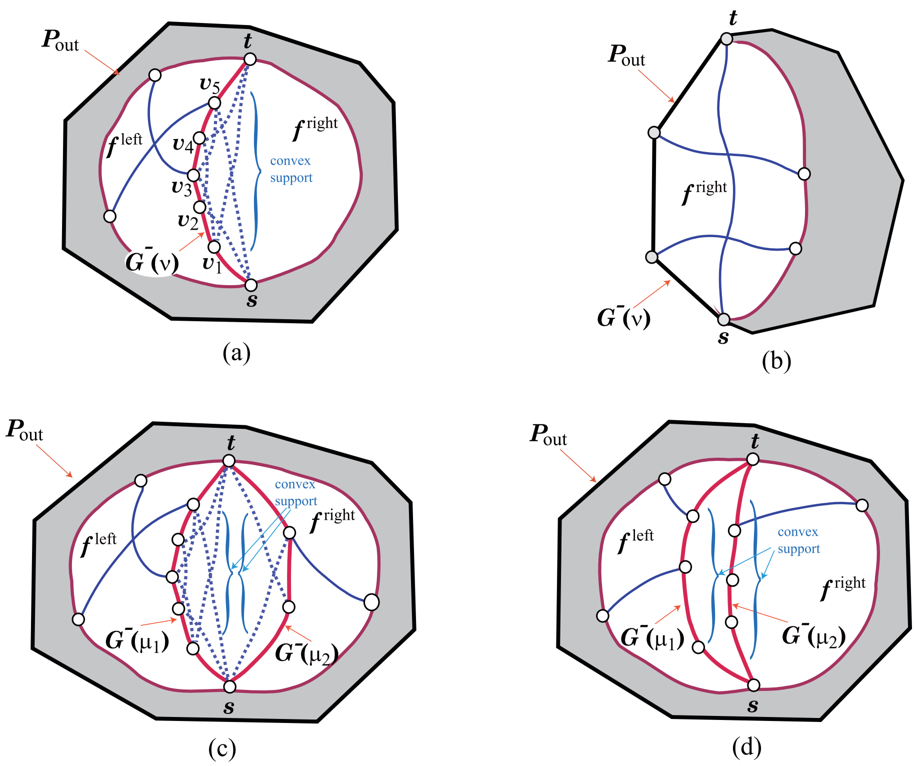

Figure 11: **(a)** Embedding with the subgraph $G^-(\nu)$ of a reduced S-node ν, where the set of edges vv' $(v, v' \in V^o_{ts}(G^-(\nu))$ within $f^{\rm right}$ is the convex-support for $G^-(\nu)$; **(b)** Embedding with the subgraph $G^-(\nu)$ of a reduced S-node ν on the polygon $P_{\rm out}$; **(c)** Embedding with the subgraph $G^-(\nu)$ of a reduced P-node ν such that $G^-(\nu)$ is required to be drawn as a convex polygon; and **(d)** Embedding with the subgraph $G^-(\nu)$ of a reduced P-node ν such that $G^-(\nu)$ is required to be drawn as a pseudo-convex polygon with a concave link $G^-(\nu_2)$.

In this paper, we simplify the subgraph $H = G^-(\nu)$ for one of P-, R- and S-nodes ν up to the following structure (see Fig. 11 in Section 11).

Reduced S-nodes We call a non-root S-node ν with no virtual edges in $\mathrm{skn}^-(\nu)$ if (i) $\mathrm{skn}^-(\nu) = G^-(\nu)$ consists of a subpath of the outer boundary f^o_M, which is now drawn as a convex polygon P_{out}; or (ii) $G^-(\nu)$ are fully exposed along $f^o_{ts}(G^-(\nu))$ and has a convex-support along $f^o_{st}(G^-(\nu))$ for (s,t) with $st = \mathrm{parent}(\nu)$.

Reduced P-nodes A P-node ν with $\{s,t\} = V(\mathrm{skn}(\nu))$ is called *reduced* if $\mathrm{skn}(\nu)$ consists of two virtual edges e_1 and e_2 which correspond to reduced S-nodes μ_1 and μ_2.

To prove Theorem 10, it suffices to design reductions for each of the following cases:
- A non-reduced P-node whose child-nodes are all reduced S-nodes;
- An R-node whose child-nodes (if any) are all reduced S- or P-nodes; and
- A non-reduced S-node whose child-nodes (if any) are all reduced P-nodes.

The details of reduction for each case can be found in Sections 12 - 15.

10 Technical Lemmas

This section provides a collection of technical lemmas which will be used in the subsequent sections.

Lemma 18 *Let $I = (G = (V,E), M, F_M, f^o_M, \alpha)$ be a standard instance with a prescribed convex polygon P_{out} for f^o_M, and assume that I has no zipped-chains or squashed chains. Let $f \in F_M$ be an inner face, and u and v be two distinct vertices in $V(f)$, and I' be the instance obtained by assigning a new edge uv within face f.*
(i) *Assume that I' contains a zipped-chain (S,S') with terminal a and b, where the a,b-chain S contains uv without loss of generality. Then $\{a,b\}$ is contained in the u,v-boundary path $f^o_{uv}(f)$ or v,u-boundary path $f^o_{vu}(f)$ of the facial cycle f, and I has a b,a-chain S' which together with the a,b-boundary path $f^o_{ab}(f)$ surrounds the region f (see* Fig. 12(a)*).*
(ii) *Assume that I' contains a squashed a,b-chain S. Then there is an a,b-component H such that $u,v \in V^o_{ab}(H)$ and $f^o_{ba}(H)$ is a b,a-path $S' = P_{ba}$ of the boundary of P_{out} from b to a in the clockwise order which contains no convex corner (see* Fig. 12(b)*).*

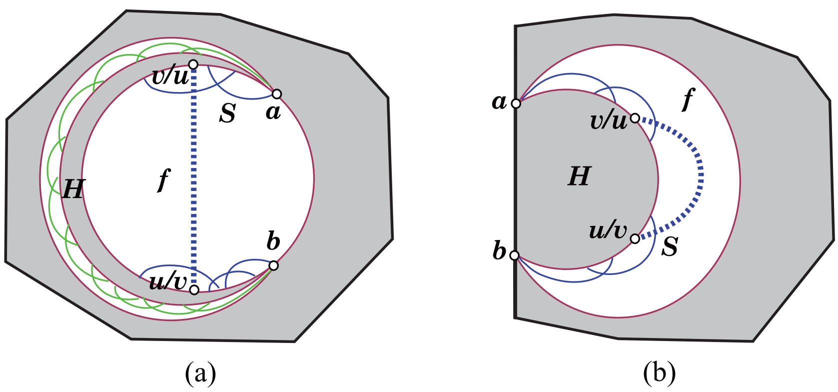

Figure 12: Illustration for embeddings with a new edge uv assigned to an inner face $f \in F_M$: **(a)** the new edge uv is contained in an a,b-chain S which gives a newly created zipped-chain; and **(b)** the new edge uv is contained in an a,b-chain S which gives a newly created squashed chain.

Proof: (i) By Lemma 2, $\{a,b\}$ is a cut-pair of G_M and the zipped-chain (S,S') surrounds an a,b-component H. Since the facial cycle f and the new edge uv give three internally disjoint paths between u and v in I', the cut-pair $\{a,b\}$ never separate u and v. Hence $\{a,b\}$ is contained in $f^o_{uv}(f)$ or $f^o_{vu}(f)$. Clearly in this case the a,b-boundary path $f^o_{ab}(H)$ of H appears along f as the b,a-boundary $f^o_{ba}(f)$. Hence the b,a-boundary path $f^o_{ba}(H)$ of H and the b,a-boundary $f^o_{ab}(f)$ surrounds the region f, as shown in Fig. 12(a).

(ii) By definition, $\{a,b\}$ is a cut-pair of G_M that appears along the facial cycle f and the b,a-path $S' = P_{ba}$ obtained from the boundary of $P_{\rm out}$ from b to a in the clockwise order, where $S' = P_{ba}$ contains no convex corner of $P_{\rm out}$, since S is a squashed chain. See Fig. 12(b). Note that path $S' = P_{ba}$ and chain S surround an a,b-component H such that $u, v \in V^o_{ab}(H)$ and $P_{ba} = f^o_{ba}(H)$. ∎

Lemma 19 *Let $I = (G = (V,E), M, F_M, f^o_M, \alpha)$ be a standard instance with no zipped-chains. Let $\{u,v\}$ is a cut-pair with $uv \notin E$ such that there are two inner faces $f_1, f_2 \in F_M$ which contain u and v on their facial cycles, where the ordering of u and v along f_1 and f_2 is assumed so that, for the subgraph H of G_M with no outer vertices/edges enclosed by f_1 and f_2, the boundary $f^o(H)$ consists of $f^o_{uv}(H) = f^o_{vu}(f_1)$ and $f^o_{vu}(H) = f^o_{uv}(f_2)$, as shown in Fig. 13(a). Assume that instance I contains neither a v,u-chain which together with f_1 surrounds the path $f^o_{uv}(H) = f^o_{vu}(f_1)$ nor a u,v-chain which together with f_2 surrounds the path $f^o_{vu}(H) = f^o_{uv}(f_2)$. Let $I_i = (G_i, M, F_M, f^o_M, \alpha_i)$, $i = 1,2$ be the instance obtained by assigning a new edge $e_i = uv$ within face f_i. Then at least one of I_1 and I_2 contains no newly created zipped-chain.*

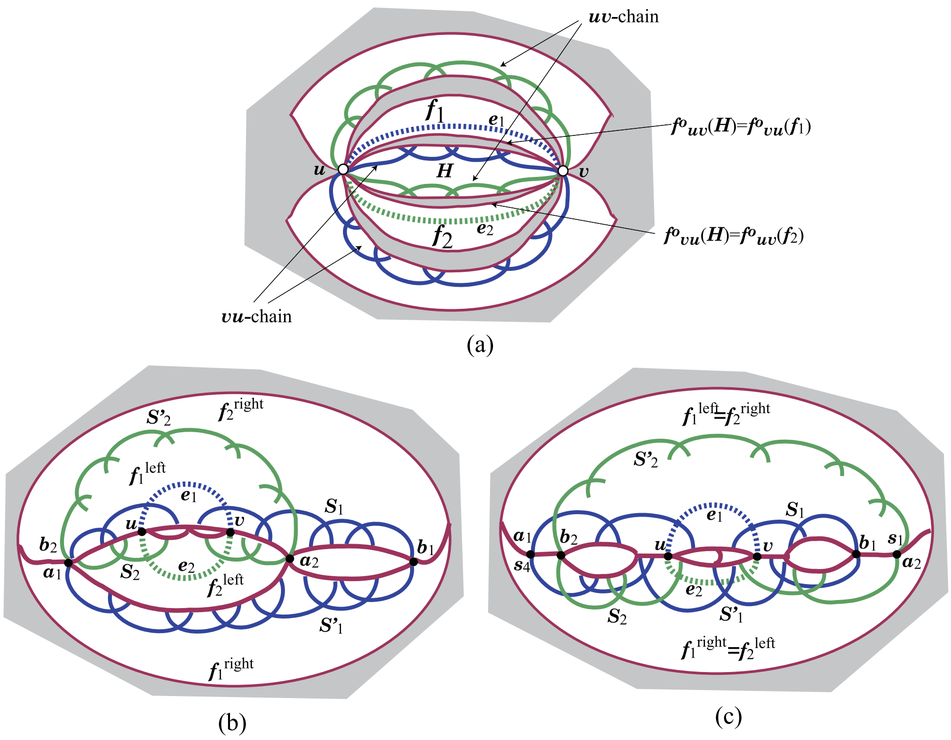

Figure 13: Illustration for embeddings with new edge $e_i = uv$ assigned to two different inner faces of F_M: **(a)** Two inner faces $f_1, f_2 \in F_M$ enclose a subgraph H of G_M with no outer vertices/edges such that the boundary $f^o(H)$ consists of $f^o_{vu}(f_1)$ and $f^o_{uv}(f_2)$, and the blue lines (resp., green lines) indicate v,u-chains which together with f_1 surrounds the path $f^o_{uv}(H) = f^o_{vu}(f_1)$ (resp., u,v-chains which together with f_2 surrounds the path $f^o_{vu}(H) = f^o_{uv}(f_2)$); **(b)** $f_2^{\rm left}$ is enclosed by the boundary of the a_1,b_1-component H_1; and **(c)** $f_2^{\rm left}$ is not enclosed by the boundary of H_1.

Proof: Fix an embedding γ of G that realizes the frame (M, F_M, f^o_M, α). Let γ_i be an embedding of I_i obtained from γ by placing edge $e_i = uv$ within face $f_i \in F_M$. The assumption that instance I has no v,u-chain which together with f_1 surrounds the path $f^o_{uv}(H) = f^o_{vu}(f_1)$ implies that adding a new edge e_1 within face f_1 does not create a new zipped-chain with terminal u and v. Symmetrically for the assumption that there is no u,v-chain which together with f_2 surrounds the path $f^o_{vu}(H) = f^o_{uv}(f_2)$.

To derive a contradiction, assume that each γ_i, $i = 1, 2$ contains a zipped-chain $\eta_i = (S_i, S'_i)$ with $e_i \in S_i$ in I_i, where S_i and S'_i are minimal. Let a_i and b_i be the terminals of the zipped-chain (S_i, S'_i), where we assume without loss of generality that S_i is an a_i, b_i-chain, where S'_i is a $b_i a_i$-chain in I_i. By the assumption, each of I_1 and I_2 contains no new zipped-chain with terminal u and v, and we have $\{a_i, b_i\} \neq \{u, v\}$ for $i = 1, 2$. Let Q_i denote the 2-vertex-cycle that surrounds η_i in the graph $\mathcal{G}(\gamma_i) = (V \cup C(\gamma_i), \mathcal{E}(\gamma_i))$ (thus $V(Q_i) = \{a_i, b_i\}$). Let H_i denote the a_i, b_i-component of $G_M = (V, M)$, where we regard H_i as the plane embedding induced from γ. The end-vertices of all edges in $S_i \cup S'_i$ appear along the outer boundary $f^o(H_i)$.

By Lemma 1, S_i and S'_i are contained in different inner faces f_i^{left} and f_i^{right} of F_M, respectively. We distinguish two cases.

(i) f_2^{left} is enclosed by the boundary $f^o(H_1)$ of the a_1, b_1-component H_1 (see Fig. 13(b)): In this case, Q_2 contains exactly two vertices along H_1 as the terminals a_2 and b_2 in $\mathcal{G}(\gamma_2)$, and $\{a_2, b_2\}$ needs to be a cut-pair of G_M, since Q_2 surrounds an a_2, b_2-component which contains u and v. By $\{a_2, b_2\} \neq \{u, v\}$, we see that Q_2 visits both faces f_1 and f_2. Then Q_2 surrounds the b_2, a_2-boundary path of $f^o(H_1)$. Hence $S_1 \cup S'_2$ contains an a_1, b_1-chain S_3 in I, and $(S_3, S'_3 = S'_1)$ gives a zipped-chain with $e_1, e_2 \notin S_3 \cup S'_3$ in the original instance I, a contradiction to the assumption on I.

(ii) f_2^{left} is not enclosed by the boundary $f^o(H_1)$ (see Fig. 13(c)): In this case, $f_1^{\text{right}} = f_2^{\text{left}} = f_2$. Assume without loss of generality that f_1^{left} is not enclosed by the boundary $f^o(H_2)$ either (otherwise we can apply the argument of (i)). Then $f_2^{\text{right}} = f_1^{\text{left}} = f_1$. Since vertices a_1, a_2, b_1 and b_2 appear in both f_1 and f_2 and H_1 and H_2 share vertices u and v, these vertices appear along f_1 in an ordering $(s_1, s_2, v, u, s_3, s_4) \in \{(a_2, b_1, v, u, b_2, a_1), (b_1, a_2, v, u, b_2, a_1), (a_2, b_1, v, u, a_1, b_2), (b_1, a_2, v, u, a_1, b_2)\}$. In any case, $S_1 \cup S'_2$ contains an s_4, s_1-chain S_3 in I, and $S_2 \cup S'_1$ contains an s_1, s_4-chain S'_3 in I, which gives a zipped-chain (S_3, S'_3) with $e_1, e_2 \notin S_3 \cup S'_3$ in the original instance I, a contradiction. ∎

For a standard instance, let $f_1 \in F_M$ be an inner face, and s and t be two distinct vertices along the facial cycle f_1. We consider how a new zipped-chain or squashed chain can be created by adding a new edge vw within region $f_1 \in F_M$ in the standard instance. In particular, we assume that there are two vertices s and t which are connected by three internally disjoint paths, and vertices v and w appear on the s, t-boundary path $f^o_{st}(f_1)$ and the t, s-boundary path $f^o_{ts}(f_1)$ of f_1, respectively. We say that edge wv is a *shift* of an edge wv' if there is a v, z-chain or z, v-chain S^* along the s, t-boundary path $f^o_{st}(f_1)$ such that the edge $v'w$ crosses some edge in S^* (see Fig. 14(a) and (b)). The next tells that introducing shifts does not create new zipped/squashed chains.

Lemma 20 *Let $I = (G = (V, E), M, F_M, f^o_M, \alpha)$ be a standard instance with a prescribed convex polygon P_{out} for f^o_M, and assume that instance I has no zipped-chains or squashed chains. Let s and t be two distinct vertices along an inner facial cycle $f_1 \in F_M$ such that G_M contains an s, t-path Q disjoint with the facial cycle f_1 except at s and t, where such a path Q is denoted by Q_1 (resp., by Q_2) if Q and the t, s-boundary path $f^o_{ts}(f_1)$ (resp., s, t-boundary path $f^o_{st}(f_1)$) of f_1 encloses the region f_1. For a vertex v on $f^o_{st}(f_1)$ (possibly $v = s$ or t), and a vertex w ($\neq s, t$) on $f^o_{ts}(f_1)$, let I' be the instance obtained from I by adding a new edge wv within f_1. Assume that I' has a zipped-chain or a squashed chain; i.e., I' has a new a, b-chain S with $vw \in S$ such that a zipped-chain of the a, b-chain S and a b, a-chain S' (or a squashed a, b-chain S and an a, b-subpath of f^o_M) surrounds an a, b-component H^*. Then the terminals a and b are on $f^o_{ts}(f_1)$. Moreover*

(i) *When b and a appear in this order from t to s along $f^o_{ts}(f_1)$ (see Fig. 14(c),(e)), $v = s = a$ holds, vertices t, b, w and a appear in this order along $f^o_{ts}(f_1)$ from t to s, and $f^o_{bs}(f_1) = f^o_{sb}(H^*)$.*

(ii) *When a and b appear in this order from t to s along $f^o_{ts}(f_1)$ (see Fig. 14(d),(f)), vertices t, w, a, b and s appear in this order along $f^o_{ts}(f_1)$ from t to s, $f^o_{ba}(f_1) = f^o_{ab}(H^*)$, and instance I has no path Q_2 and no edge vw such that vw is a shift of $v'w$.*

Proof: When I' has a new zipped-chain (S, S'), $\{a, b\}$ is a cut-pair of G_M and (S, S') surrounds an a, b-component H^* of G_M by Lemma 2. Similarly by definition, when I' has a new squashed

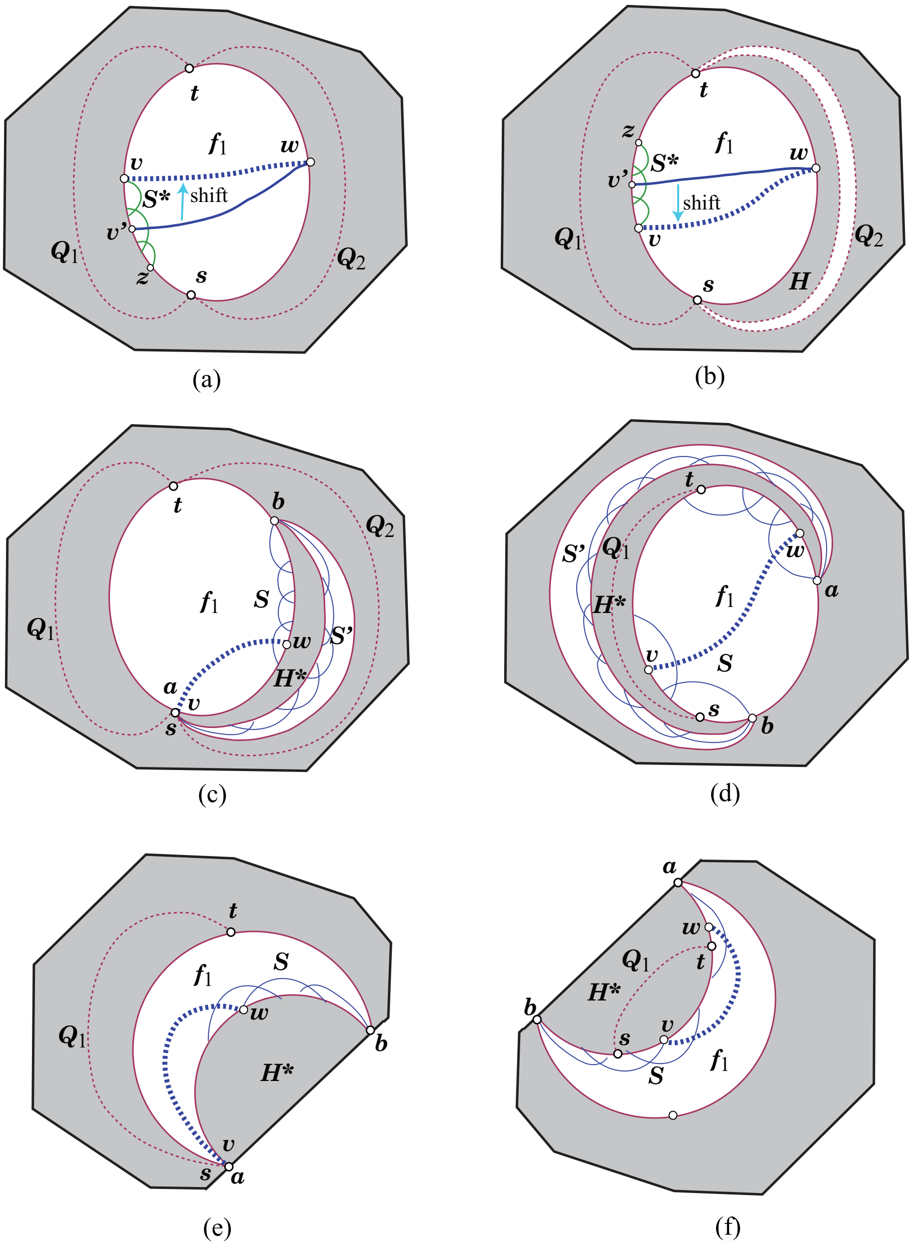

Figure 14: Illustration for two vertices s and t along an inner face $f \in F_M$ such that G_M contains an s,t-path Q_1 or Q_2 disjoint with the facial cycle f except at s and t: **(a)** vw is a shift of edge $v'w$ with a v,z-chain S^*; **(b)** vw is a shift of edge $v'w$ with a z,v-chain S^*, and an s,t-component H next to f implies the existence of path Q_2; **(c)** vertices t, b, w and $v = a = t$ appear in the clockwise order along f_1 for a zipped-chain (S, S') such that the added edge vw; **(d)** vertices t, w, a, b, s and v appear in the clockwise order along f_1 for a zipped-chain (S, S') such that the added edge vw; **(e)** vertices t, b, w and $v = a = t$ appear in the clockwise order along f_1 for a squashed a,b-chain S containing the added edge vw; and **(f)** vertices t, w, a, b, s and v appear in the clockwise order along f_1 for a squashed a,b-chain S containing the added edge vw.

a, b-chain S, $\{a, b\}$ is a cut-pair of G_M and we see that chain S and an s, b-subpath of f^o_M surround an a, b-component H^*.

Since G_M has three internally disjoint s, t-paths (Q and two from f_1) by assumption, the cut-pair $\{a, b\}$ is on $f^o_{ts}(f_1)$ or $f^o_{st}(f_1)$. Since $w \in V(H^*)$ and $w \notin V(f^o_{st}(f_1))$, we see that $\{a, b\}$ must be on $f^o_{ts}(f_1)$. We distinguish two cases.

(i) b and a appear in this order from t to s along $f^o_{ts}(f_1)$ (see Fig. 14(c),(e)): In this case, the b, a-boundary path $f^o_{ba}(f_1)$ of f_1 is the a, b-boundary path of H^* (i.e., $f^o_{bs}(f_1) = f^o_{sb}(H^*)$). Note that this can happen only when v is on $f^o_{ba}(f_1)$ (i.e., $v = s = a$). Since w is also on the the b, a-boundary path, we see that vertices t, b, w and $v = s = a$ appear in this order along $f^o_{ts}(f_1)$.

(ii) a and b appear in this order from t to s along $f^o_{ts}(f_1)$ (see Fig. 14(d),(f)): Now the b, a-boundary path of f is part of $f^o(H^*)$, and hence vertices t, w, a, b and s appear in this order along $f^o_{ts}(f_1)$ from t to s (possibly $w = a$ and $v = s = b$). Note $a \neq t$ by $w \neq s, t$ by assumption. Then H^* contains the b, a-boundary path $f_{b,a}$ of f_1 as its a, b-boundary path (i.e., $f^o_{ba}(f_1) = f^o_{ab}(H^*)$), and this means that G_M cannot have the second type of s, t-path Q_2 (see Fig. 14(b)).

Finally we show that instance I has no edge $v'w$ which is a shift of vw. Assume that vw is a shift of an edge $v'w$ for a z, v-chain S^* along $f^o_{st}(f_1)$. Then we see that $(S - \{vw\}) \cup \{v'w\} \cup S^*$ will be an a, b-chain in I, which together with the b, a-chain S' (or the a, b-subpath of f^o_M) gives a zipped-chain (or a squashed chain), contradicting the assumption that instance I has no zipped-chains. ∎

We call the a, b-component H^* in (i) (resp., (ii)) of the lemma *type I* (resp., *type II*) *bad component* for the vertex pair $\{v, w\}$.

11 Preliminaries for Proving Theorem 10

11.1 Inner Convex Drawings of Triconnected Plane Graphs

A straight-line drawing of a plane embedding is called *inner convex* if every inner facial cycle is drawn as a convex polygon. It is known that a given plane embedding admits an inner convex drawing when it is triconnected or internally triconnected. To establish a reduction for R-nodes for proving Theorem 10, we use the following result, a slight extension of the main result in [13] (Theorem 10).

Theorem 21 *For a plane embedding $\gamma = (F, f^o)$ of a triconnected planar graph $G = (V, E)$, the outer facial cycle f^o is drawn as a star-shaped polygon P^o whose kernel $K(P^o)$ has a positive area. Let K' be a convex region contained in the region $K(P^o)$. Then P^o can be extended to an inner convex drawing D_G of G such that all inner vertices appear strictly inside K'. Such a drawing D_G can be computed in linear time.*

Proof: It is shown [13] (Lemma 7) that G contains a tree T (so-called an "arch-free tree") whose leaf set is equal to the set $V(f^o)$ of the boundary of the plane embedding γ with the following properties:
(i) T can be drawn as a straight-line drawing D_T within in P^o;
(ii) all non-leaf vertices of T are placed strictly inside $K(P^o)$ in D_T; and
(iii) P^o together with D_T forms an inner convex drawing D' with convex inner faces $f_1, \ldots, f_q \in F(D')$, where the subgraph G_i of G enclosed by the boundary of each face f_i admits a convex drawing D_{G_i} as an extension of the convex polygon for f_i.

This implies that a convex drawing D_G of G can be obtained by placing the convex drawing D_{G_i} in each face f_i. In the above argument, we can further restrict an area where non-leaf vertices of T will be located to a sub-region K' of $K(P^o)$ (instead of $K(P^o)$) without affecting the correctness of the proof. Note that all vertices in each G_i automatically appear inside the convex region K' in any convex drawing D_{G_i} of G_i, since otherwise the inner face D_{G_i} containing an outer edge in f^o cannot be convex. ∎

In an inner convex drawing D_G obtained in the theorem, a convex polygon P_f drawn for an inner face f may have a flat corner for some inner vertex on the facial cycle. We can slightly move such vertices so that the corner for each inner vertex along any convex polygon P_f become convex. Formally, as in Section 8, we define $\delta(P)$ to be the minimum of $\min\{|L[p,p']| :$ for every two distinct points p and p' along $P\}$ and $\min\{\delta(p;p',p'') :$ for every three non-co-linear points p, p' and p'' along P $\}$, and set $\epsilon = (1/4)\min\{\delta(P_f) :$ for every polygon P_f in D_G drawn for an inner face $f\}$. Then we see that a straight-line drawing D'_G obtained by changing the position of each vertex v within distance ϵ from that in D_G preserves the convexity of all corners in D_G. We only need to choose new positions of vertices whose corners are flat in D_G so that they become convex corners in D'_G. For each side $S = L[u,v]$ of P_f which contains at least one flat corner in D_G, where u and v are convex corners of P_f, we replace S with a convex link to P_f selecting new positions of the flat corners on S within distance ϵ from their initial positions on S. Summarizing these we have the next result.

Corollary 22 *For a plane embedding $\gamma = (F, f^o)$ of a triconnected planar graph $G = (V,E)$, the outer facial cycle f^o is drawn as a star-shaped polygon P^o whose kernel $K(P^o)$ has a positive area. Let K' be a convex region contained in the region $K(P^o)$. Then P^o can be extended to an inner convex drawing D_G of G such that all inner vertices appear strictly inside K' and no flat corner appears at any inner vertex. Such a drawing D_G can be computed in polynomial time.*

11.2 SPQR decomposition of graphs

We here review a decomposition of a given graph into "triconnected components" and a tree representation for the components.

Triconnected components of a graph $G = (V,E)$ are defined as follows [14]. If G is triconnected, then G itself is the unique triconnected component of G. Otherwise, let $\{u,v\}$ be a cut-pair of G. We split the edges of G into two disjoint subsets E_1 and E_2, such that $|E_1| > 1$, $|E_2| > 1$, and the subgraphs G_1 and G_2 induced by E_1 and E_2 only have vertices u and v in common. Form the graph G'_1 from G_1 by adding an edge (called a *virtual edge*) between u and v that represents the existence of the other subgraph G_2; similarly form G'_2. We continue the splitting process recursively on G'_1 and G'_2. The process stops when each resulting graph reaches one of three forms: a triconnected simple graph, a set of three multiple edges (a triple bond), or a cycle of length three (a triangle). The triconnected components of G are obtained from these resulting graphs: (i) a triconnected simple graph; (ii) a *bond*, formed by merging the triple bonds into a maximal set of multiple edges; and (iii) a *polygon*, formed by merging the triangles into a maximal simple cycle.

One can define a tree structure, sometimes called the *3-block tree*, using triconnected components as follows. The nodes of the 3-block tree are the triconnected components of G. The edges of the 3-block tree are defined by the virtual edges, that is, if two triconnected components have a virtual edge in common, then the nodes that represent the two triconnected components in the 3-block tree are joined by an edge that represents the virtual edge. There are many variants of the 3-block tree in the literature; the first was defined by Tutte [25]. In this paper, we use the terminology of the *SPQR tree*, a data structure with efficient operations defined by di Battista and Tamassia [3].

Each node ν in the SPQR tree is associated with a graph called the *skeleton* of ν, denoted by $\mathrm{skn}(\nu) = (V_\nu, E_\nu)$ $(V_\nu \subseteq V)$, which corresponds to a triconnected component. There are four types of nodes in the SPQR tree. The node types and their skeletons are:

1. Q-node: the skeleton consists of two vertices connected by two edges. Each Q-node corresponds to an edge of the original graph.

2. S-node: the skeleton is a simple cycle with at least three vertices (this corresponds to a polygon triconnected component).

3. P-node: the skeleton consists of two vertices connected by at least three edges (this corresponds to a bond triconnected component).

4. R-node: the skeleton is a triconnected graph with at least four vertices.

The SPQR tree is unique, and can be computed in linear-time [3, 10, 14]. In our case, G is simple, and no Q-nodes appear.

We treat the SPQR tree as a rooted tree $\mathcal{T}$ by choosing a node ν^* as its root. For a node ν, let $\mathrm{Ch}(\nu)$ denote the set of all children of ν, and let η be the parent of ν. The graph $\mathrm{skn}(\eta)$ has exactly one *virtual edge* e in common with $\mathrm{skn}(\nu)$. The edge e is called the *parent virtual edge* $\mathrm{parent}(\nu)$ of $\mathrm{skn}(\nu)$, and a *child virtual edge* of $\mathrm{skn}(\eta)$. Non-virtual edges in $\mathrm{skn}(\nu)$ are called *real edges*, which are some of the edges in G. We define the *parent cut-pair* of ν as the two end vertices of $\mathrm{parent}(\nu)$. We denote the graph formed from $\mathrm{skn}(\nu)$ by deleting its parent virtual edge as $\mathrm{skn}^-(\nu) = (V_\nu, E_\nu^-)$, $E_\nu^- = E_\nu - \{\mathrm{parent}(\nu)\}$. Let $G^-(\nu)$ denote the subgraph of G which consists of the vertices and real edges in the graphs $\mathrm{skn}^-(\mu)$ for all descendants μ of ν, including ν itself. For notational convenience, we let $G^-(\nu)$, $\mathrm{skn}^-(\nu)$ and E_ν^- denote $G(\nu)$, $\mathrm{skn}(\nu)$ and E_ν if ν is the root. By the definition, no S-node (resp., P-node) has a child S-node (resp., child P-node), and no P-node can be a leaf in the SPQR tree.

11.3 Construct SPQR-trees for Frame Graphs $G_M = (V, M)$

We compute the SPQR-tree $\mathcal{T}$ for the biconnected graph $G_M = (V, M)$. In what follows, the SPQR-tree $\mathcal{T}$ always means that for $G_M = (V, M)$ (not for $G = (V, E)$ in an instance I).

Choosing Roots Let $\mathcal{T}$ be the SPQR tree of $G_M = (V, M)$. We distinguish two case: (i) The outer facial cycle $f^o(\psi)$ contains two vertices $u, v \in V(f^o(\psi))$ such that $\{u, v\}$ is a cut-pair of the biconnected spanning graph $G_M = (V, M)$; and (ii) Otherwise.

In (i), there is a P-node ν whose skeleton consists of multiple edges uv. We choose such a cut-pair $\{u, v\}$ so that u and v are as close as possible on $f^o(\psi)$ (hence no other outer vertex a (resp., b) appears on the u, v-boundary path (resp., v, u-boundary path) such that $\{u, a\}$ (resp, $\{v, b\}$) is a cut-pair). Then we choose the P-node for such a cut-pair $\{u, v\}$ as the root ν^* of the SPQR tree $\mathcal{T}$. In (ii), there is an R-node ν such that both $f^o(\mathrm{skn}(\nu))$ and $f^o(G(\nu))$ consists of the same set of crossing-free edges in M, and we designate such an R-node as the root ν^* of $\mathcal{T}$.

Lemma 23 *Let $I = (G = (V, E), M, F_M, f_M^o, \alpha)$ be a standard instance. For an S-node ν in the rooted SPQR tree of G_M, denote $st = \mathrm{parent}(\nu)$. Then G_M contains three internally disjoint s, t-paths, each from the subgraphs $H = G^-(\nu)$, $\mathrm{face}^{st}(H) - (V(H) - \{s, t\})$ and $\mathrm{face}^{st}(H) - (V(H) - \{s, t\})$, respectively.*

Proof: By the choice of the root ν^* of $\mathcal{T}$, any S-node is a non-root node in $\mathcal{T}$. Clearly $G_M - (V(H) - \{s, t\})$ contains two internally disjoint s, t-paths when the parent of ν is an R-node or a non-root P-node. When the parent of ν is the root P-node ν^*, we see that each vertex in $V(\mathrm{skn}(\nu)) - \{s, t\}$ is an inner vertex in the plane embedding of G_M by the choice of the cut-pair $\{s, t\}$ on the outer boundary $f^o(\eta)$ for the root P-node ν^*, and thereby $G_M - (V(H) - \{s, t\})$ contains two internally disjoint s, t-paths. Hence G_M contains three internally disjoint s, t-paths in $H = G^-(\nu)$, $\mathrm{face}^{ts}(H) - (V(H) - \{s, t\})$ and $\mathrm{face}^{st}(H) - (V(H) - \{s, t\})$. ∎

11.4 Detecting Forbidden Configurations

W here examine the structure of P-, R- and S-nodes for standard instances, which provides how to detect whether a given instance contains zipped-chains or squashed chains.

Structure of R-nodes

Lemma 24 *Let $I = (G = (V, E), M, F_M, f_M^o, \alpha)$ be a standard instance. For a non-root R-node ν in the SPQR tree of G_M, let $H = G^-(\nu)$ and $st = \mathrm{parent}(\nu)$. Then:*
(i) *If H is not exposed along $f_{ts}^o(H)$ and along $f_{st}^o(H)$, then there is a zipped-chain or a squashed chain; and*
(ii) *Assume that the parent node of ν is an R- or S-node, and that $f^{\mathrm{left}} = \mathrm{face}^{st}(H) \in F_M$ and $f^{\mathrm{right}} = \mathrm{face}^{ts}(H) \in F_M$ are inner faces. If H is exposed along both $f_{ts}^o(H)$ and $f_{st}^o(H)$ and instance I has no edge st, then adding a new edge st within f^{left} or f^{right} does not create a zipped-chain or a squashed chain.*

Proof: (i) We see that there is a zipped-chain (S, S') of an s,t-chain S and a t,s-chain S' or a squashed s,t- or t,s-chain S (possibly S or S' consists of a single edge st).

(ii) We apply Lemma 19 to cut-pairs $\{s,t\}$ and inner faces $f^{\text{left}}, f^{\text{right}} = \text{face}^{ts}(H) \in F_M$. Since the parent of ν is now an R- or S-node, G_M has no other s,t-component H' other than H and its complement. Hence no st- or t,s-chain stated in the lemma exists in I, and adding edge st within f^{left} or f^{right} creates no zipped-chain. Assume that adding a new edge st within f^{right} creates a squashed a,b-chain S (otherwise we are done). By Lemma 18(ii), the terminals a and b of the chain S gives a cut-pair that appears along f^{left} and the b,a-path P_{ba} obtained from the boundary of P_{out} from b to a in the clockwise order. Note that path P_{ba} and chain S surround f^{left} or f^{left} is the outer face f^o_M. By assumption, f^{left} is an inner face in F_M. If adding a new edge st within f^{left} creates another squashed a',b'-chain S', then by Lemma 18(ii), the b',a'-path $P_{b'a'}$ obtained from the boundary of P_{out} from b' to a' in the clockwise order must be a line segment. However, this is impossible because a and b' appear on $L[b,a]$ in this order from b to a, since f^{left} is surrounded by P_{ba} and S. Therefore, adding st to f^{left} or f^{right} does not create a squashed chain. ∎

Structure of S-nodes For an S-node ν with $st = \text{parent}(\nu)$ and $H = G^-(\nu)$, we denote $f^{\text{left}} = \text{face}^{st}(H) \in F_M$ and $f^{\text{right}} = \text{face}^{ts}(H) \in F_M$. Also denote the s,t-path $\text{skn}^-(\nu)$ by $(v_0 = s, v_1, \ldots, v_k, v_{k+1} = t)$, and for each virtual edge $e_i = v_i v_{i+1}$, let $\mu_i \in \text{Ch}(\nu)$ denote the child node corresponding to e_i and H_i denote $G^-(\mu_i)$; for each real edge $e_i = v_i v_{i+1}$, let H_i denote the graph consisting of the real edge e_i. For two indices $i < j$, let $H(i,j)$ denote the union of subgraphs $H_i, H_{i+1}, \ldots, H_j$, which is a v_i, v_{j+1}-component of G_M.

Lemma 25 *Let $I = (G = (V,E), M, F_M, f^o_M, \alpha)$ be a standard instance. For an S-node ν in the rooted SPQR tree of G_M, denote $st = \text{parent}(\nu)$ and $\text{skn}^-(\nu) = (v_0 = s, v_1, \ldots, v_k, v_{k+1} = t)$. Then:*
(i) *If there are indices $0 \le i < j \le k+1$ such that $H(i,j)$ is not exposed along $f^o_{v_{j+1}v_i}(H(i,j))$ and along $f^o_{v_i v_{j+1}}(H(i,j))$, then instance I contains a zipped-chain or a squashed chain.*
(ii) *Assume that the parent node of ν is an R- or S-node, and that $f^{\text{left}} = \text{face}^{st}(H) \in F_M$ and $f^{\text{right}} = \text{face}^{ts}(H) \in F_M$ are inner faces. If H is exposed along both $f^o_{ts}(H)$ and $f^o_{st}(H)$ and instance I has no edge st, then adding a new edge st within f^{left} or f^{right} does not create a zipped-chain or a squashed chain.*

Proof: (i) We see that there is a zipped-chain (S, S') of an s,t-chain S and a t,s-chain S' or a squashed s,t- or t,s-chain S (possibly S or S' consists of a single edge st).

(ii) Analogously with Lemma 24(ii). ∎

Structure of P-nodes For each P-node ν with $\{s,t\} = V(\text{skn}(\nu))$, we always index the virtual edges in $\text{skn}^-(\nu)$ as $e_1, e_2, \ldots, e_k$ by traversing these edges from left to right, placing s on the bottom level and t on the top level, as shown Fig. 15(a). The child node in $\text{Ch}(\nu)$ corresponding to the virtual edge e_i is denoted by μ_i. Possibly, $f^o_{ts}(G^-(\mu_1))$ or $f^o_{st}(G^-(\mu_k))$ is a subpath of the outer boundary f^o_M. When ν is the root of $\mathcal{T}$, it holds $\text{skn}^-(\nu) = \text{skn}(\nu)$ and $f^o(\psi)$ consists of the boundary paths $f^o_{ts}(G^-(\mu_1))$ and $f^o_{st}(G^-(\mu_k))$.

Lemma 26 *Let $I = (G = (V,E), M, F_M, f^o_M, \alpha)$ be a standard instance with a prescribed convex polygon P_{out}. For a P-node ν, let $V(\text{skn}(\nu)) = \{s,t\}$ and let $e_1, e_2, \ldots, e_k$ denote the virtual edges in $\text{skn}(\nu)$. Then there is a zipped-chain or a squashed chain if there are indices $1 \le i < j \le k$ that satisfy one of the following* (i)-(iii)*:*
(i) *$G^-(\mu_i)$ is not exposed along $f^o_{ts}(G^-(\mu_i))$ and $G^-(\mu_j)$ is not exposed along $f^o_{st}(G^-(\mu_j))$;*
(ii) *$G^-(\mu_i)$ is not exposed along $f^o_{ts}(G^-(\mu_i))$, and a real edge $st \in E$ is assigned in the face f between $G^-(\mu_{j-1})$ and $G^-(\mu_j)$ (where $f = \text{face}^{ts}(G^-(\mu_j))$); and*
(iii) *$G^-(\mu_j)$ is not exposed along $f^o_{ts}(G^-(\mu_j))$, and a real edge $st \in E$ is assigned in the face f between $G^-(\mu_i)$ and $G^-(\mu_{i+1})$.*

Proof: In any of (i)-(iii), there is a zipped-chain (S, S') of an s,t-chain S and a t,s-chain S' or a squashed s,t- or t,s-chain S (possibly S or S' consists of a single edge st). ∎

For each P-node ν, we choose the following index j^* ($1 \leq j^* \leq k$) such that $G^-(\mu_i)$ ($i \leq j^*$) is exposed along $f^o_{ts}(G^-(\mu_i))$; $G^-(\mu_i)$ ($i > j^*$) is exposed along $f^o_{st}(G^-(\mu_j))$; and if $st \in E$ (possibly $st \in M$), then st is assigned to the face f between $G^-(\mu_{j^*})$ and $G^-(\mu_{j^*+1})$. If there is no such j^*, then the frame has a forbidden configuration by Lemma 26. We call the virtual edges e_i with $i \leq j^*$ (resp., $i > j^*$) the *left edges* (resp., *right edges*) in the skeleton $\mathrm{skn}^-(\nu)$.

Lemma 27 *Let $I = (G = (V, E), M, F_M, f^o_M, \alpha)$ be a standard instance with a prescribed convex polygon P_{out}. For a P-node ν, let $V(\mathrm{skn}(\nu)) = \{s, t\}$, and let $e_1, e_2, \ldots, e_{j^*}$ and $e_{j^*+1}, e_{j^*+2}, \ldots, e_k$ denote the left edges and the right edges in $\mathrm{skn}(\nu)$, respectively. If $st \notin E$, none of $G^-(\mu_1)$ and $G^-(\mu_k)$ is a subpath of P_{out}, and $1 \leq j^* < k$, then adding a new edge st within the face f between $G^-(\mu_{j^*})$ and $G^-(\mu_{j^*+1})$ does not create a zipped-chain or a squashed chain.*

Proof: By $1 \leq j^* < k$ and the assumption on $G^-(\mu_1)$ and $G^-(\mu_k)$, we see that G_M contains two s,t-paths Q_1 and Q_2 such that the cycle formed by Q_1 and Q_2 encloses the region f and each of Q_1 and Q_2 is disjoint with the facial cycle f except at s and t. We apply Lemma 18 to f and a new edge $st = uv$. Then for any a,b-chain S in a zipped-chain or a squashed chain created by adding a new edge st within the region f, it must hold $a = t$ and $s = b$ in the lemma due to the existence of the two s,t-paths Q_1 and Q_2. However, in this case, the a,b-component H would give an s,t-chain outside the region f or an s,t-subpath of P_{out} having no convex corners on it. The former contradicts the choice of j^*, since $G^-(\mu_j)$ for each left edge e_j is exposed along its left side $f^o_{st}(G^-(\mu_j))$. The latter contradicts the assumption that none of $G^-(\mu_1)$ and $G^-(\mu_k)$ is a subpath of P_{out}. Therefore, adding a new edge st within the face f does not a zipped-chain or a squashed chain. ∎

In what follows, we assume that for any P-node ν with $st = \mathrm{parent}(\nu)$ satisfying the condition of Lemma 27, an edge st is added to $E - M$ within the face f between $G^-(\mu_{j^*})$ and $G^-(\mu_{j^*+1})$.

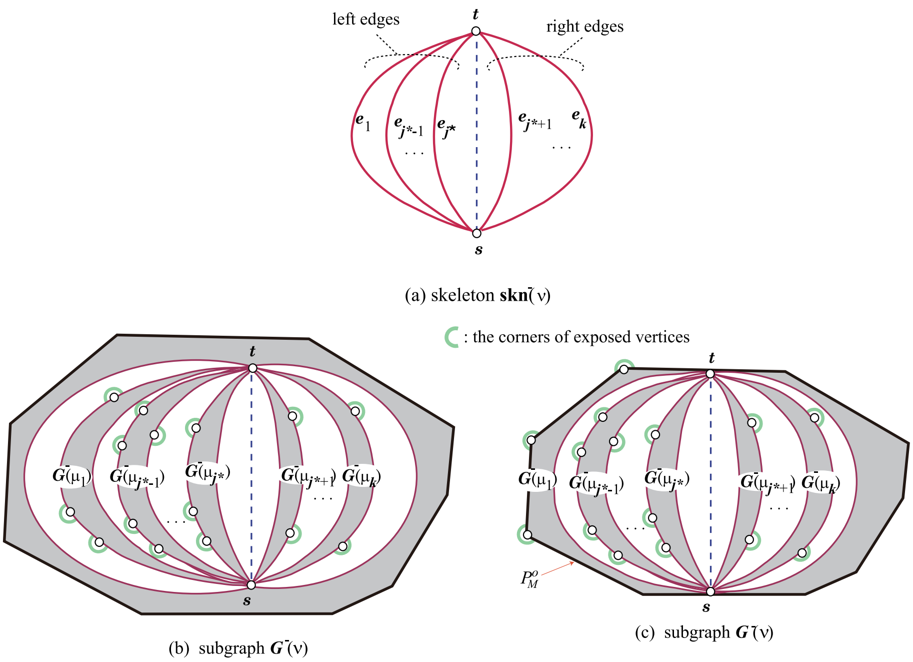

Figure 15: **(a)** A plane embedding of skeleton $\mathrm{skn}^-(\nu)$ of a P-node ν, where the virtual edges are categorized into left edges and right edges; **(b)** The subgraphs $G^-(\mu_i)$ of child-nodes $\mu_i \in \mathrm{Ch}(\nu)$ such that no virtual edge in $\mathrm{skn}^-(\nu)$ is an outer edge; and **(c)** The subgraphs $G^-(\mu_i)$ of child-nodes $\mu_i \in \mathrm{Ch}(\nu)$ such that the leftmost virtual edge in $\mathrm{skn}^-(\nu)$ is an outer edge.

Since any zipped-chain appears around a u,v-component H of G_M by Lemma 2, we see that any zipped-chain in a given standard instance I appears as one of the zipped-chains in Lemma 24(i), Lemma 25(i) and Lemma 26. Similarly any squashed chain in I appears as one of those in these lemmas. Hence we can detect any zipped-chains or squashed chains in a given instance I in polynomial time. In what follows, we assume that a given standard instance has no zipped-chains or squashed chains.

12 Reduction for P-nodes

In this section, we assume that the rooted SPQR tree $\mathcal{T}$ of a given standard instance I has a non-reduced P-node ν whose child-nodes are all reduced S-nodes, and give a reduction procedure that converts such a standard instance I into a standard instance I' with a smaller number of edges in M.

For a non-reduced P-node ν whose child-nodes are all reduced S-nodes, let $\{s,t\} = V(\mathrm{skn}(\nu))$, $e_1, e_2, \dots, e_k$ be the virtual edges in $\mathrm{skn}^-(\nu)$, and $\mu_i \in \mathrm{Ch}(\nu)$ denote the child S-node corresponding to e_i, where $e_1, e_2, \dots, e_{j^*}$ are the left edges and $e_{j^*+1}, \dots, e_k$ are the right edges. Recall that for each left edge e_i, the graph $G^-(\mu_i)$ is fully exposed along its left side $f^o_{st}(G^-(\mu_i))$ while it has a convex-support along its right side $f^o_{ts}(G^-(\mu_i))$. Symmetrically for each right edge e_i, the graph $G^-(\mu_i)$ is fully exposed along $f^o_{ts}(G^-(\mu_i))$ and has a convex-support along $f^o_{st}(G^-(\mu_i))$. We distinguish two cases:
1. $G^-(\mu_1)$ or $G^-(\mu_k)$ is a subpath of the prescribed polygon P_{out}; and
2. Neither of $G^-(\mu_1)$ and $G^-(\mu_k)$ is a subpath of the prescribed polygon P_{out}.

Case 1. $G^-(\mu_1)$ or $G^-(\mu_k)$, say $G^-(\mu_1)$ is a subpath of P_{out}. Since ν is not a reduced P-node yet, skeleton $\mathrm{skn}^-(\nu)$ contains the second virtual edge e_2, which is a left edge or a right edge in $\mathrm{skn}^-(\nu)$ (i.e., $j^* \geq 2$ or $j^* = 1$). We denote the s,t-path $G^-(\mu_2)$ by $(v_0 = s, v_1, v_2, \dots, v_k, v_{k+1} = t)$ and the s,t-path $G^-(\mu_1)$ by $(u_0 = s, u_1, u_2, \dots, u_\ell, u_{\ell+1} = t)$, where each u_i is an outer vertex and its position is now fixed on P_{out}. Let $f^{\mathrm{right}} = \mathrm{face}^{ts}(G^-(\mu_2)) \in F_M$. See Fig. 16(a) and (b).

Case 1a. e_2 is a left edge (see Fig. 16(a)): In this case, we convert I into a standard instance I' as follows.

Reduction

1. Let T be the triangle enclosed by three segments $L[s,u_\ell]$, $L[t,u_1]$ and $L[s,t]$. Realize the s,t-path $G^-(\mu_2)$ as a convex link within T to form a pseudo-convex polygon $P_{1,2}$ for $(s, u_1, u_2, \dots, u_\ell, t, v_k, v_{k-1}, \dots, v_1)$ such that any two vertices u_i in $G^-(\mu_1)$ and v_j in $G^-(\mu_2)$ are M-visible (see Fig. 16(b));
2. Modify the outer polygon P_{out} into P'_{out} by replacing $G^-(\mu_1)$ with the above fixed path $G^-(\mu_2)$, where the edges in $E - M$ that are incident to a vertex u_i in $G^-(\mu_1)$ are also removed. Let I' be the resulting instance.

Since each vertex v_j in $G^-(\mu_2)$ is realized as a convex corner along P'_{out}, no new squashed chain is created. By induction hypothesis on the size of M, I' admits an FSL-drawing D', as shown in Fig. 16(c).

Construction of Drawing
We easily see that D' can be extended to an FSL-drawing D of I by drawing the removed edges in $E - M$ within the pseudo-convex polygon $(s, u_1, u_2, \dots, u_\ell, t, v_k, v_{k-1}, \dots, v_1)$. The resulting drawing D is an FSL-drawing of I.

Case 1b. e_2 is a right edge (see Fig. 16(d)): Possibly the vertices in $G^-(\mu_1) - \{s,t\}$ are realized as flat corners along P'_{out}. In this case, we convert I into a standard instance I' as follows.
Reduction

1. Place the vertices in $G^-(\mu_2)$ along segment $L[s,t]$;

2. Modify the outer polygon $P_{\rm out}$ into $P'_{\rm out}$ by replacing $G^-(\mu_1)$ with the above fixed path $G^-(\mu_2)$, where the edges in $E - M$ that are incident to a vertex u_i in $G^-(\mu_1)$ are also removed. Let I' be the resulting instance, as illustrated in Fig. 16(e).

Although each vertex v_j in $G^-(\mu_2)$ is realized as a flat corner along $P'_{\rm out}$, no new squashed chain is created, since $G^-(\mu_2)$ is fully exposed along $f^o_{ts}(G^-(\mu_2))$ and no edge assigned within $f^{\rm right}$ joins two vertices v_i and v_j ($\{i, j\} \neq \{0, k+1\}$). By induction hypothesis on the size of M, I' admits an FSL-drawing D', as shown in Fig. 16(f).

Construction of Drawing
We now show that D' can be extended to an FSL-drawing D of I. For each vertex v_i in $G^-(\mu_2)$, let W_i denote the set of vertices w on the t,s-boundary $f^{\rm right}_{ts}$ of the facial cycle $f^{\rm right}$ such that there is an edge $wv_i \in E-M$. For each vertex $w \in W_i$ ($1 \leq i \leq k$), we define ${\rm cone}_w$ to be the set of half-lines L starting from w that do not intersect any segment in D' except segment $L[s, t]$. We call the intersection K_i of ${\rm cone}_w$ over all $w \in W_i$ and the convex polygon $P'_{\rm out}$, the *kernel* for the vertex v_i in $G^-(\mu_2)$. Clearly, K_i contains the point for v_i in D'. We see that K_i has a positive area, since each $w \in W_i$ has segment $L[w, v_i]$ which are separate apart with some positive distance from any edges in M except at w and v_i. We next move the position of each vertex v_i ($1 \leq i \leq k$) in $G^-(\mu_2)$ within the interior of K_i so that $G^-(\mu_1)$ and $G^-(\mu_2)$ form a convex polygon, as shown in Fig. 16(g). This is possible because each K_i contains the current position for v_i and has a positive area. Let D' be the resulting drawing for I. Note that the new position for each v_i in K_i is M-visible from any vertices $w \in W_i$. Hence D is a correct FSL-drawing of I.

Case 2. Neither of $G^-(\mu_1)$ and $G^-(\mu_k)$ is a subpath of the prescribed polygon $P_{\rm out}$. Since ν is not reduced, it has at least three virtual edges in ${\rm skn}^-(\nu)$, where $e_1, e_2, \ldots, e_{j^*}$ are the left edges and $e_{j^*+1}, \ldots, e_k$ are the right edges. Without loss of generality that the number of left edges is not less than that of right ones, where e_1 and e_2 are left edges and e_3 is a left or right edge. We denote the s,t-path $G^-(\mu_1)$ by $(u_0 = s, u_1, u_2, \ldots, u_\ell, u_{\ell+1} = t)$. the s,t-path $G^-(\mu_2)$ by $(v_0 = s, v_1, v_2, \ldots, v_k, v_{k+1} = t)$, and the s,t-path $G^-(\mu_3)$ by $(w_0 = s, w_1, w_2, \ldots, w_h, w_{h+1} = t)$. See Fig. 17(a) and (c).

Reduction
Let $X = V(G^-(\mu_2)) - \{s, t\}$. Remove the vertices in X and the edges in $E(X)$ from I, and let I' be the resulting instance.

Since I' is obtained from I by simply removing vertices/edges, I' has no new zipped-chains. By induction hypothesis on the size of M, I' admits an FSL-drawing D', as shown in See Fig. 17(b) and (d).

Construction of Drawing
We now show that D' can be extended to an FSL-drawing D of I. Recall that $G^-(\mu_1) = (s, u_1, \ldots, u_\ell, t)$ has a convex-support on its right side in I, and D' contains segments $L[s, u_\ell]$ and $L[t, u_1]$ for edges su_ℓ and tu_1. Currently the polygon for the cycle $(s, u_1, u_2, \ldots, u_\ell, u, t, w_h, w_{h-1}, \ldots, w_1)$ of $G^-(\mu_1)$ and $G^-(\mu_3)$ is a convex polygon $P_{1,3}$ (resp., pseudo-convex polygon) when $j^* = 2$ (resp., $j^* \geq 3$). Let K be the intersection of the kernel $K(P_{1,3})$ of the polygon $P_{1,3}$ and the convex polygon $(s, u_1, u_2, \ldots, u_\ell, t)$ for $G^-(\mu_1)$. We place the vertices in $G^-(\mu_1) - \{s, t\}$ within the interior of K so that $G^-(\mu_1)$ and $G^-(\mu_2)$ form a pseudo-convex polygon, as shown in Fig. 16(b) and (d). Let D' be the resulting drawing for I. Note that each vertex v_i in $G^-(\mu_2)$ is M-visible from any vertices $G^-(\mu_1)$ and $G^-(\mu_3)$ since it is placed inside K. Hence D is a correct FSL-drawing of I.

13 Cactus Instances

We are given a non-root S-node ν in a standard instance I such that every child node of ν is a reduced P- or S-nodes. Hence the subgraph $G^-(\nu)$ is a concatenation of paths/cycles. Our aim is to reduce such an S-node ν to a reduced S-node, i.e., to replace the subgraph $G[V(H)]$ induced by the vertex set of $H = G^-(\nu)$ with a single path with a convex-support in a given embedding of I.

Before we establish an entire reduction, we in this section focus on how to construct a straight-line drawing for the induced subgraph $G[V(H)]$, ignoring the rest of the graph $G-V(H)$. However, finding a straight-line drawing of $G[V(H)]$ is not trivial, because $G[V(H)]$ may have some crossing edges in $E-M$ that join two vertices in H. We also introduce a way of controlling the area for a drawing D_H of $G[V(H)]$ so that we can plug the drawing D_H in an FSL-drawing of a reduced instance I'.

In what follows, we formulate a "cactus instance" which represents the structure of the induced graphs $G[V(H)]$ for $H = G^-(\nu)$, where we will ignore any edges in $E - E(H)$ joining two vertices in the same cycle in $H = G^-(\nu)$ and we instead impose a constraint on the shape of a polygon drawn for each cycle $H = G^-(\nu)$. In the rest of section, we design a procedure for constructing a straight-line drawing of cactus instances.

We call a cactus a *line-cactus* if it consists of q (≥ 0) cycles

$$Q_i = (s_{i-1}, v_{i,1}, v_{i,2}, \ldots, v_{i,k_i}, s_i, v'_{i,k'_i}, v'_{i,k'_i-1}, \ldots, v'_{i,1}),\ i = 1, 2, \ldots, q$$

such that Q_i and Q_{i+1} share a vertex s_i ($1 \leq i < q$), where vertices $s_{i-1}, v_{i,1}, v_{i,2}, \ldots, v_{i,k_i}, s_i, v'_{i,k'_i}, v'_{i,k'_i-1}, \ldots, v'_{i,1}$ appear in this order when we traverse Q_i in clockwise order. Possibly $k_i = 0$ or $k'_i = 0$, i.e., Q_i is an $s_{i-1}s_i$-path (Q_i is a single edge when $k_i = k'_i = 0$). See Fig. 18(a). We call vertices $v_{i,j}$ (resp., $v'_{i,j}$) in some Q_i *left vertices* (resp., *right vertices*) whereas we call vertices

$$s_0, s_1, \ldots, s_q$$

joint vertices. When $q = 0$, the above line-cactus is a single vertex. We call s_0 and s_q the terminal of the line-cactus, and call a line-cactus with terminals s and t an *s,t-cactus*.

Formally a *cactus instance* (G, γ, M) is defined to be a tuple of a graph $G = (V, E)$, an embedding γ of G [1], an s,t-cactus $G_M = (V, M) = (Q_1, Q_2, \ldots, Q_q)$ of crossing-free edges that spans G, and such that

(i) the terminal s and t of (V, M) are on the boundary of γ;
(ii) no edge $E - M$ joins two vertices in the same cycle Q_i (except edge $s_{i-1}s_i \in E - M$); and
(iii) no edge in $E - M$ joins a left vertex in Q_i and a right vertex in Q_j for any i, j.

For two distinct vertices $u, u' \in V^o_{st}(G_M)$ (resp., $u, u' \in V^o_{ts}(G_M)$), we denote $u \prec u'$ if u' appears after u when we traverse $f^o_{st}(G_M)$ (resp., $f^o_{ts}(G_M)$) from s to t (i.e., u' is closer to t than u), and denote $u \preceq u'$ if $u \prec u'$ or $u = u'$. Every edge $uu' \in E - M$ and the boundary of M enclose a new region $R_{uu'}$ (not the one inside some cycle Q_i). We call edge $uu' \in E - M$ ($u \preceq u'$) a *left edge* if u' appears immediately after u along the boundary $R_{uu'}$ in the clockwise order; otherwise it is called a *right edge*. Let E^{right} and E^{left} denote the set of right and left edges in $E - M$, respectively. No left edge is incident to any right vertex. Similarly for right edges.

Polygon constraint We assume that each cycle Q_i is one of *central*, *left* and *right types*, which specify the shape of polygon P_i drawn for Q_i as follows:

- Each central type cycle Q_i is required to be drawn as a convex polygon P_i (where a single edge Q_i is always of central type);
- Each right type cycle Q_i has edge $s_{i-1}s_i \in E^{\text{left}}$, and Q_i is required to be drawn as a pseudo-convex polygon P_i that consists of a concave link $(s_{i-1}, v_{i,1}, v_{i,2}, \ldots, v_{i,k_i}, s_i)$ and a convex link $(s_{i+1}, v'_{i,k'_i}, v'_{i,k'_i-1}, \ldots, v'_{i,1})$; and
- Each left type cycle Q_i has edge $s_{i-1}s_i \in E^{\text{right}}$, and Q_i is required to be drawn as a pseudo-convex polygon P_i that consists of a convex link $(s_{i-1}, v_{i,1}, v_{i,2}, \ldots, v_{i,k_i}, s_i)$ and a concave link $(s_{i+1}, v'_{i,k'_i}, v'_{i,k'_i-1}, \ldots, v'_{i,1})$.

In that follows, for a straight-line (or a segment) L in the xy-plane not parallel to the y-axis, let $\lambda_L(x)$ denote a function that outputs the y-coordinate of the point on L with the x-coordinate x (i.e., point $(x, \lambda_L(x))$ is on L).

[1] Graph G and set M here are now reset for cactus instances in this section, not necessarily the same ones from which a particular S-node ν is taken.

We assume that the x-coordinates of all vertices $v \in V$ are predetermined to be values $a(v)$ such that

$$a(s_{i-1}) < a(v_{i,1}) < a(v_{i,2}) < \cdots < a(v_{i,k_i}) < a(s_i)$$

and

$$a(s_{i-1}) < a(v'_{i,1}) < a(v'_{i,2}) < \cdots < a(v'_{i,k'_i}) < a(s_i)$$

(possibly $a(v_{i,h}) = a(v'_{i,\ell})$ for some h and ℓ) for all $i = 1, 2, \ldots, q$. Hence $a(s_0) < a(s_1) < \cdots < a(s_q)$. For the terminals s_0 and s_q, their permanent y-coordinates are also predetermined to be some values:

$$y(s_0) = b_0^* \text{ and } y(s_q) = b_q^*.$$

The other non-terminal vertices $v \in V - \{s_0, s_q\}$ are temporarily placed on the segment $L[s_0, s_q] = L[(a(s_0), b_0^*), (a(s_q), b_q^*)]$; i.e., the temporary y-coordinate $y(v)$ of them is

$$\lambda_{L[s_0,s_q]}(a(v)).$$

See Fig. 18(b).

We wish to determine a (permanent) value $b^*(v)$ for the y-coordinate of each non-terminal $v \in V - \{s_0, s_q\}$ so that they give an FSL-drawing of a cactus instance with a polygon constraint (possibly after computing temporary values for the y-coordinate of them several times). We here introduce another constraint in order to control the drawing area for a final FSL-drawing.

Band constraint We are given a positive $\epsilon > 0$ such that a permanent value $b^*(v)$ for the y-coordinate of each non-terminal $v \in V - \{s_0, s_q\}$ is required to be chosen from

$$[\lambda_{L[s_0,s_q]}(a(v)) - \epsilon, \lambda_{L[s_0,s_q]}(a(v)) + \epsilon],$$

i.e., a final position of v is within distance ϵ from the initial position $(a(v), \lambda_{L[s_0,s_q]}(a(v)))$.

Our task is to find an FSL-drawing which satisfies the polygon and band constraints by selecting appropriate y-coordinates $y(v)$ for all non-terminal vertices $v \in V - \{s_0, s_q\}$. The problem is described as follows.

Input: A cactus instance $I = (G = (V, E), \gamma, (V, M) = (Q_1, Q_2, \ldots, Q_q), b_0^*, b_q^*, \epsilon)$ with cycles Q_i of type of central/left/right; permanent x-coordinates $x(v) = a(v)$ of $v \in V$; permanent y-coordinates $y(s_0) = b_0^*$ and $y(s_q) = b_q^*$; and a band parameter $\epsilon > 0$, where we call segment $L[s_0, s_q] = L[(a(s_0), b_0^*), (a(s_q), b_q^*)]$ the *guideline* of I.
Output: A set of y-coordinates $b^*(v)$ of non-terminal vertices $v \in V - \{s_0, s_q\}$ which satisfies the band constraint: $|b^*(v) - \lambda_{L[s_0,s_q]}(a(v))| < \epsilon$ for all $v \in V - \{s_0, s_q\}$, and gives an FSL-drawing $D = \{(a(v), b^*(v)) : v \in V\}$ of γ satisfying the constraint on polygon P_i for each Q_i.

We construct such an FSL-drawing of a cactus instance I by a divide-and-conquer procedure, where we divide the instance into two subinstances I_1 and I_2 and combine FSL-drawings of them into an FSL-drawing for I. More formally, we choose a joint vertex s_{j-1} (or a cycle Q_j) adequately and fix the y-coordinate of s_{j-1} (or the vertices in Q_j) permanently. For the newly determined permanent y-coordinate b_{j-1}^* of s_{j-1} (or b_v^* and b_j^* of s_{j-1} and s_j), we generate two subinstances

$$I_1 = (G_1, \gamma_1, (Q_1, Q_2, \ldots, Q_{j-1}), b_0^*, b_{j-1}^*, \epsilon') \text{ and}$$

$$I_2 = (G_2, \gamma_2, (Q_j, Q_{j+1}, \ldots, Q_q), b_{j-1}^*, b_q^*, \epsilon')$$

(or $I_2 = (G_2, \gamma_2, (Q_{j+1}, Q_{j+2}, \ldots, Q_q), b_j^*, b_q^*, \epsilon')$), where (G_1, γ_1) and (G_2, γ_2) are the subgraphs and sub-embeddings induced from (G, γ) by $(Q_1, Q_2, \ldots, Q_{j-1})$ and $(Q_{j'}, Q_{j'+1}, \ldots, Q_q)$ ($j' = j$ or $j + 1$), respectively.

In the following, we show how to choose s_{j-1} (or choose/fix cycle Q_j) and $\epsilon'(< \epsilon/4)$ so that arbitrary FSL-drawings D_1 and D_2 for I_1 and I_2 will constitute an FSL-drawing D for I.

We say that an edge $uu' \in E^{\text{left}}$ with $u \prec u'$ *covers* a left or joint vertex v if $u \prec v \prec u'$. If no edge in E^{left} covers a left or joint vertex v, then v is called *exposed* on its *left* side. Note that all left vertices of each right type cycle Q_i are covered by edge $s_{i-1}s_i \in E^{\rm left}$. Symmetrically define edges in $E^{\rm right}$ covering right/joint vertices and right/joint vertices exposed on their right side.

In a straight-line drawing of γ, an edge $uu' \in E - M$ is called *M-visible* if the segment $L[u, u']$ does not intersect the segment of any edge $e \in M$ (except at the end-points u and u'). Thus, if all edges in $E - M$ are M-visible, then the current drawing is an FSL-drawing of γ.

If there is no vertex in $V - \{s_0, s_q\}$ which is exposed on its left or right side, then the current embedding γ would be a zipped-chain with terminals s_0 and s_q. Then there is a vertex v^* in $V - \{s_0, s_q\}$ which is exposed on its left or right side. Without loss of generality that v^* is a joint or left vertex which is exposed on its left side. Hence v^* is a joint vertex s_{j-1} $(2 \le j \le q)$ or a left vertex in a cycle Q_j, where Q_j is of central or left type.

When $q = 0$, we easily see that I has a desired FSL-drawing, the current point for the single vertex $(s_0 = s_q)$ in the instance. Assume that $q \ge 1$. We distinguish three cases:
Case 1. $v^* = s_{j-1}$ for some $2 \le j \le q$;
Case 2. $v^* = v_{j,h} \in V(Q_j)$ for some $1 \le j \le q$ and $1 \le h \le k_i$, and Q_j is of central type; and
Case 3. $v^* = v_{j,h} \in V(Q_j)$ for some $1 \le j \le q$ and $1 \le h \le k_i$, and Q_j is of left type.

Case 1. $v^* = s_{j-1}$ for some $2 \le j \le q$: In this case, we determine a permanent y-coordinate $y(s_{j-1})$ of vertex s_{j-1} to be

$$b^*_{j-1} = \lambda_{L[s_0,s_q]}(a(s_{j-1})) + \epsilon/2.$$

Then we generate two instances $I_1 = (G_1 = (V_1, E_1), \gamma_1, (V_1, M_1) = (Q_1, Q_2, \ldots, Q_{j-1}), b^*_0, b^*_{j-1}, \epsilon')$ and $I_2 = (G_2 = (V_2, E_2), \gamma_2, (V_2, M_2) = (Q_j, Q_{j+1}, \ldots, Q_q), b^*_{j-1}, b^*_q, \epsilon')$, where $V_1 = V(Q_1) \cup V(Q_2) \cup \cdots \cup V(Q_{j-1})$, $V_2 = V(Q_j) \cup V(Q_{j+1}) \cup \cdots \cup V(Q_q)$ and E_i and M_i are the sets of edges induced from E and M by the vertices in V_i, respectively.

Now we place vertices in $G_1 - \{s_0, s_{j-1}\}$ (resp., $G_2 - \{s_{j-1}, s_q\}$) on a new guideline segment $L[s_0, s_{j-1}]$ (resp., $L[s_{j-1}, s_q]$), which automatically determines their temporary y-coordinates from their permanent x-coordinate a, as shown in Fig. 18(c). Denote this embedding by $D(b^*_0, b^*_{j-1}, b^*_q)$, and let $b(v)$ be the y-coordinate of each vertex v in this embedding (i.e., $b(v) = \lambda_{L[s_0,s_{j-1}]}(a(v))$ for $v \in V_1 - \{s_0, s_{j-1}\}$ and $b(v) = \lambda_{L[s_{j-1},s_q]}(a(v))$ for $v \in V_2 - \{s_{j-1}, s_q\}$). Note that any edge in $E - E_1 - E_1$ joins vertices $u \in V_1 - \{s_{j-1}\}$ and $u' \in V_2 - \{s_{j-1}\}$ and belongs to $E^{\rm right}$, since s_{j-1} is exposed on its left side. Hence every edge in $E - E_1 - E_1$ is M-visible currently in $D(b^*_0, b^*_{j-1}, b^*_q)$. Since the y-coordinates of the end-vertices u and u' are temporary ones (except $u = s_0$ or $u' = s_q$), they may change in FSL-drawings D_1 and D_2 for I_1 and I_2, and uu' may not be M-visible in the combined drawing D for I. We can keep uu' M-visible in D if the band parameter ϵ' for I_1 and I_2 is chosen as a sufficiently small value as follows.

For each vertex $v \in V - \{s_0, s_q\}$ and each pair of vertices $u, u' \in V$ with $a(u) < a(v) < a(u')$, we define the *y-distance* $\delta(v; uu')$ between v and segment $L[u, u']$ to be the distance between them in the y-direction; i.e.,

$$\delta(v; uu') = |b(v) - \lambda_{L[(a(u),b(u)),(a(u'),b(u'))]}(a(v))|,$$

where b denotes the current y-coordinate of vertices in $D(b^*_0, b^*_{j-1}, b^*_q)$. Let $\delta(v)$ be the minimum of $\delta(v; uu')$ over all edges $uu' \in E - E_1 - E_2$ $(\subseteq E^{\rm right})$ that cover v. We set

$$\epsilon' = \min[\epsilon/4,\ \min\{\delta(v) : v \in V - \{s_0, s_q\}\}]\ (> 0).$$

For the above instances I_1 and I_2 with this ϵ', the next holds.

Lemma 28 *For each $j = 1, 2$, let D_j be an FSL-drawing of I_j which satisfies the polygon and band constraints. Then the drawing D obtained by combining D_1 and D_2 is an FSL-drawing of I which satisfies the polygon and band constraints.*

Proof: Let $b^*(v)$ denote the y-coordinate of a vertex $v \in V_i$ in D_i $(i = 1, 2)$.

Clearly the polygon constraint is satisfied in D and no two edges $e \in E_1$ and $e' \in E_2$ cross each other in D, since x-coordinates of all vertices are predetermined so that $a(v) < a(s_{j-1}) < a(v')$ for all vertices $v \in V_1 - \{s_{j-1}\}$ and $v' \in V_2 - \{s_{j-1}\}$.

To show that D is an FSL-drawing, we only need to show that no edge $uu' \in E - E_1 - E_2$ intersects any edge vv' in M in D. Recall that in $D(b_0^*, b_{j-1}^*, b_q^*)$, no edge $uu' \in E - E_1 - E_2$ intersects any edge $vv' \in M$; i.e., segments $L[(a(u), b(u)), (a(u'), b(u'))]$ and $L[(a(v), b(v)), (a(v'), b(v'))]$ have no intersection except at their end-points.

Since each D_j satisfies the band constraint with ϵ', it holds that $\max\{|b^*(u) - b(u)|, |b^*(u') - b(u')|, |b^*(v) - b(v)|, |b^*(v') - b(v')|\} \leq \epsilon' \leq \min\{\delta(v)/4 : v \in V - \{s_0, s_n\}\}$, and we see that the segments $L[(a(u), b^*(u)), (a(u'), b^*(u'))]$ and $L[(a(v), b^*(v)), (a(v'), b^*(v'))]$ remain separate apart in the combined drawing D. Also $|b^*(u) - b(u)| \leq \epsilon' \leq \epsilon/4$ means that $|b^*(u) - \lambda_{L[s_0,s_q]}(a(u))| \leq \epsilon/2 + \epsilon' < \epsilon$. Therefore D also satisfies the band constraint of I. ∎

Case 2. $v^* = v_{j,h} \in V(Q_j)$ for some $1 \leq j \leq q$ and $1 \leq h \leq k_i$, and Q_j is of central type: See Fig. 19(a). In this case, we fix the y-coordinates of all vertices v in Q_j as some values $b^*(v)$ permanently and generate two instances $I_1 = (G_1, \gamma_1, (Q_1, Q_2, \ldots, Q_{j-1}), b_0^*, b_{j-1}^*, \epsilon')$ and $I_2 = (G_2, \gamma_2, (Q_{j+1}, Q_j, \ldots, Q_q), b_j^*, b_q^*, \epsilon')$ in a similar manner of Case 1.

We first determine a permanent y-coordinate of vertex $v_{j,h}$ to be

$$b^*(v_{j,h}) = \lambda_{L[s_0,s_q]}(a(v_{j,h})) + \epsilon/2.$$

Then we determine permanent y-coordinates b^* of the other vertices in Q_j so that the following polygons P_A, P_B, P_C and P_j will be formed (see Fig. 19(b) for the relationship among these polygons):
(i) points $s_0, s_{j-1}, v_{j,1}, v_{j,2}, \ldots, v_{j,h}$ form a pseudo-convex polygon P_A with a concave link $(s_{j-1}, v_{j,1}, v_{j,2}, \ldots, v_{j,h})$ such that each vertex in the link is M-visible from any vertex on segment $L[s_0, (a(s_{j-1}), b^*(s_{j-1}))]$;
(ii) points $v_{j,h+1}, v_{j,h+2}, \ldots, v_{j,k_j}, s_j, s_q$ form a pseudo-convex polygon P_B with a concave link $(v_{j,h+1}, v_{j,h+2}, \ldots, v_{j,k_j}, s_j)$ such that each vertex in the link is M-visible from any vertex on segment $L[(a(s_j), b^*(s_j)), s_q]$;
(iii) points $s_0, s_{j-1}, v'_{j,1}, v'_{j,2}, \ldots, v'_{j,k'_j}, s_j, s_q$ form a pseudo-convex polygon P_C with a concave link $(s_{j-1}, v'_{j,1}, v'_{j,2}, \ldots, v'_{j,k'_j}, s_j)$ such that each vertex in the link is M-visible from any vertex on segments $L[s_0, (a(s_{j-1}), b^*(s_{j-1}))]$ and $L[(a(s_j), b^*(s_j)), s_q]$; and
(iv) points $s_{j-1}, v_{j,1}, v_{j,2}, \ldots, v_{j,k_j}, s_j, v'_{j,k'_j}, v'_{j,k'_j-1}, \ldots, v'_{j,1}$ form a convex polygon P_j for Q_j (in order to satisfy the polygon constraint for Q_j).

Such points can be chosen as follows. First we place s_{j-1} between $L[s_0, s_q]$ and $L[s_0, (a(v_{j,h}), b^*(v_{j,h}))]$, say set the y-coordinate of s_{j-1} to be

$$b_{j-1}^* = \min\{\frac{1}{2}[\lambda_{L[s_0,s_q]}(a(s_{j-1})) + \lambda_{L[s_0,v_{j,h}]}(a(s_{j-1}))], \lambda_{L[s_0,s_q]}(a(s_{j-1})) - \epsilon/4\}.$$

Similarly set the y-coordinate of s_j to be

$$b_j^* = \min\{\frac{1}{2}[\lambda_{L[s_0,s_q]}(a(s_j)) + \lambda_{L[v_{j,h},s_q]}(a(s_j))], \lambda_{L[s_0,s_q]}(a(s_j)) - \epsilon/4\}.$$

Now points $s_0, s_{j-1}, v_{j,h}$ form a convex polygon P_A, $s_{j-1}, v_{j,h}, s_j, s_q$ form a convex polygon P_B, s_0, s_{j-1}, s_j, s_q form a convex polygon P_C, and $s_{j-1}, v_{j,h}, s_j$ from a convex polygon P_j. By Lemma 15, we can place vertices $v_{j,1}, v_{j,2}, \ldots, v_{j,h-1}$ over segment $L[s_{j-1}, v_{j,h}]$ (resp., $v_{j,h+1}, v_{j,h+2}, \ldots, v_{j,k_j}$ over $L[v_{j,h}, s_j]$) to form a concave link of P_A (resp., P_B), while we can place vertices $v'_{j,1}, v'_{j,2}, \ldots, v'_{j,k'_j}$ under segment $L[s_{j-1}, s_j]$ to form a concave link of P_C.

Let $b^*(v)$ denote the y-coordinate of vertex v in Q_j determined in the above way, and $b(v)$ denote the current y-coordinate of each vertex $v \in V - \{s_0, s_q\} - V(Q_j)$ on a new guideline $L[s_0, s_{j-1}]$ or $L[s_j, s_q]$. Since all these points are in pseudo-convex polygons P_A, P_B and P_C, we see that $|b^*(v) - \lambda_{L[s_0,s_q]}(a(v))| \leq \epsilon/4$ for all $v \in V(Q_j)$, and $|b(v) - \lambda_{L[s_0,s_q]}(a(u))| \leq \epsilon/4$ for all $v \in V - \{s_0, s_q\} - V(Q_j)$.

Next we choose ϵ' for the new instances $I_1 = (G_1 = (V_1, E_1), \gamma_1, (V_1, M_1) = (Q_1, Q_2, \ldots, Q_{j-1}), b_0^*, b_{j-1}^*, \epsilon')$ and $I_2 = (G_2 = (V_2, E_2), \gamma_2, (V_2, M_2) = (Q_{j+1}, Q_j, \ldots, Q_q), b_j^*, b_q^*, \epsilon')$. See Fig. 19(c).

Since $v^* = v_{j,h}$ is exposed on its left side, there is no left edge uu' that covers v^* and any edge covering v^* is a right edge. As in Case 1, let $\delta(v)$ be the minimum of $\delta(v; uu')$ over all edges $uu' \in E - E_1 - E_2$ that cover v, where some left edge in $E - E_1 - E_2$ may cover vertices in V. Then we set

$$\epsilon' = \min[\epsilon/4,\ \min\{\delta(v) : v \in V - \{s_0, s_q\}\}]\ (> 0).$$

For the above instances I_1 and I_2 with this ϵ', we have the next analogously with Lemma 28.

Lemma 29 *Let P_j be a convex polygon for Q_j defined in the above. For each $j = 1, 2$, let D_j be an FSL-drawing of I_j which satisfies the polygon and band constraints. Then the drawing D obtained by combining D_1, D_2 and P_j is an FSL-drawing of I which satisfies the polygon and band constraints.*

Case 3. $v^* = v_{j,h} \in V(Q_j)$ for some $1 \le j \le q$ and $1 \le h \le k_i$, and Q_j is of left type: See Fig. 20(a). We can handle this case analogously with Case 2. We first determine permanent y-coordinates of vertices in Q_j so that so that the following polygons P_A, P_B, P_C and P_j will be formed (see Fig. 20(b) for the relationship among these polygons):
(i) points $s_0, s_{j-1}, v_{j,1}, v_{j,2}, \ldots, v_{j,h}$ form a pseudo-convex polygon P_A with a concave link $(s_{j-1}, v_{j,1}, v_{j,2}, \ldots, v_{j,h})$ such that each vertex in the link is M-visible from any vertex on segment $L[s_0, (a(s_{j-1}), b^*(s_{j-1}))]$;
(ii) points $v_{j,h+1}, v_{j,h+2}, \ldots, v_{j,k_j}, s_j, s_q$ form a pseudo-convex polygon P_B with a concave link $(v_{j,h+1}, v_{j,h+2}, \ldots, v_{j,k_j}, s_j)$ such that each vertex in the link is M-visible from any vertex on segment $L[(a(s_j), b^*(s_j)), s_q]$;
(iii) points $s_0, s_{j-1}, v'_{j,1}, v'_{j,2}, \ldots, v'_{j,k'_j}, s_j, s_q$ form a convex polygon P_C; and
(iv) points $s_{j-1}, v_{j,1}, v_{j,2}, \ldots, v_{j,k_j}, s_j, v'_{j,k'_j}, v'_{j,k'_j-1}, \ldots, v'_{j,1}$ form a pseudo-convex polygon P_j for Q_j with a "convex" link $(s_{j-1}, v'_{j,1}, v'_{j,2}, \ldots, v'_{j,k_j}, s_j)$.

Thus the difference from Case 2 is to construct the link $(s_{j-1}, v'_{j,1}, v'_{j,2}, \ldots, v'_{j,k'_j}, s_j)$ as a "convex" link to P_C, which is a "concave" link to P_j (in order to satisfy the polygon constraint for Q_j). This is again possible by Lemma 15. Finally we set

$$\epsilon' = \min[\epsilon/4,\ \min\{\delta(v) : v \in V - \{s_0, s_q\}\}]\ (> 0)$$

for the new instances I_1 and I_2. Then we have the next analogously with Lemma 28. See Fig. 20(c).

Lemma 30 *Let P_j be a pseudo-convex polygon for Q_j defined in the above. For each $j = 1, 2$, let D_j be an FSL-drawing of I_j which satisfies the polygon and band constraints. Then the drawing D obtained by combining D_1, D_2 and P_j is an FSL-drawing of I which satisfies the polygon and band constraints.*

Lemma 28, Lemma 29 and Lemma 30 establish a divide-and-conquer method that constructs an FSL-drawing of a given cactus instance with no zipped-chains in polynomial time.

14 Reduction for S-nodes

In this section, we give a reduction procedure that converts a standard instance I with the subgraph $G^-(\nu)$ of G_M for an S-node ν into a standard instance I' with a smaller number of edges in M.

Let ν be a non-reduced S-node with parent edge parent$(\nu) = st$ such that each child-node of ν is a reduced S- or P-node. Now ν is not the root of the SPQR tree by the choice of root. If graph $G^-(\nu) - \{s, t\}$ contains an outer vertex on f_M^o, then ν has no child P-nodes and any child S-node μ of ν induces its subpath $G^-(\mu)$ from the outer facial cycle f_M^o, and then $G^-(\nu)$ is also a subpath of the boundary f_M^o, indicating that ν is already a reduced S-node. Hence each child node $\mu \in \mathrm{Ch}(\nu)$, the subgraph $G^-(\mu)$ contains no outer vertices/edges of the plane embedding of G_M.

Let $H = G^-(\nu)$, and denote $f^{\rm left} = {\rm face}^{st}(H)$ and $f^{\rm right} = {\rm face}^{ts}(H)$, where $f^{\rm left}$ and $f^{\rm right}$ are inner faces in F_M. Let $V^{\rm right}$ (resp., $V^{\rm left}$) denote the set of vertices in $f^{\rm right} - V^o_{ts}(H) - \{s,t\}$ (resp., $f^{\rm left} - V^o_{st}(H) - \{s,t\}$). On the left/right relationship with respect to (s,t), we here assume the following without of generality:
(i) If H is not exposed along $f^o_{st}(H)$ or $f^o_{ts}(H)$, then it is not exposed along $f^o_{ts}(H)$, i.e., there is a t,s-chain S^* along $f^o_{ts}(H)$ (possibly $S^* = \{ts\}$);
(ii) Otherwise (H is exposed along both $f^o_{st}(H)$ and $f^o_{ts}(H)$), if the parent node of ν is an R- or S-node, then an edge $st \in E - M$ is assigned within $f^{\rm right}$ (see Lemma 25(ii)), where $S^* = \{ts\}$ is a t,s-chain along $f^o_{ts}(H)$; and
(iii) Otherwise, if the parent node of ν is a P-node, then ν corresponds to a left edge in the skeleton of the P-node and an edge $st \in E - M$ is assigned within the face f' in Lemma 27, where $f^o_{ts}(f')$ and $f^o_{ts}(H)$ surround the region $f^{\rm right}$.

By the above assumption on the ordering (s,t), we see that H is exposed $f^o_{ts}(H)$.

Denote the skeleton ${\rm skn}^-(\nu)$, i.e., an s,t-path by $P = (s_0 = s, s_1, \ldots, s_q, s_{q+1} = t)$ $(q \geq 2)$, and let each virtual edge $e_i = s_is_{i+1}$ correspond to a reduced S- or P-node $\mu_i \in {\rm Ch}(\nu)$. See Fig. 21(a).

For two distinct vertices $u, u' \in V^o_{st}(H)$ (resp., $u, u' \in V^o_{ts}(H)$), we denote $u \prec u'$ (i.e., u' is closer to t than u) if u' appears after u when we traverse $f^o_{st}(H)$ (resp., $f^o_{ts}(H)$) from s to t, and denote $u \preceq u'$ if $u \prec u'$ or $u = u'$.

Let W denote the set of vertices $w \in V^{\rm right}$ such that an edge $wv \in E - M$ for some vertex $v \in V^o_{ts}(H) - \{s,t\}$ is assigned to $f^{\rm right}$.

Let $\{v^*_1, v^*_2, \ldots, v^*_r\}$ be the set of all vertices in $V^o_{st}(H)$ exposed on their left sides, where $v^*_1, v^*_2, \ldots, v^*_r$ appear in this order along the left side $f^o_{st}(H)$ of H from s to t. Let $v^*_0 = s$ and $v^*_{r+1} = t$. By definition, for each $i = 1, 2, \ldots, r+1$, there is a v^*_{i-1}, v^*_i-chain along $f^o_{v^*_{i-1}v^*_i}(H)$. For each $1 \leq i \leq r+1$, let U_i denote the set of vertices $u \in V^{\rm left}$ such that an edge $uv \in E - M$ is assigned to $f^{\rm left}$ for some vertex $v \in V^o_{st}(H)$ with $v^*_{i-1} \prec v \prec v^*_i$. In an illustration in Fig. 21(a), we have $u_1 \in U_1$, $u_3 \in U_3$, $u_4 \in U_{r+1}$, and $w_1, w_2 \in W$.

Lemma 31 (i) *For each vertex $w \in W$ and vertex $v \in V^o_{ts}(H) - \{s,t\}$, adding a new edge wv within face $f^{\rm right}$ does not create a new zipped-chain or squashed chain;*
(ii) *For each vertex $u \in U_i$ with $2 \leq i \leq r+1$, adding a new edge uv^*_{i-1} within face $f^{\rm right}$ does not create a new zipped-chain or squashed chain;*
(iii) *For each vertex $u \in U_i$ with $1 \leq i \leq r$, adding a new edge uv^*_i within face $f^{\rm right}$ does not create a new zipped-chain or squashed chain;*
(iv) *For each vertex $u \in U_1$, either adding a new edge uv^*_0 $(= us)$ within face $f^{\rm right}$ does not create a new zipped-chain/squashed chain or there is an s,u'-chain outside $f^{\rm left}$ for some vertex $u' \in V^{\rm left}$ (possibly $u' = u$) between t and u (see vertices $u_1 \in U$ and u' in* Fig. 21(a)); *and*
(v) *For each vertex $u \in U_{r+1}$, either adding a new edge uv^*_{r+1} $(= ut)$ within face $f^{\rm right}$ does not create a new zipped-chain/squashed chain or there is a u',t-chain outside $f^{\rm left}$ for some vertex $u' \in V^{\rm left}$ between s and u (possibly $u' = u$).*

Proof: (i) We apply Lemma 20 to $f^{\rm right}$ and vertices s and t on it. Note that the s,t-boundary path of $f^{\rm left}$ gives an s,t-path Q_1 disjoint with $f^{\rm right}$ except at s and t by Lemma 23. We show that instance I has neither of types I and II bad component for $\{w,v\}$ in the lemma. Clearly $\{w,v\} \cap \{s,t\} = \emptyset$, and instance I has no type I bad component for $\{w,v\}$ (since $v = s$ needs to hold for (i) of Lemma 20). By the assumption on the ordering (s,t), there is a t,s-chain S^* along $f^o_{ts}(H)$ or an edge $st \in E$ assigned to a face f' such that $f^o_{ts}(f')$ and $f^o_{ts}(H)$ surround the region $f^{\rm right}$. In other words, edge wv with $w \in W$ is a shift of some edge wv' due to the t,s-chain $S^* = \{ts\}$, or there is an s,t-path Q_2 of second type. Hence instance I has no type II bad component for $\{w,v\}$ either. This proves (i).

(ii) We show (ii) (the cases of (iii) can be treated symmetrically). We apply Lemma 20 to $f^{\rm left}$ and vertices s and t on it. Clearly $\{w, v^*_{i-1}\} \cap \{s,t\} = \emptyset$ for $2 \leq i \leq r+1$, and instance I has no type I bad component for $\{w, v^*_{i-1}\}$. Since there is a v^*_{i-1}, v^*_i-chain along $f^o_{st}(H)$, we see that uv^*_{i-1} is a shift of some edge uv with $v^*_{i-1} \prec v \prec v^*_i$ (by $u \in U_i$), and instance I has no type II bad component for $\{w, v^*_{i-1}\}$ either. This proves (ii).

(iv) We show (iv) (the cases of (v) can be treated symmetrically). Again apply Lemma 20 to $f^{\rm left}$ and vertices s and t on it. Since there is a v_0^*, v_1^*-chain along $f^o_{st}(H)$, we see that uv_0^* is a shift of some edge uv with $s = v_0^* \prec v \prec v_1^*$ (by $u \in U_1$), and instance I has no type II bad component for $\{w, v_0^*\}$ either. However, instance I may have a type I bad component for $\{w, v_0^*\}$ since $\{w, v_0^*\} \cap \{s, t\} = \{s\}$ holds. Lemma 20 tells that this occurs only when there is an s, u'-chain outside $f^{\rm left}$ for some vertex $u' \in V^{\rm left}$. This proves (iv). ∎

We are ready to describe our reduction to S-nodes.

Reduction

1. Let $E' := E$ and $M' := M$. First we add to E' edges $\{uv_{i-1}^* : \ u \in U_i\}$, $(1 \le i \le r+1)$ and $\{uv_i^* : \ u \in U_i\}$ $(0 \le i \le r)$ assigned to face $f^{\rm left}$. Also add to E' each of new edges $\{us : \ u \in U_1\} \cup \{ut : \ u \in U_{r+1}\}$ assigned to face $f^{\rm left}$ as long as no new zipped-chain or squashed chain is created;

2. Let $X = V(H) - \{s, v_1^*, v_2^*, \ldots, v_r^*, t\}$. We remove the vertices in X from the current graph (letting $V' := V - X$, $E' := E' - E(X)$ and $M' := M' - E(X)$), and replace $H = G^-(\nu)$ with a new s, t-path
$$P = (s = v_0^*, v_1^*, v_2^*, \ldots, v_r^*, t = v_{q+1}^*),$$
adding $E(P)$ to M'. Add to E' a convex-support for the right side P (i.e., edges $\{v_j^* v_{j+2}^* : \ 0 \le j \le q-1\} \cup \{sv_r^*, tv_1^*\}$ assigned to $f^{\rm right}$);

3. Finally add to E' edges $\{wv_1^*, wv_r^* : \ w \in W\}$ assigned to face $f^{\rm right}$. Let I' be the resulting instance (note that the edges $\{uv_i^* \in E : \ u \in V^{\rm left}\}$, $1 \le i \le r$ in I still exits in I'). See Fig. 21(b).

Lemma 32 *The new instance I' has no zipped-chains or squashed chains.*

Proof: By Lemma 31, the augmented embedding after Step 1 in the reduction contains no new zipped-chains or squashed chains. To prove the lemma, we regard Steps 2 and 3 as the following set of sub-steps, which changes I into I' more gently.
Step A1. Add to E' edges $\{ws_i : \ w \in W\}$ $(1 \le i \le q)$ assigned to $f^{\rm right}$;
Step A2. Remove all vertices in $V(H) - V^o_{st}(H)$ (those not on the facial cycle $f^{\rm left}$) from H (now H has been replaced with its left side $f^o_{st}(H)$);
Step A3. Add to E' edges $\{wv_1^*, wv_r^* : \ w \in W\}$ assigned to $f^{\rm right}$;
Step A4. Remove all edges in E' that join two vertices in $V^o_{st}(H)$;
Step A5. Remove all edges in E' (and those added in Step A1) that are assigned in $f^{\rm right}$ and incident to some vertex in $V(H) - \{s, v_1^*, v_2^*, \ldots, v_r^*, t\}$;
Step A6. Replace each v_{i-1}^*, v_i^*-path $(1 \le i \le r+1)$ on $f^o_{st}(H)$ by a single edge in $v_{i-1}^* v_i^* \in M'$;
Step A7. Finally add to E' a convex-support for the right side $P = (s, v_1^*, , \ldots, v_r^*, t)$.

Note that Steps A2, A4, A5 and A6 never introduce new zipped-chains or squashed chains, since they simply remove vertices/edges or ignore degree 2 vertices in a path of G. Step A1 does not introduce new zipped-chains or squashed chains by Lemma 31(i). We see that Step A3 also does not introduce new zipped-chains or squashed chains, since we can obtain a similar property of Lemma 31(i) in the graph after Step A2.

Finally we prove that Step A7 does not introduce any new zipped-chains or squashed chains. To prove this, we use the following properties:
(a) By the assumption on the ordering (s, t), there is a t, s-chain S^* along $f^o_{ts}(H)$ or an edge $st \in E$ assigned to a face f' such that $f^o_{ts}(f')$ and $f^o_{ts}(H)$ surround the region $f^{\rm right}$; and
(b) After Step A6, $f^o_{st}(f^{\rm right})$ forms a single s, t-path P which is fully exposed along its left side (i.e., no edge assigned to $f^{\rm left}$ joins two veritces in the s, t-path P).

To derive a contradiction, we assume that introducing an edge $e = v_j^* v_{j'}^*$ $(j' \ge j+2)$ creates a new a, b-chain S with $e \in S$ such that S and a b, a-chain S' (or a ba-subpath S' of $P_{\rm out}$) give a zipped-chain (or a squashed chain). Let H be the a, b-component surrounded by S and S'.

We apply Lemma 18 with $uv = v_j^* v_{j'}^*$ and $f = f^{\text{right}}$. Since there are three internally disjoint s,t-path, two along f^{right} and one outside f^{right}, we see that any cut-pair along facial cycle f^{right} appears on $f_{ts}^o(f^{\text{right}})$ or $f_{st}^o(f^{\text{right}})$. By property (b), the b,a-chain S' (or the b,a-subpath S' of P_{out}) cannot appear along P. Therefore, the cut-pair $\{a,b\}$ appear along the right side $f_{ts}^o(f^{\text{right}})$ of the face $f = f^{\text{right}}$. In this case, $f_{ab}^o(f^{\text{right}})$ and the a,b-boundary path $f_{ab}^o(H)$ form the facial cycle $f = f^{\text{right}}$ (as shown in Fig. 12(a)(b)). By property (a), there is a t,s-chain S^* along $f_{ts}^o(H)$ or an edge $st \in E$ assigned to a face f' on the right hand side of $f = f^{\text{right}}$. In the former, $(S - \{e = v_j^* v_{j'}^*\}) \cup S^*$ contains an a,b-chain in I, which together with S' gives a zipped-chain or a squashed chain, contradicting that instance I has no zipped-chains or squashed chains. In the latter, the face f' also provides another s,t-path Q' of G_M which together with $f_{ts}^o(H)$ surrounds the region $f = f^{\text{right}}$ in I. This is possible only when $a = t$ and $b = s$. However, in this case, S^* together with S' gives a zipped-chain or a squashed chain in I, a contradiction.

This completes a proof that instance I' has no zipped-chains or squashed chains. ∎

By induction hypothesis on the size of M, I' admits an FSL-drawing D'. Before we proceed to construction of an FSL-drawing of I from D', we observe an important property on D' attained by the edges added in Steps 1 and 3.

For each vertex $u \in U_1 \cup U_2 \cup \cdots \cup U_{r+1}$, let cone_u be the set of half-lines L starting from u that do not intersect any edges in $E(f^{\text{left}}) - E(P)$ in the FSL-drawing D'. Similarly define cone_w ($w \in W$) to be the set of half-lines L starting from w that do not intersect any edges in $E(f^{\text{right}}) - E(P)$ in D'. See Fig. 21(c).

We define the *drawing area* for the set of all right/joint vertices in H to be the intersection K^{right} of cone_w for all vertices $w \in W$. Similarly, for each $i = 1, 2, \ldots, r+1$, the *drawing area* for the set $V_{v_{i-1}^* v_i^*}^o(H)$ of all left/joint vertices in H between exposed vertices v_{i-1}^* and v_i^* is defined to be the intersection K_i^{left} of cone_u for all vertices $u \in U_i$.

Lemma 33 *Drawing area K^{right} contains $L[v_{i-1}^*, v_i^*]$ for all $i = 2, \ldots, r$. For each $i = 2, \ldots, r$, K_i^{left} contains $L[v_{i-1}^*, v_i^*]$, $K^{\text{right}} \cap K_1^{\text{left}}$ contains a segment $L[p, v_1^*]$ for some point p ($\neq s$) on $L[s = v_0^*, v_1^*]$, and $K^{\text{right}} \cap K_{r+1}^{\text{left}}$ contains a segment $L[v_r^*, p']$ for some point p' ($\neq t$) on $L[v_r^*, t = v_{r+1}^*]$.*

Proof: For each vertex $w \in W$, E' contains two edges wv_1^* and wv_r^* within f^{right}. For each vertex $u \in U_i$ with $2 \leq i \leq r$, E' contains two edges uv_{i-1}^* and uv_i^* within f^{left}. Hence we see that the whole segment $L[v_{i-1}^*, v_i^*]$ is contained in each of K^{right} and K_i^{left}. Also E' contains an edge uv_1^* within f^{right} for each $w \in W$. Since v_1^* is a convex corner from the interior of f^{left} in D', we see that the intersection of K^{right} and segment $L[s = v_0^*, v_1^*]$ is given by $L[p_a, v_1^*]$ for some point p_a ($\neq s$) on $L[s = v_0^*, v_1^*]$ in D'. Similarly the intersection of K^{right} and $L[v_r^*, t = v_{r+1}^*]$ is given by $L[v_r^*, p_b]$ for some point p_b ($\neq t$) on $L[v_r^*, t = v_{r+1}^*]$.

We now show that K_1^{left} contains a segment $L[p'_a, v_1^*]$ for some point p'_a ($\neq s$) on $L[s = v_0^*, v_1^*]$. To show this, we prove that, for any vertex $u \in U_1$, the angle at the point v_1^* between $L[s, v_1^*]$ and $L[v_1^*, u]$ is less than π (in other words, the triangle suv_2^* encloses v_1^*). This is trivial if D' has an edge $us \in E'$ (since it cannot intersect the edges $E(P) \subseteq M'$). Consider the case where edge us has not been added to E' in Step 1. In this case, by Lemma 31, G (hence G') has a u',s-chain outside f^{left} for some vertex $u' \in V^{\text{left}}$ between u and t, as shown in Fig. 21(a) and (b). Hence in D' the u',s-chain and the path $f_{su'}^o(f^{\text{left}})$ must be drawn within the triangle $su'v_2^*$, which implies that the angle at the point v_1^* between $L[s, v_1^*]$ and $L[v_1^*, u]$ is less than π.

Analogously K_{r+1}^{left} also contains a segment $L[v_r^*, p'_b]$ for some point p'_b ($\neq t$) on $L[v_r^*, t = v_{r+1}^*]$. From the above argument, we have the lemma. ∎

Construction of Drawing

We show how to convert the FSL-drawing D' of I' into that of I.

Due to the convex-support introduced in Step 2, the s,t-path P is drawn as a sequence of segments between adjacent exposed vertices $L[s = v_0^*, v_1^*]$, $L[v_1^*, v_2^*]$, $\ldots$, $L[v_r^*, t = v_{r+1}^*]$ in D' which together with $L[t, s]$ form a convex $(r+2)$-gon. We keep the current position of each vertex v_i^* $(1 \le i \le r)$ in D' as those in a final drawing D for the original instance I, and select adequate positions of the other vertices from their drawing areas.

Recall that the subgraph $H = G^-(\nu)$ and the set of edges in E joining vertices in H is a cactus instance $(Q_1, Q_2, \ldots, Q_q)$.

We call a cycle $Q = G^-(\mu)$, $\mu \in \mathrm{Ch}(\nu)$ a *corner cycle* if it contain at least one exposed vertex in $\{v_1^*, \ldots, v_r^*\}$, where possibly Q is a single path (see cycles Q_5 and Q_9 in Fig. 21(d) for an illustration of corner cycles). Denote by $Q_{i_1}, Q_{i_2}, \ldots, Q_{i_{r'}}$ $(1 \le i_1 < i_2 < \cdots < r')$ all corner cycles, as shown in Fig. 22(a). Note that if exposed vertices appear along each Q_{i_1} consecutively (i.e., if $v_i^*, v_{i'}^* \in V(Q_{i_j})$, then $v_{i''}^* \in V(Q_{i_j})$ for any $i < i'' < i'$), since cycle Q_{i_j} with a vertex exposed on its left side is fully exposed along the left side $f^o_{s_{i_j-1} s_{i_j}}(Q_{i_j})$.

Let I_j be the cactus instance induced from I by the vertices in H between $s_{i_{j-1}}$ and s_{i_j}. It is not difficult to see that we can find an adequate FSL-drawing D_j of I_j so that a drawing D obtained by replacing P in D' with these drawings D_j becomes an FSL-drawing if we construct D_j within an area sufficiently close to the drawing P. In the following we given a concrete procedure for constructing such a drawing D.

Fix the current positions of exposed vertices $v_1^*, \ldots, v_r^*$ as those in a final drawing for $H = G^-(\nu)$. In the following, we always keep each left/joint vertex within the corresponding area K_i^{left} and each right/joint vertex within K^{right}.

1. Regard segments $L[v_0^*, v_1^*]$, $L[v_1^*, v_2^*], \ldots, L[v_r^*, v_{r+1}^*]$ as guidelines, and place the other vertices in H along guidelines according to the order $\prec$, where the right vertices in a corner cycle Q_j can be placed on any guideline between s_{j-1} and s_j as long as they obey the order $\prec$. See Fig. 22(b).;

2. Regarding the line $L\langle s, t\rangle$ as the x-axis with the y-coordinate which increases in the left direction, we fix the x-coordinates $a(v)$ of the current positions $(a(v), b(v))$ for all vertices v in G, and the y-coordinates $b(v)$ of all vertices v in $G - (V(H) - \{v_1^*, \ldots, v_r^*\})$. We only decrease the y-coordinates $b(v)$ of the vertices v in $H - \{v_1^*, \ldots, v_r^*\}$. For each left/right (resp., joint) vertex v in $H - \{v_1^*, \ldots, v_r^*\}$, let $(a(v), b_{\mathrm{right}}(v))$ be the rightmost point of v within within its corresponding area $K_i^{\mathrm{left}}/K^{\mathrm{right}}$ (resp., $K_i^{\mathrm{left}} \cap K^{\mathrm{right}}$). We set $\delta_{D'}$ to be the minimum of the following
$$\min\{b(v) - b_{\mathrm{right}}(v) : v \in V(H) - \{v_1^*, \ldots, v_r^*\}\}$$
and
$$(1/2)\min\{\delta(v; uu') :\ v, u \in V(H),\ u' \in U_1 \cup U_2 \cup \cdots \cup U_{r+1} \cup W\},$$
where $\delta(v; uu')$ is the y-distance between v and segment $L[u, u']$ defined in Section 13;

3. Decrease the y-coordinates of joint vertices s_{j-1}, s_j $(\notin \{v_1^*, \ldots, v_r^*\})$ in each corner cycle Q_j by at most $\delta_{D'}/4$ so that the new positions of s_{j-1} and s_j form a convex polygon P_j. Fix the y-coordinates of the joint vertices of all corner cycles Q_j, and move the other vertices on the corresponding sides of the convex polygons P_j by decreasing their y-coordinates, as shown in Fig. 22(c);

4. Move the remaining vertices v $(\notin \{s_{j-1}, s_j\} \cup \{v_1^*, \ldots, v_r^*\})$ in each corner cycle Q_j by at most $\delta_{D'}/4$ (fixing the vertices not on corner cycles) so that the following (i)-(iv) hold:
(i) P_j of a central type of corner cycle Q_j becomes a convex polygon when Q_j is of central type;
(ii) P_j of a left type of corner cycle Q_j becomes a pseudo-convex polygon with a concave link along its right side $f^o_{s_j s_{j-1}}(Q_j)$;
(iii) Polygon P_C drawn for the cycle of the right side $f^o_{ts}(H)$ of H and $L[st]$ becomes a pseudo-convex polygon with concave links along central type of corner cycles Q_j; and
(iv) The polygon $P'_{i_j} = (v_h^*, \ldots, s_{i_{j-1}}, \ldots, s_{i_j}, \ldots, v_\ell^*) = f^o_{v_h^* v_\ell^*}(H)$ between every two consecutive corner cycles $Q_{i_{j-1}}$ and Q_{i_j} becomes a pseudo-convex polygon with concave links $(v_h^*, \ldots, s_{i_{j-1}})$ and $(s_{i_j}, \ldots, v_\ell^*)$, where v_h^* is the last exposed vertex on $Q_{i_{j-1}}$ and v_ℓ^* is the

first exposed vertex on Q_{i_j}.
Such a set of pseudo-convex polygons can be obtained by applying Lemma 15 with $\epsilon = \delta_{D'}/4$ (where we can find a desired set of pseudo-convex polygons just by changing the y-coordinates in the proof I of Lemma 15 as long as no side of a given polygon is parallel to y-axis). See Fig. 22(d);

5. Determine the position of vertices between Finally we the joint vertices $s_{i_{j-1}}$ and s_{i_j} of every two consecutive corner cycles $Q_{i_{j-1}}$ and Q_{i_j}. Let I_j be the cactus instance induced from instance I by the vertices in H between $s_{i_{j-1}}$ and s_{i_j}, where the positions of the terminals $s_{i_{j-1}}$ and s_{i_j} have been determined. See Fig. 21(d). We set $\epsilon = \delta_{D'}/4$, and construct an FSL-drawing D_j for each I_j with the procedure described in Section 13. See Fig. 21(e);

6. Let D be a straight-line drawing D obtained from D' by plugging FSL-drawings D_j of all cactus instances I_j, wherein we draw a segment $L[u, v]$ (resp., $L[w, v]$) for every edge $uv \in E$, $u \in U_1 \cup U_2 \cup \cdots \cup U_{r+1}$ and $v \in V(H)$ (resp., $wv \in E$, $w \in W$ and $v \in V(H)$).

Since $\delta_{D'}$ is the maximum change of the y-cooridinate for all vertices $v \in V(H) - \{v_1^*, \ldots, v_r^*\}$ such that each of them stays within the corresponding drawing area, the segments $L[u, v]$ and $L[u', v']$ for any two edges $uv, u'v' \in E$ that do not cross in D' remain separate apart as long as the x-coordinates of all vertices $v \in V(H) - \{v_1^*, \ldots, v_r^*\}$ remain fixed to the one $a(v)$. After all steps in the construction, the maximum possible change of the x-coordinate of each vertex $v \in V(H) - \{v_1^*, \ldots, v_r^*\}$ is bounded by $(3/4)\delta_{D'}$, which implies that every edge uv or wv between H and $G - V(H)$ is M-visible in the final drawing D. Therefore D is an FSL-drawing for instance I.

15 Reduction for R-nodes

In this section, given a non-root R-node ν in a standard instance I such that any child node of ν is a reduced P- or S-node, we present a reduction procedure that converts the instance I into a standard instance I' with a smaller number of edges in M by simplifying the subgraph $G[V(H)]$ induced by the vertex set of $H = G^-(\nu)$.

One easy and tricky reduction for an R-node ν with at least one real edge in its skeleton is to simply regard one edge $e^* \in E(\mathrm{skn}^-(\nu))$ $(\subseteq M)$ as an edge in $E - M$ to obtain I'. This simply completes a reduction for such an R-node ν since M one edge less still induces a biconnected spanning subgraph G_M and $E - M$ can contain crossing-free edges (recall that M can be a proper subset of $E^{(0)}$). However, there is a case where the skeleton $\mathrm{skn}^-(\nu)$ contains only virtual edges (although the figures in this section contain real edges of skeletons for readability). In this section, we assume that

$$\text{the skeleton } \mathrm{skn}^-(\nu) \text{ of R-node } \nu \text{ contains only virtual edges.} \tag{1}$$

Now each child of ν is a reduced S- or P-node. Then the subgraph $G^-(\nu)$ of G_M will be obtained from the skeleton $\mathrm{skn}^-(\nu)$ by replacing each virtual edge uv with a single u, v-path or a cycle of two u, v-paths, which is required to be drawn as a convex/concave link or a pair of convex/concave links to its incident inner faces in an FSL-drawing of I.

We distinguish three cases:
1. ν is the root R-node;
2. ν is not the root node, but the subgraph $G^-(\nu)$ contains a subpath of the prescribed polygon P_{out}; and
3. the subgraph $G^-(\nu)$ contains no subpath of the prescribed polygon P_{out}.

Case 1. ν is the root R-node (see Fig. 23(a)-(d)): In this case, we convert I into a standard instance I' as follows.

Reduction

1. Remove all edges $E - M$ from the graph, and replace the subgraph $G^-(\mu)$ of each child P- or S-node $\mu \in \mathrm{Ch}(\nu)$ with a real edge e_μ (i.e., replace the interior of G_M with the interior of the skeleton $\mathrm{skn}(\nu)$). Let M' be the set of all current edges including those in f^o_M;

2. For each inner face f of length at least four in the resulting plane embedding, assign a new edge vw for every adjacent edges $vu, uw \in E(f)$ sharing an inner vertex u (see Fig. 23(b)). Let E' be the set of edges introduced in Step 2. Let I' be the resulting instance.

Lemma 34 *The new instance I' has no zipped-chains or squashed chains.*

Proof: Clearly Step 1 creates no zipped-chain or squashed chain. We show that no zipped-chain or squashed chain will be created either during Step 2. After Step 2, the graph $G_{M'}$ in I' can have a cut-pair $\{a, b\}$ only along a subpath of the outer facial cycle $f^o_M = f^o_{M'}$. We show that adding a new edge vw within an inner face f with $|V(f)| \geq 4$ creates no zipped-chain or squash chains. Since the end-vertices v and w of vw are two non-adjacent vertices in the skeleton $\mathrm{skn}(\nu)$, there are two other vertices $s, t \in V(f) - \{v, w\}$ such that s, v, t and w appear in the clockwise order along f and there is an s,t-path Q in G_M disjoint with $V(f) - \{s, t\}$, as shown in Fig. 14(a).

By Lemma 20, if adding a new edge vw within such a face f, then there is a bad component of type I or II for $\{v, w\}$. Since $\{v, w\} \cap \{s, t\} = \emptyset$, there is no type I bad component for $\{v, w\}$ by Lemma 20(i). By Lemma 20(ii), a type I bad component is an a, b-component H^* for a cut-pair $\{a, b\}$ such that a and b appear along $f^o_{ws}(f)$, as shown in Fig. 14(d),(f). This, however, is impossible since the skeleton $\mathrm{skn}(\nu)$ has no such cut-pair along each inner facial cycle. This proves that I' has no zipped-chain or squashed chain. ∎

By (1), it holds $|M'| < |M|$. By induction hypothesis on the size of M, I' admits an FSL-drawing D', as shown in Fig. 23(c).

Construction of Drawing
Due to the edges assigned to all inner faces of $F_{M'}$ in Step 2, every inner face $f \in F_{M'}$ is now drawn as a convex polygon P_f. The remaining task is to replace each inner edge that corresponds to a virtual edge e in the skeleton $\mathrm{skn}(\nu)$ with the subgraph $G^-(\mu_e)$ of G_M, which is a convex/concave link or a pair of convex/concave link. By Lemma 16, we can replace all virtual edges with such links so that the convex polygon P_f drawn for each inner face f becomes a pseudo-convex polygon. See Fig. 23(c). This gives a straight-line drawing D for I. Recall that when a u, v-path in $G^-(\mu_e)$ for a virtual edge $e = uv$ is required to be a concave link to a face $f \in \{f(uv), f(vu)\}$, the subgraph $G^-(\mu_e)$ is fully exposed along its side facing f. Therefore, now in D, for each edge $ab \in E - M$ is M-visible in the assigned inner face f which is now drawn as a pseudo-convex polygon. Therefore D is an FSL-drawing for I.

Case 2. ν is not the root node, but the subgraph $G^-(\nu)$ contains a subpath of P_{out} (see Fig. 24(a)-(f)): Let $st = \mathrm{parent}(\nu)$, $H = G^-(\nu)$, and assume without loss of generality that $f^o_{ts}(H)$ is a subpath of P_{out}, as shown in Fig. 24(a) (the case where all corners on the subpath are flat is a hard instance). Now $f^{\mathrm{left}} = \mathrm{face}^{st}(H) \in F_M$ is an inner face.

Since ν is an R-node, any cut-pair $\{a, b\}$ of the skeleton $\mathrm{skn}(\nu)$ separates s and t (i.e., one of a and b is in $V^o_{ts}(\nu) - \{s, t\}$ and the other in $V^o_{st}(\nu) - \{s, t\}$).

Let $F_{\mathrm{skn}^-(\nu)}$ denote the set of all inner faces in the induced plane embedding of $\mathrm{skn}^-(\nu)$. Let $(s_0 = s, s_1, s_2, \ldots, s_q, s_{q+1} = t)$ denote the s, t-boundary path $f^o_{st}(\mathrm{skn}^-(\nu))$ of the skeleton $\mathrm{skn}^-(\nu)$. Let $\mathrm{Ch}_{st}(\nu)$ denote the set of child nodes $\mu_i \in \mathrm{Ch}(\nu)$ of ν such that the corresponding virtual edge appears as an edge $s_{i-1}s_i$ along $f^o_{st}(\mathrm{skn}^-(\nu))$, and let $Q_i = G^-(\mu_i)$, which is an s_{i-1}, s_i-path of G_M or a cycle consisting of two s_{i-1}, s_i-path of G_M, since each child node μ_i is a reduced S- or P-node. Let H^{left} be the subgraph induced from $H = G^-(\nu)$ by the vertices in $\cup_{\mu \in \mathrm{Ch}_{st}(\nu)} V(G^-(\mu))$. Thus H^{left} is a concatenation of cycles/paths $Q_1, \ldots, Q_{q+1}$, which isl a line-cactus.

We convert I into a standard instance I' as follows.

Reduction

1. Let $M' := M$ and $E' := E$. For each reduced child S- or P-node $\mu \in \mathrm{Ch}(\nu) - \mathrm{Ch}_{st}(\nu)$, we remove vertices in $G^-(\mu) - \{u, v\}$ (where $uv = \mathrm{parent}(\mu)$) from the embedding and from M', and add a single edge uv to the embedding and to M'. We remove any edges that were incident to vertices in $V(G^-(\mu)) - \{u, v\}$ from the embedding and from E', as shown in Fig. 24(b). Now the set of inner faces enclosed by $f^o(H)$ consists of those in $F_{\mathrm{skn}^-(\nu)}$ and in the line-cactus H^{left};

2. Within each inner face $f \in F_{\mathrm{skn}^-(\nu)}$, add a new edge vw for every adjacent edges $vu, uw \in E(f)$ unless v and w are contained in the same path of $G^-(\mu)$ of a child $\mu \in \mathrm{Ch}_{st}(\nu)$. Let I' be the resulting instance.

For example, in Step 1, each facial cycle $f \in \{f_1, f_2, \ldots, f_5\}$ in Fig. 24(b) contains such a path from the subgraph $G^-(\mu)$ of a child $\mu \in \mathrm{Ch}_{st}(\nu)$, while the other face f will receive new edges as in the reduction for Case 1.

Lemma 35 *The new instance I' has no zipped-chains or squashed chains.*

Proof: The lemma can be proved analogously with Lemma 34 for Case 1.

Clearly Step 1 creates no zipped-chain or squashed chain. We show that no zipped-chain or squashed chain will be created either during Step 2. After Step 2, the graph $G_{M'}$ in I' can have a cut-pair $\{a, b\}$ only along a subpath of the outer facial cycle $f^o_M = f^o_{M'}$. We show that adding a new edge vw within an inner face f with $|V(f)| \geq 4$ creates no zipped-chain or squash chains. Since the end-vertices v and w of vw are two non-adjacent vertices in the skeleton $\mathrm{skn}(\nu)$, there are two other vertices $s, t \in V(f) - \{v, w\}$ such that s, v, t and w appear in the clockwise order along f and there is an s,t-path Q in G_M disjoint with $V(f) - \{s, t\}$, as shown in Fig. 14(a).

By Lemma 20, if adding a new edge vw within such a face f creates a zipped-chain or a squashed chain, then there is a bad component of type I or II for $\{v, w\}$. Since $\{v, w\} \cap \{s, t\} = \emptyset$, there is no type I bad component for $\{v, w\}$ by Lemma 20(i). By Lemma 20(ii), a type I bad component is an a,b-component H^* for a cut-pair $\{a, b\}$ such that a and b appear in the clockwise order along $f^o_{ws}(f)$ from t to s, as shown in Fig. 14(d),(f). This can happen only when $f^o_{ab}(f)$ is a subpath of $G^-(\mu)$ of a child $\mu \in \mathrm{Ch}_{st}(\nu)$. However, in this case G_M is given by the union of the a,b-path $f^o_{ab}(f)$ and H^*, which cannot be connected to the outer boundary P_{out}, contradicting the biconnectivity of G_M. This proves that I' has no zipped-chain or squashed chain. ∎

By (1), it holds $|M'| < |M|$. By induction hypothesis on the size of M, I' admits an FSL-drawing D', as shown in Fig. 24(c).

Construction of Drawing

In D', the polygon P_f drawn for each inner face $f \in F_{\mathrm{skn}^-(\nu)}$ is a convex polygon or a pseudo-convex polygon P_f with one concave link which is a convex link to a cycle Q_i in H^{left} (such as $f \in \{f_1, f_2, \ldots, f_5\}$ in Fig. 24(b)). Note that these convex links appear only along $f^o_{st}(H)$. Hence the straight-line drawing D_ν that consists of polygons P_f with $f \in F_{\mathrm{skn}^-(\nu)}$ is a pseudo-convex drawing. In Fig. 24(b), D_ν is given by the polygons enclosed by $(s, v_1, v_2, \ldots, v_{17}, t)$. As in Case 1, the remaining task is to replace each inner virtual edge that corresponds to a child node $\mu \in \mathrm{Ch}(\nu) - \mathrm{Ch}_{st}(\nu)$ with the subgraph $G^-(\mu)$ of G_M, which is a convex/concave link or a pair of convex/concave link. By Lemma 17, we can replace all virtual edges with such links so that all inner faces become pseudo-convex polygons, as shown in Fig. 24(d). This gives a straight-line drawing D for I. In D, any two vertices u and v in the same inner face $f \in F_{\mathrm{skn}^-(\nu)}$ is now M-visible within a pseudo-convex polygon P_f unless u and v are on the same concave link of P_f. This gives an FSL-drawing D for I.

Case 3. ν is not the root node, and the subgraph $G^-(\nu)$ contains no subpath of P_{out}: Let $st = \mathrm{parent}(\nu)$. See Fig. 25(a)-(b):

Let $H = G^-(\nu)$, and denote $f^{\mathrm{left}} = \mathrm{face}^{st}(H)$ and $f^{\mathrm{right}} = \mathrm{face}^{ts}(H)$, where f^{left} and f^{right} are inner faces in F_M. Let V^{right} (resp., V^{left}) denote the set of vertices in $f^{\mathrm{right}} - V^o_{ts}(H) - \{s, t\}$

(resp., $f^{\rm left} - V^o_{st}(H) - \{s,t\}$). As in the case of S-nodes, we here assume the following left/right relationship with respect to (s,t) without loss of generality:
(i) If H is not exposed along $f^o_{st}(H)$ or $f^o_{ts}(H)$, then it is not exposed along $f^o_{ts}(H)$, i.e., there is a t,s-chain S^* along $f^o_{ts}(H)$ (possibly $S^* = \{ts\}$);
(ii) Otherwise (H is exposed along both $f^o_{st}(H)$ and $f^o_{ts}(H)$), if the parent node of ν is an R- or S-node, then an edge $st \in E - M$ is assigned within $f^{\rm right}$ (see Lemma 24(ii)), where $S^* = \{ts\}$ is a t,s-chain along $f^o_{ts}(H)$; and
(iii) Otherwise, if the parent node of ν is a P-node, then ν corresponds to a left edge in the skeleton of the P-node and an edge $st \in E - M$ is assigned within the face f' in Lemma 27, where $f^o_{ts}(f')$ and $f^o_{ts}(H)$ surround the region $f^{\rm right}$.

By the above assumption on the ordering (s,t), we see that H is exposed along $f^o_{ts}(H)$ (note that $st \notin M$ even if $st \in E$).

Let W denote the set of vertices $w \in V^{\rm right}$ such that an edge $wv \in E - M$ for some vertex $v \in V^o_{ts}(H) - \{s,t\}$ is assigned to $f^{\rm right}$. Let $w_1, w_2, \ldots, w_\ell$ denote the vertices in W which appear in this order along $f^o_{ts}(f^{\rm right})$ from t to s. Analogously with Lemma 31(i), we have the next result on additional new edges within $f^{\rm right}$.

Lemma 36 *For each vertex $w \in W$ and vertex $v \in V^o_{ts}(H) - \{s,t\}$, adding a new edge wv within face $f^{\rm right}$ does not create a new zipped-chain or squashed chain.*

By (1), the skeleton $\mathrm{skn}^-(\nu)$ contains only virtual edges. Analogously with Case 2, we define $\mathrm{Ch}_{st}(\nu)$ to be the set of child nodes corresponding virtual edges on the left side $f^o_{st}(\mathrm{skn}^-(\nu))$, let $Q_i = G^-(\mu_i)$ for each $\mu_i \in \mathrm{Ch}_{st}(\nu)$, and let $H^{\rm left} = (Q_1, \ldots, Q_{q+1})$ be the line-cactus induced from $H = G^-(\nu)$ by the vertices in $\cup_{\mu \in \mathrm{Ch}_{st}(\nu)} V(G^-(\mu))$. Let $V^o_{ts}(\mathrm{skn}^-(\nu)) = \{v_0\ (=t), v_1, \ldots, v_{q'+1}\ (= s)\}$ denote the vertices in $f^o_{ts}(\mathrm{skn}^-(\nu))$, where $v_0\ (=t), v_1, \ldots, v_{q'+1}\ (=s)$ appear in this order from t to s along $f^o_{ts}(\mathrm{skn}^-(\nu))$).

In Case 3, we present two reduction methods (A) and (B). The first one (A) uses a result on inner convex drawings with star-shaped boundaries (Corollary 22), and the second (B) does not rely on it.

(A) We design a reduction using Corollary 22.
Reduction

1. Let $M' := M$ and $E' := E$. Choose a vertex $v^*\ (\neq s,t)$ along the right side $f^o_{ts}(H)$, and add to E' edges $\{v^*w :\ w \in W\}$ assigned to $f^{\rm right}$;
2. Let $X = V(H) - V^o_{ts}(H) - V(H^{\rm left})$ (i.e., the set of vertices surrounded by the right side $f^o_{ts}(H)$ and the left line-cactus $H^{\rm left}$). Remove X from the current graph (letting $V' = V - X$, $E' := E' - E(X)$ and $M' := M' - E(X)$). See Fig. 26(a);
3. Replace the remaining boundary $f^o_{ts}(H)$ with a t,s-path of two edges tv^* and v^*s, updating $M' := (M' - E(f^o_{ts}(H)) \cup \{tv^*, v^*s\}$;
4. Let f_ν be the inner face enclosed by $H^{\rm left}$ and the new path (tv^*, v^*s). Add to E' edges $\{v^*z :\ z \in V^o_{ts}(H^{\rm left})\}$ (see Fig. 26(b)). Let I' denote the resulting instance.

Lemma 37 *The new instance I' has no zipped-chains or squashed chains.*

Proof: Note that Steps 2 and 3 never introduce new zipped-chains or squashed chains, since they simply remove vertices/edges or ignore degree 2 vertices in a path of G. Step 1 does not introduce new zipped-chains or squashed chains by Lemma 36.

Finally we prove that adding a new edge v^*z in Step 4 does not introduce any new zipped-chains or squashed chains. To see this, we apply Lemma 20 to the face $f = f_\nu$ with a cut-pair $\{s,t\}$ and the new edge between $v = v^*$ and $w = z$. After Step 3, along $f^{\rm right}$ and $f^{\rm left}$, there are s,t-paths Q_1 and Q_2 each of which is disjoint with f_ν except at s and t, and paths Q_1 and Q_2 surrounds the region f_ν. Since $\{s,t\} \cap \{v = v^*, w = z\} = \emptyset$, no type I bad component for $\{v = v^*, w = z\}$

exists in I' by the condition (i) of Lemma 20. We also see that no type II bad component for $\{v = v^*, w = z\}$ exists due to the path Q_2 by the condition (ii) of Lemma 20.

This completes a proof that I' has no zipped-chains or squashed chains. ∎

By (1), it holds $|M'| < |M|$. By induction hypothesis on the size of M, I' admits an FSL-drawing D', as shown in Fig. 26(c).

Construction of Drawing

We construct an FSL-drawing D for the original instance I by replacing the interior of f_ν in D' with a straight-line drawing D_ν for the subgraph $H = G^-(\nu)$. In what follows, we fix the positions of vertices other than v^* in D' as those in a final drawing D for I.

An adequate drawing D_ν for $H = G^-(\nu)$ will be constructed by several steps:
(1) First construct a convex-interior drawing $D_{\mathrm{skn}(\nu)}$ for the skeleton $\mathrm{skn}^-(\nu)$ plus edge st; and
(2) Then convert $D_{\mathrm{skn}(\nu)}$ into a desired drawing D_ν for $H = G^-(\nu)$.

To describe these steps, we introduce some more notations. Let Q^* be the cycle formed by the right side $f^o_{ts}(\mathrm{skn}^-(\nu))$ of the skeleton $\mathrm{skn}^-(\nu)$ plus edge st assigned within f^{right} (even if $st \notin E'$). Let f^* denote the face whose boundary is given by Q^* (see Fig. 26(d)). Let $\mathrm{skn}(\nu)$ denote the plane embedding obtained from $\mathrm{skn}^-(\nu)$ plus edge st within f^{right}, as shown in Fig. 26(d). The important observation here is that $\mathrm{skn}(\nu)$ is triconnected. Note that the current outer boundary $f^o(\mathrm{skn}(\nu))$ forms a star-shaped polygon P_{f_ν}, since all the vertices on the face f_ν are joined to the vertex v^* in I', and the kernel $K(P_{f_\nu})$ contains v^* in D'.

For each vertex $w \in W$, we define cone_w to be the set of half-lines L starting from w that do not intersect any segment in D' except segment $L[s, v^*]$ or $L[v^*, t]$. Let K^* be the intersection of $K(P_{f_\nu})$ and cone_w over all $w \in W$, where K^* contains v^* properly inside and has a positive area. We are ready to describe how to construct an FSL-drawing D for I.

1. Compute an inner convex drawing $D^{\mathrm{convex}}_{\mathrm{skn}(\nu)}$ of the triconnected plane graph $\mathrm{skn}(\nu)$ with the star-shaped polygon drawn for the outer boundary $f^o(\mathrm{skn}(\nu))$ such that all the inner vertices are contained in the prescribed area K^* ($\subseteq K(P_{f_\nu})$) and no flat corner appears at any inner vertex. This can be done in polynomial time by Corollary 22;

2. For each virtual edge $e = zz'$ along the left side of $D^{\mathrm{convex}}_{\mathrm{skn}(\nu)}$ (i.e., the edges corresponding child nodes in $\mu_e \in \mathrm{Ch}_{st}(\nu)$), replace its current drawing $L[z, z']$ with the straight-line drawing of $G^-(\mu_e)$ obtained in D'. Let $D_{\mathrm{skn}(\nu)}$ be the resulting straight-line drawing consisting of the polygons P_f with $f \in F(\mathrm{skn}^-(\nu)) \cup \{f^*\}$ (thus $D_{\mathrm{skn}(\nu)}$ is obtained from by replacing the left side of $D^{\mathrm{convex}}_{\mathrm{skn}(\nu)}$ with the right side of H^{left} in D'). See Fig. 27(a). Note that $D_{\mathrm{skn}(\nu)}$ is a convex-interior drawing;

3. Let $P_{f^{\mathrm{right}}}$ be the polygon drawn for the region f^{right} in D'. We choose a vertex subset $\widetilde{W}$ with $W \subseteq \widetilde{W} \subseteq V^{\mathrm{right}}$ so that the position of vertices in $V^o_{ts}(H) \cup \widetilde{W}$ in D' form a polygon $P_{\widetilde{W}}$ whose convex corners are only from W (hence the region $P_{\widetilde{W}}$ is contained in $P_{f^{\mathrm{right}}}$). Let $D^+_{\mathrm{skn}(\nu)}$ be the drawing obtained from $D_{\mathrm{skn}(\nu)}$ by replacing P_{f^*} with $P_{\widetilde{W}}$. Since all inner vertices in $D_{\mathrm{skn}(\nu)}$ are placed inside K^*, for each edge $v_i v_{i+1}$ along $f^o_{ts}(H) - \{s, t\}$, its drawing $L[v_i, v_{i+1}]$ with $1 < i < q'$ is visible from any vertex in $\widetilde{W}$, and $L[a, v_2]$ for some point $a \in L[t, v_2]$ ($a \neq t$) and $L[v_{q'}, b]$ for some point $b \in L[v_{q'}, s]$ ($b \neq s$) are commonly visible from any vertex in $\widetilde{W}$. Hence $D^+_{\mathrm{skn}(\nu)}$ is still a convex-interior drawing;

4. Apply Lemma 17 to $D^+_{\mathrm{skn}(\nu)}$ to replace all inner virtual edges in $D^+_{\mathrm{skn}(\nu)}$ with the corresponding required concave/convex links so that the convex-interior polygons P_f for all inner faces f in $D^+_{\mathrm{skn}(\nu)}$ attain the visibility of two vertices $u, v \in V(f)$ as long as they are not on the same link or on the outer boundary of $D_{\mathrm{skn}^+(\nu)}$. Let D_ν be the resulting drawing converted from $D_{\mathrm{skn}^+(\nu)}$. See Fig. 27(b).

Let D be the resulting drawing for the original instance I obtained by extending D_ν with the positions of the other vertices in D'.

Lemma 38 *The resulting drawing D is an FSL-drawing for I.*

Proof: Clearly the set of M induces a straight-line plane drawing from D. It suffices to show that each edge in $E - M$ is M-visible. We consider the followings cases:
(i) edges in $E - M$ assigned to an inner face $f \in F_M$ such that the region f is contained inside the cycle formed by $f^o_{ts}(H^{\text{right}})$ and $f^o_{ts}(H)$;
(ii) edges in $E - M$ assigned to f^{right} and incident to only vertices in $V^o_{ts}(H) - \{s, t\}$;
(iii) edges in $E - M$ assigned to f^{right} and incident to a vertex $v \in V^o_{ts}(H) - \{s, t\}$ and a vertex $w \in W$; and
(iv) edges in $E - M$ not satisfying (i) or (ii).

Clearly the edges in $E - M$ in case (iv) are M-visible in the FSL-drawing D' (by definition) and remain M-visible in D (since the construction step is applied only inside the region enclosed by $f^o_{ts}(H^{\text{right}})$ and $f^o_{ts}(H)$).

The edges in $E - M$ in case (i) are M-visible in D because each of them is assigned to an inner face $f \in F_M$ whose polygon P_f is drawn in D_ν such that two vertices $u, v \in V(f)$ are visible as long as they are on the same link or on the outer boundary of $D_{\text{skn}^+(\nu)}$.

The edges vv' $E - M$ in case (ii) are M-visible in D because vertices v and v' are inner vertices in an internally convex-interior drawing $D_{\text{skn}^+(\nu)}$ and they remain visible in the resulting polygon $P_{\widetilde{W}}$ in D_ν.

Similarly, the edges $vw \in E - M$ are also M-visible in D because an inner vertex v and an outer vertex w remains visible in the resulting polygon $P_{\widetilde{W}}$ in D_ν. ∎

(B) We design another reduction without using Corollary 22.

Lemma 39 *For any two vertices $v_, v_h \in V^o_{ts}(\text{skn}^-(\nu))$ with $0 \le j$ and $j + 2 \le h \le q' + 1$ and $\{v_j, v_h\} \neq \{s, t\}$, adding a new edge $v_j v_h$ within face f^{right} does not create a new zipped-chain or squashed chain.*

Proof: By the assumption on (s, t), recall that there is a t, s-chain S^* along $f^o_{ts}(H)$ or the current R-node ν corresponds to a left edge in the skeleton of the parent P-node. To prove the lemma, we apply Lemma 18 with $uv = v_j v_h$ and $f = f^{\text{right}}$. Let I' be the instance obtained by assigning a new edge $uv = v_j v_h$ within face $f = f^{\text{right}}$. We distinguish two cases according to (i) and (ii) in Lemma 18.

(i) Assume that I' contains a zipped-chain (S, S') with terminal a and b, where the a, b-chain S contains uv without loss of generality. Then by Lemma 18(i), $\{a, b\}$ is contained in the u, v-boundary path $f^o_{uv}(f)$ or v, u-boundary path $f^o_{vu}(f)$ of the facial cycle f, and instance I has a b, a-chain S' which together with the a, b-boundary path $f^o_{ab}(f)$ surrounds the region f (see Fig. 12(a)). Let H' be the a, b-component surrounded by S and S'. Since $\{a, b\}$ is a cut-pair in I, it appears either along $f^o_{st}(G^-(\nu))$ or $f^o_{ts}(G^-(\nu))$. First consider the case where a and b appear in this order along $f^o_{v_j v_h}(G^-(\nu))$ from v_j to v_h. Since any cut-pair of I along $f^o_{st}(G^-(\nu))$ is either $\{s, t\}$ or $v_j v_{j+1}$ for some j, vertices a and b must appear along $f^o_{ts}(G^-(\nu))$. In this case, if there is a t, s-chain S^* along $f^o_{ts}(H)$, then (S^*, S') would be a zipped-chain, a contradiction. Hence the current R-node ν must correspond to a left edge in the skeleton of the parent P-node. This case can occur only when $a = t$ and $b = s$, since f^{right} is shared by the subgraph $G^-(\nu')$ of another child ν' of the parent P-node. However, in this case, the b, a-chain S' is an s, t-chain along $f^o_{st}(H')$, which contradicts that ν corresponds to a left edge in the skeleton of the P-node (see Lemma 26).

Consider the remaining case, where a and b appear in this order along $f^o_{v_h v_j}(G^-(\nu))$ from v_h to v_j. This case can happen only when $a = s$ and $b = t$, since the boundary of f^{left} needs to be disjoint with $f^o(H')$ except at s and t. However, this is impossible since a and b are contained in $f^o_{v_h v_j}(G^-(\nu))$ and $\{v_j, v_h\} \neq \{s, t\}$ by the choice of j and h.

(ii) Assume that I' contains a squashed a, b-chain S. Then by Lemma 18(ii), there is an a, b-component H such that $u, v \in V^o_{ab}(H)$ and $f^o_{ba}(H)$ is a b, a-path $S' = P_{ba}$ of the boundary of

$P_{\rm out}$ from b to a in the clockwise order which contains no convex corner (see Fig. 12(b)). Let H' be the a,b-component surrounded by S and S'. Since $\{a,b\}$ is a cut-pair in I, it appears either along $f^o_{st}(G^-(\nu))$ or $f^o_{ts}(G^-(\nu))$. First consider the case where a and b appear in this order along $f^o_{v_jv_h}(G^-(\nu))$ from v_j to v_h. Since any cut-pair of I along $f^o_{st}(G^-(\nu))$ is either $\{s,t\}$ or v_jv_{j+1} for some j, vertices a and b must appear along $f^o_{ts}(G^-(\nu))$. In this case, if there is a t,s-chain S^* along $f^o_{ts}(H)$, then (S^*,S') would be a squashed chain, a contradiction. Hence the current R-node ν must correspond to a left edge in the skeleton of the parent P-node. This case can occur only when $a=t$ and $b=s$, since $f^{\rm right}$ is shared by the subgraph $G^-(\nu')$ of another child ν' of the parent P-node. However, in this case, the b,a-path S' would contradicts that ν corresponds to a left edge in the skeleton of the P-node (see Lemma 26).

Consider the remaining case, where a and b appear in this order along $f^o_{v_hv_j}(G^-(\nu))$ from v_h to v_j. This case can happen only when $a=s$ and $b=t$, since no vertex in $f^o_{ts}(G^-(\nu))$ except s or t is an inner vertex. However, this is impossible since a and b are contained in $f^o_{v_hv_j}(G^-(\nu))$ and $\{v_j,v_h\}\neq\{s,t\}$ by the choice of j and h. ∎

Reduction

1. Let $M':=M$ and $E':=E$. Add to E' edges $\{wv_2:\ w\in W,\ wv_2\notin E\}\cup\{wv_{q'}:\ w\in W,\ wv_{q'}\notin E\}$ assigned to $f^{\rm right}$; when $q'\geq 3$, add to E' a convex-support $\{v_jv_{j+2}:1\leq j\leq q'-1\}\cup\{tv_{q'},v_2s\}$ assigned to $f^{\rm right}$ (see Fig. 28(a));

2. Let $X=V(H)-V(H^{\rm left})-V({\rm skn}^-(\nu))$ (recall that $H^{\rm left}=(Q_1,\ldots,Q_{q+1})$ is the line-cactus along the left side of H), and remove X from the current graph (letting $V'=V-X$, $E':=E'-E(X)$ and $M':=M'-E(X)$). Let E^* be the set of virtual edges in $E({\rm skn}^-(\nu))-E(f^o_{st}({\rm skn}^-(\nu)))$ (i.e., those not appear along $f^o_{st}({\rm skn}^-(\nu))$), and add E^* to M' (see Fig. 28(b)).

3. Within each inner face $f\in F_{{\rm skn}^-(\nu)}$, add a new edge vw for every adjacent edges $vu,uw\in E(f)$ unless v and w are contained in the same path of $G^-(\mu)$ of a child $\mu\in{\rm Ch}_{st}(\nu)$ (see Fig. 28(b)). Let I' denote the resulting instance.

Lemma 40 *The new instance I' has no zipped-chains or squashed chains.*

Proof: By Lemma 34, adding to E' edges $\{wv_2:\ w\in W,\ wv_2\notin E\}\cup\{wv_{q'}:\ w\in W,\ wv_{q'}\notin E\}$ assigned to $f^{\rm right}$ does not create a zipped-chain or squashed chain. By Lemma 39, adding to E' a convex-support $\{v_jv_{j+2}:1\leq j\leq q'-1\}\cup\{tv_{q'},v_2s\}$ assigned to $f^{\rm right}$ does not create a zipped-chain or squashed chain, either. Analogously with Lemma 35, we see that neither of zipped-chains and squashed chains will be created by adding a new edge vw for every adjacent edges $vu,uw\in E(f)$ in a face $f\in F_{{\rm skn}^-(\nu)}$ unless v and w are contained in the same path of $G^-(\mu)$ of a child $\mu\in{\rm Ch}_{st}(\nu)$. ∎

By (1), it holds $|M'|<|M|$. By induction hypothesis on the size of M, I' admits an FSL-drawing D', as shown in Fig. 28(c).

Construction of Drawing
We construct an FSL-drawing D for the original instance I from D' as follows.

1. Let $F({\rm skn}^-(\nu))$ denote the set of inner faces of the skeleton ${\rm skn}^-(\nu)$, where D' contains a star-shaped polygon P_f for each face $f\in F({\rm skn}^-(\nu))$. We see that the drawing $D_{{\rm skn}^-(\nu)}$ which is a collection of P_f, $f\in F({\rm skn}^-(\nu))$ is a convex-interior drawing. Let $P_{f^{\rm right}}$ be the polygon drawn for the region $f^{\rm right}$ in D'. We choose a vertex subset $\widetilde{W}$ with $W\subseteq\widetilde{W}\subseteq V^{\rm right}$ so that the position of vertices in $V^o_{ts}(H)\cup\widetilde{W}$ in D' form a polygon $P_{\widetilde{W}}$ whose convex corners are only from W (hence the region $P_{\widetilde{W}}$ is contained in $P_{f^{\rm right}}$). Let $D^+_{{\rm skn}(\nu)}$ be the drawing obtained from $D_{{\rm skn}(\nu)}$ by adding $P_{\widetilde{W}}$. Since all inner vertices in $D_{{\rm skn}(\nu)}$ are placed inside K^*, for each edge v_iv_{i+1} along $f^o_{ts}(H)-\{s,t\}$, its drawing $L[v_i,v_{i+1}]$ with $1<i<q'$ is visible from any vertex in $\widetilde{W}$, and $L[a,v_2]$ for some point $a\in L[t,v_2]$ $(a\neq t)$ and $L[v_{q'},b]$ for some point $b\in L[v_{q'},s]$ $(b\neq s)$ are commonly visible from any vertex in $\widetilde{W}$. Hence $D^+_{{\rm skn}(\nu)}$ is still a convex-interior drawing;

2. Apply Lemma 17 to $D^+_{\mathrm{skn}(\nu)}$ to replace all inner virtual edges in $D^+_{\mathrm{skn}(\nu)}$ with the corresponding required concave/convex links so that the convex-interior polygons P_f for all inner faces f in $D^+_{\mathrm{skn}(\nu)}$ attain the visibility of two vertices $u, v \in V(f)$ as long as they are not on the same link or on the outer boundary of $D_{\mathrm{skn}^+(\nu)}$. Let D_ν be the resulting drawing converted from $D_{\mathrm{skn}^+(\nu)}$. Let D be the resulting drawing for the original instance I obtained by extending D_ν with the positions of the other vertices in D'. See Fig. 28(d).

Analogously with Lemma 38, we have the next.

Lemma 41 *The resulting drawing D is an FSL-drawing for I.*

This completes design of reductions for all types of P-, R- and S-nodes. It is not difficult to see that the entire constructive proof for Theorem 10 can be implemented to run in polynomial time.

16 Concluding Remarks

In this paper, we have shown that there are examples of embeddings of graphs that have no straight-line drawings but have none of natural extensions of forbidden configurations of B- and W-configurations. Such examples contain 3-plane and quasi-plane embeddings. To seek a straight-line drawing problem that can be characterized by our collection of forbidden configurations, we have formulated the frame straight-line drawability when crossing-free edges induce biconnected spanning subgraphs. We have shown that our forbidden configurations completely characterize the set of instances that admit no straight-line drawings by a divide-and-conquer method on SPQR decomposition of biconnected graphs. Our constructing proof can be implemented to run in polynomial time to test whether a given instance has a forbidden configuration or not and to construct a straight-line drawing if any. Our result is not only an extension of the straight-line drawability of 1-plane graphs but also a generalization of convex drawability of internally triconnected plane graphs with prescribed convex boundaries.

The followings are left open in the new direction in this paper:

- Can the running time of our algorithm be improved, say to linear?

- For PSL-drawability, is there any 2-plane (or 2-plane and quasi-plane) embedding that has no straight-line drawings but also contains none of our forbidden configurations?

- The current "fame" assumes the biconnectivity on the set of crossing-free edges. What if we only assume the connectivity of the set of crossing-free edges to define the "frame" straight-line drawability? We conjecture that Theorem 8 still holds for such a connectivity one case.

Acknowledgement

This research was partially supported by a Scientific Grant in Aid from the Ministry of Education, Science, Sports and Culture of Japan. The author would like to acknowledge Prof. Seokhee Hong for providing related papers and for her encouragement.

References

[1] P. Angelini, G. Di Battista, F. Frati, M. Patrignani, and I. Rutter, Testing the simultaneous embeddability of two graphs whose intersection is a biconnected or a connected graph. J. Discrete Algorithms 14, pp. 150-172, 2012.

[2] G. Di Battista, P. Eades, R. Tamassia and I. G. Tollis, Graph Drawing: Algorithms for the Visualization of Graphs, Prentice-Hall, 1999.

[3] G. Di Battista and R. Tamassia, On-line planarity testing, SIAM J. on Comput. 25(5), pp. 956-997, 1996.

[4] O. V. Borodin, A. V. Kostochka, A. Raspaud and E. Sopena, Acyclic colouring of 1-planar graphs, Discrete Applied Mathematics, 114(1-3), pp. 29-41, 2001.

[5] Z. Chen and M. Kouno, A Linear-time algorithm for 7-coloring 1-plane graphs, Algorithmica 43(3), pp. 147-177, 2005.

[6] P. Eades, S. Hong, N. Katoh, G. Liotta, P. Schweitzer and Y. Suzuki, Testing maximal 1-planarity of graphs with a rotation system in linear time, Proc. of Graph Drawing 2012, pp. 339-345, 2012.

[7] R. B. Eggleton, Rectilinear drawings of graphs. Utilitas Math. 29, pp. 149-172, 1986.

[8] I. Fabrici and T. Madaras, The structure of 1-planar graphs, Discrete Mathematics, 307(7-8), pp. 854-865, 2007.

[9] I. Fáry, On straight line representations of planar graphs, Acta Sci. Math. Szeged, 11, pp. 229-233, 1948.

[10] C. Gutwenger and P. Mutzel, A linear time implementation of SPQR-trees, Proc. of the 8th International Symposium on Graph Drawing Proc. GD 2000, LNCS 1984, Springer, pp. 77-90, 2001.

[11] S.-H. Hong, P. Eades, G. Liotta, and S.-H. Poon, Fary's theorem for 1-planar graphs. Proc. COCOON 2012, LNCS 7434, Springer, pp. 335-346, 2012.

[12] S.-H. Hong and H. Nagamochi, Star-shaped drawings of graphs with fixed embedding and concave corner constraints, Proc. COCOON 2008, LNCS 5092, Springer, pp. 405-414, 2008.

[13] S.-H. Hong and H. Nagamochi, Convex drawings of graphs with non-convex boundary constraints, Discrete Applied Mathematics, 156(12), pp. 2368-2380, 2008.

[14] J. E. Hopcroft and R. E. Tarjan,Dividing a graph into triconnected components, SIAM J. on Comput., 2, pp. 135-158, 1973.

[15] D. Hudak, T. Madaras and Y. Suzuki, On properties of maximal 1-planar graphs, Discussiones Mathematicae Graph Theory 32(4), pp. 737-747, 2012.

[16] M. Kaufmann and D. Wagner (eds.), Drawing Graphs: Methods and Models, Lecture Notes in Computer Science Tutorial 2025, Springer, 2001.

[17] V. P. Korzhik and B. Mohar, Minimal obstructions for 1-immersions and hardness of 1-planarity testing, Proc. of Graph Drawing 2008, pp. 302-312, 2009.

[18] T. Nishizeki and M. S. Rahman, Planar Graph Drawing, World Scientific, 2004.

[19] J. Pach and G. Toth, Graphs drawn with few crossings per edge, Combinatorica, 17(3) (1997) 427-439.

[20] G. Ringel, Ein Sechsfarbenproblem auf der Kugel, Abh. Math. Semin. Univ. Hamb., 29, pp. 107-117, 1965.

[21] K. S. Stein, Convex maps, Proc. Amer Math. Soc., 2, pp. 464-466, 1951.

[22] Y. Suzuki, Re-embeddings of maximum 1-planar graphs, SIAM J. Discrete Math., 24(4), pp. 1527-1540, 2010.

[23] C. Thomassen, Rectilinear drawings of graphs, J. Graph Theory, 10(3), pp. 335-341, 1988.

[24] C. Thomassen, Plane representations of graphs, Progress in Graph Theory, Academic Press, pp. 43-69, 1984.

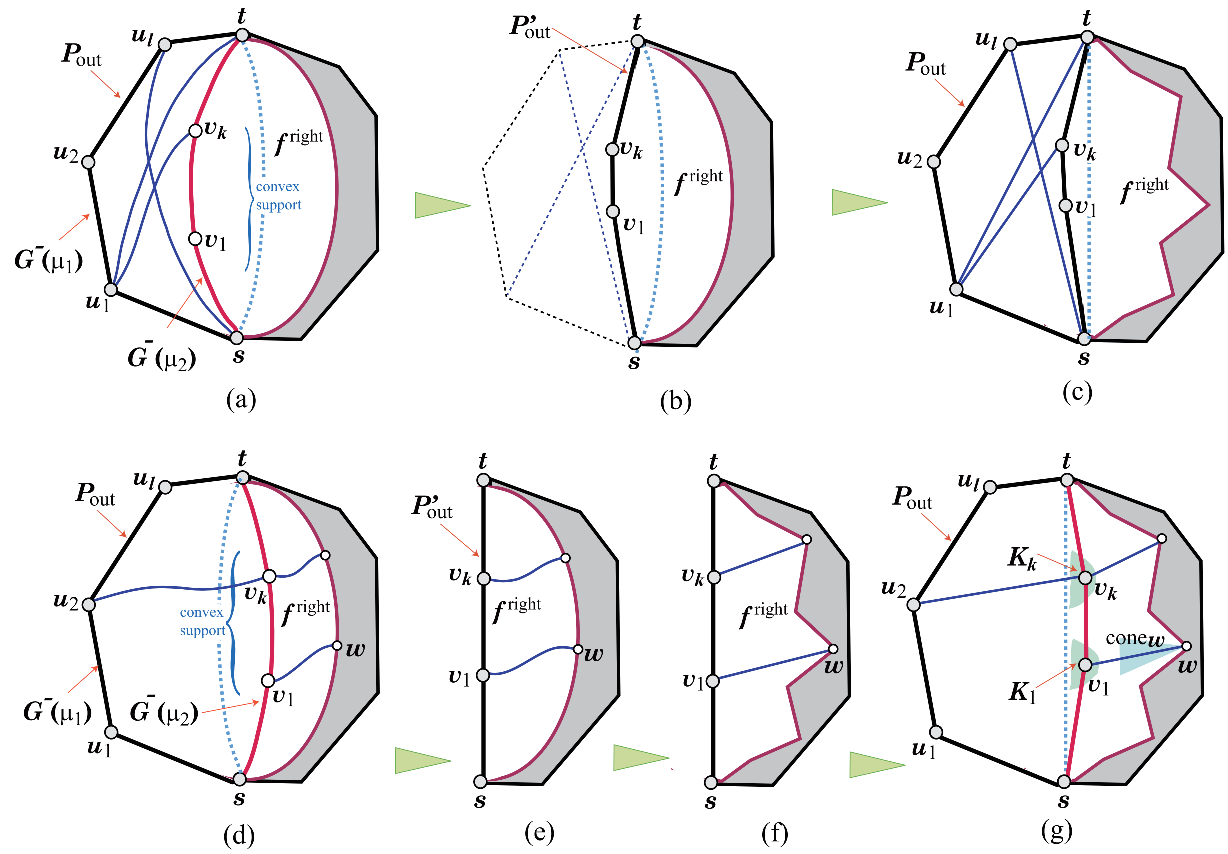

Figure 16: Illustration for reducing a P-node ν: **(a)** A P-node ν such that $j^* \geq 2$ and $G^-(\mu_1) = (s, u_1, \ldots, u_\ell, t)$ is a subpath of the polygon P_{out}; **(b)** Reduce to an instance I' by removing the vertices in $G^-(\mu_1) - \{s, t\}$ and fixing $G^-(\mu_2) = (s, v_1, \ldots, v_k, t)$ as a convex link of a new convex polygon P'_{out}; **(c)** Putting back the removed vertices/edges to a straight-line drawing D' of the reduced instance I'; **(d)** A P-node ν such that $j^* = 1$ and $G^-(\mu_1) = (s, u_1, \ldots, u_\ell, t)$ is a subpath of the polygon P_{out}; **(e)** Reduce to an instance I' by removing the vertices in $G^-(\mu_1) - \{s, t\}$ and fixing $G^-(\mu_2) = (s, v_1, \ldots, v_k, t)$ to be segment $L[s, t]$ as a side of a new convex polygon P'_{out} (all vertices v_i in $G^-(\mu_2) - \{s, t\}$ will be flat corners on it); **(f)** Find an FSL-drawing drawing D' of the reduced instance I'; and **(g)** Putting back the removed vertices/edges to D' after slightly pushing the flat corners towards inside to obtain an FSL-drawing D of the original instance I.

[25] W. T. Tutte, Convex representations of graphs, Proc. of London Math. Soc., 10, no. 3, pp. 304-320, 1960.

[26] K. Wagner, Bemerkungen zum Vierfarbenproblem, Jahresbericht Deutsch Math. Verein, 46, pp. 26-32, 1936.

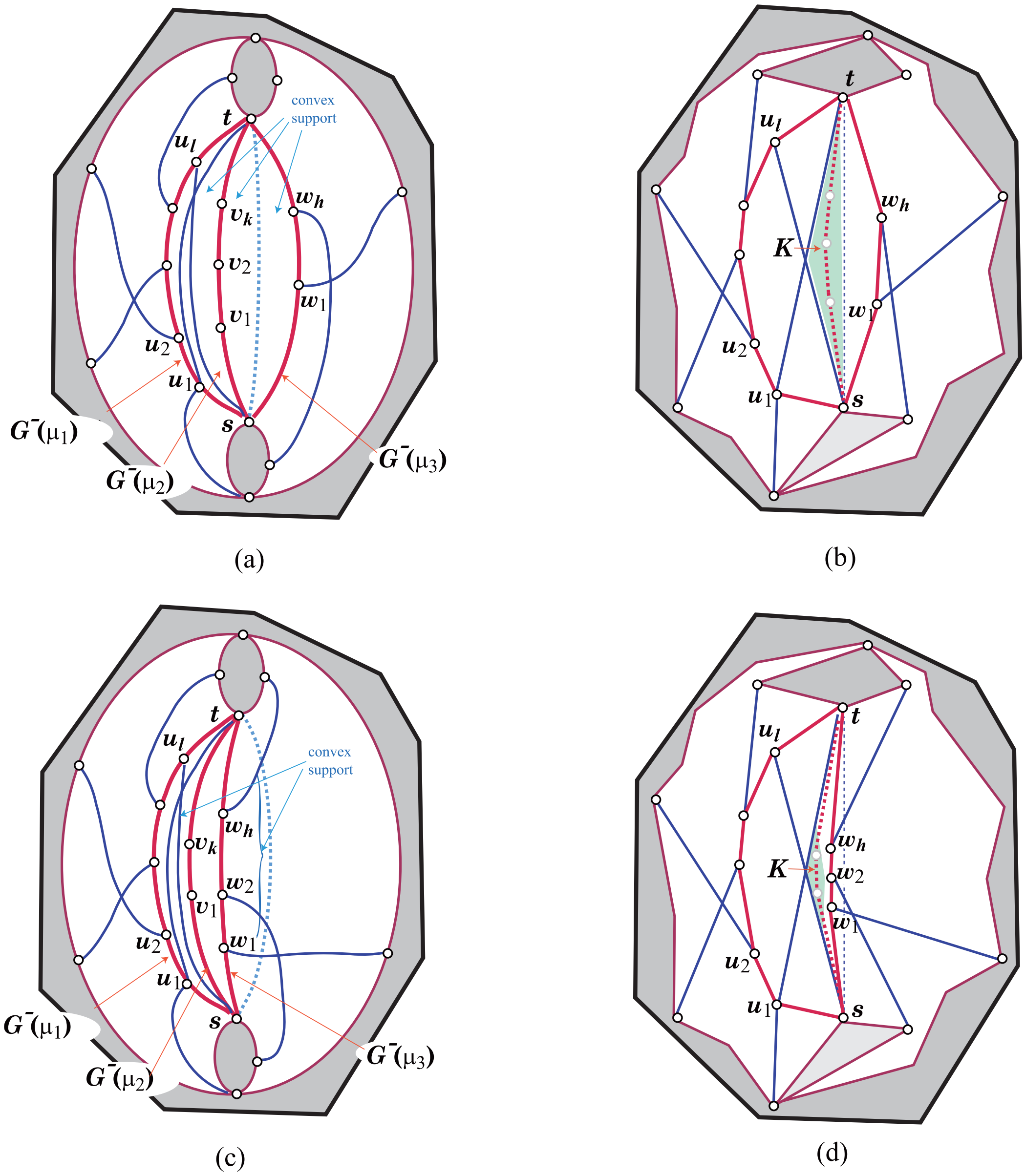

Figure 17: Illustration for reducing a P-node ν: **(a)** A P-node ν whose child nodes are reduced S-nodes, where $j^* = 2$ and $G^-(\mu_1)$ is not a subpath of the polygon P_{out}; **(b)** From an FSL-drawing D' of the reduced instance I' from I in (a), an FSL-drawing D for I is obtained by realizing $G^-(\mu_1)$ as a concave link to the pseudo-convex polygon for the cycle $G^-(\mu_1)$ and $G^-(\mu_2)$; **(c)** A P-node ν whose child nodes are reduced S-nodes, where $j^* \geq 3$ and $G^-(\mu_1)$ is not a subpath of the polygon P_{out}; and **(d)** From an FSL-drawing D' of the reduced instance I' from I in (b), an FSL-drawing D for I is obtained by realizing $G^-(\mu_1)$ as a concave link to the pseudo-convex polygon for the cycle $G^-(\mu_1)$ and $G^-(\mu_2)$.

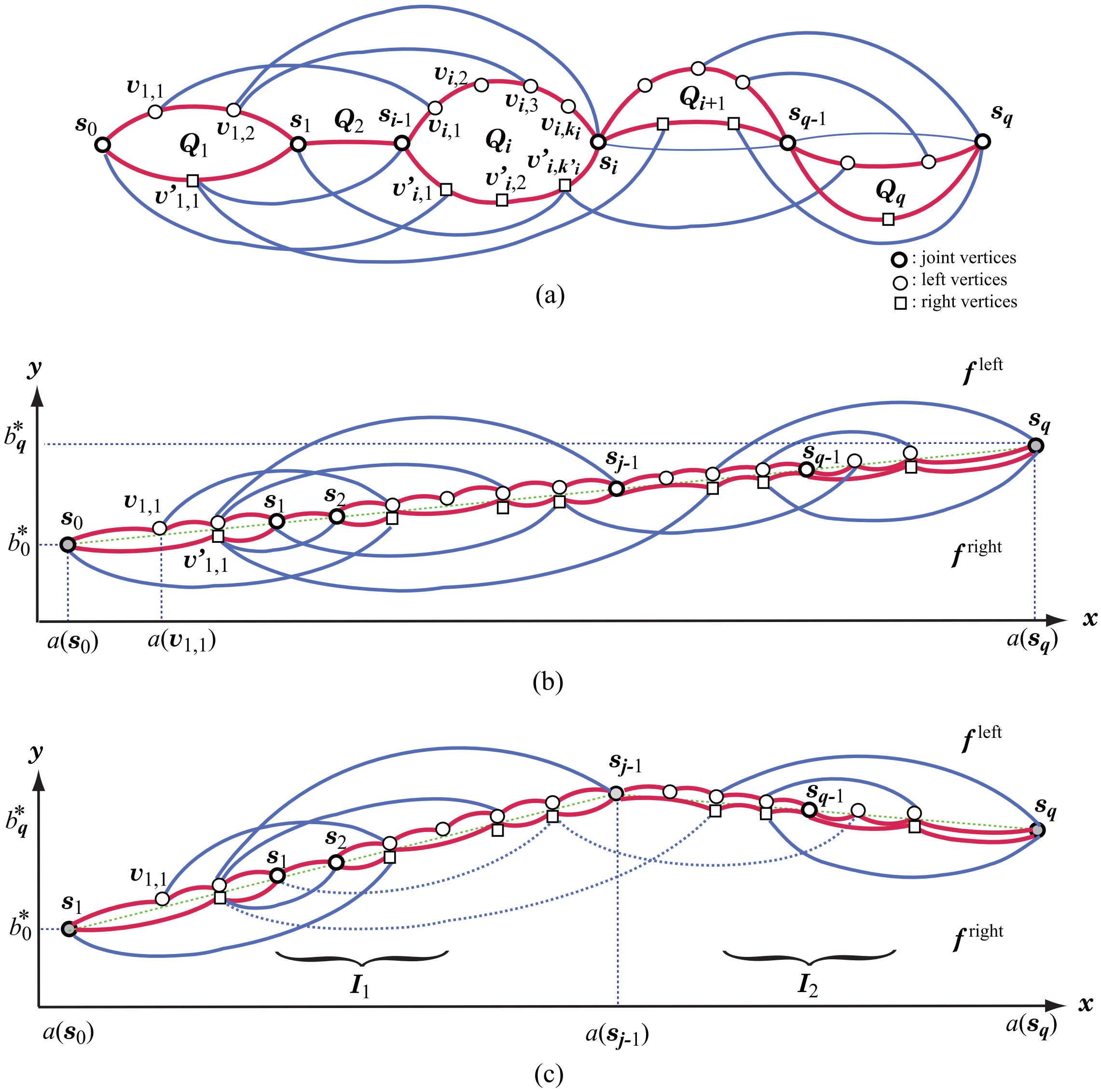

Figure 18: **(a)** An illustration for a cactus instance $(G, \gamma, (V, M) = (Q_1, Q_2, \ldots, Q_q)$, where Q_1, Q_2 and Q_i are of central type, Q_q is of right type, and Q_{i+1} is of left type; **(b)** A drawing of a cactus instance, where the positions of s_0 and s_q are permanent while those of the other vertices are temporarily placed on segment $L[(a(s_0), b_0^*), (a(s_q), b_q^*)]$ joining the terminals s_0 and s_q; and **(c)** An embedding $D(b_0^*, b_{j-1}^*, b_q^*)$ in Case 1, which generates two instances I_1 and I_2 by fixing a joint vertex s_{j-1} on a permanent position $(a(s_{j-1}), b_{j-1}^*)$.

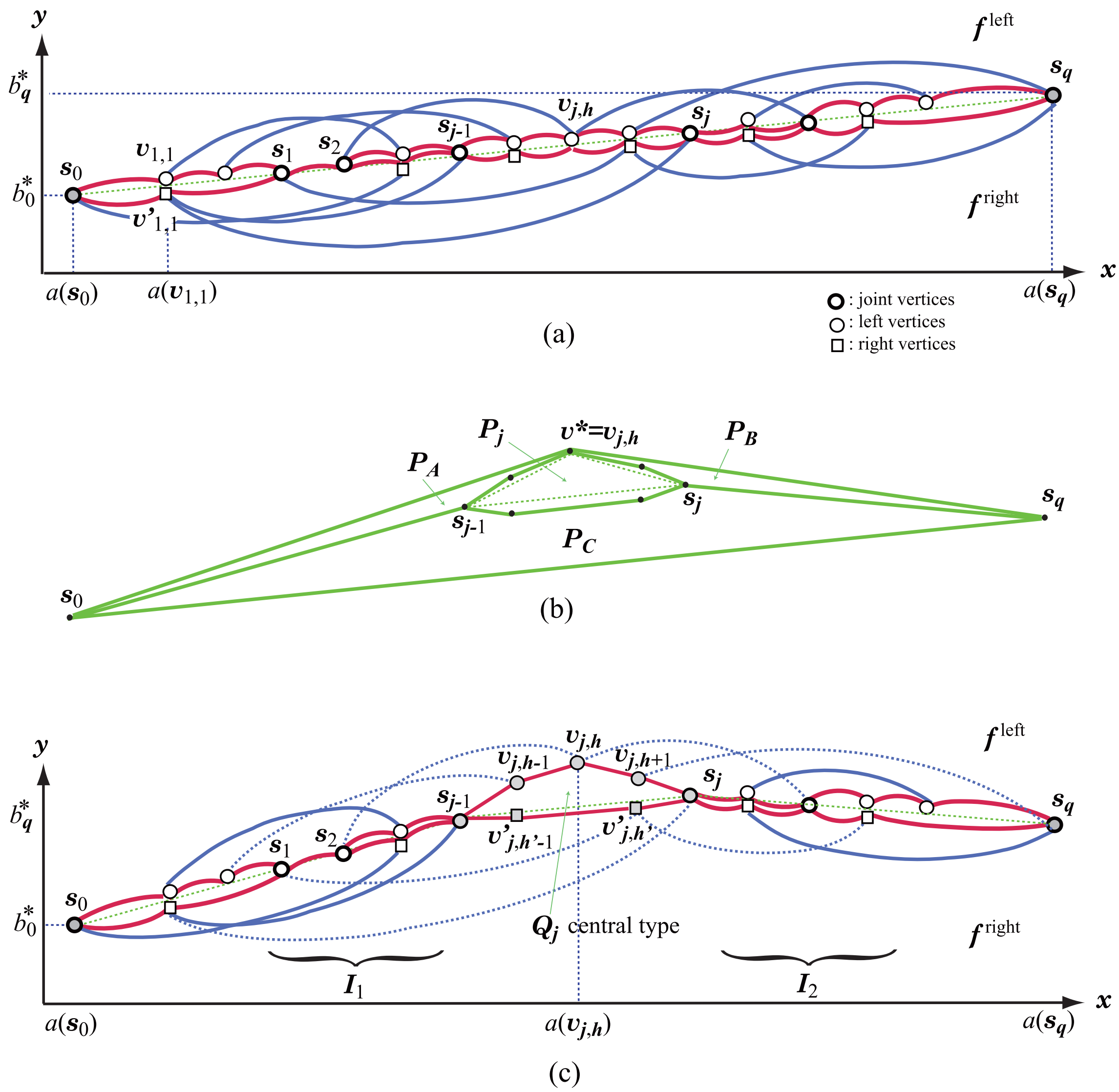

Figure 19: **(a)** A drawing of a cactus instance, where the positions of s_0 and s_q are permanent while those of the other vertices are temporarily placed on segment $L[(a(s_0), b_0^*), (a(s_q), b_q^*)]$ joining the terminals s_0 and s_q; **(b)** Relationship among polygons P_A, P_B, P_C and P_j; and **(c)** Two instances I_1 and I_2 in Case 2, which are generated by drawing the vertices in a central type cycle Q_j as a convex polygon with permanent positions.

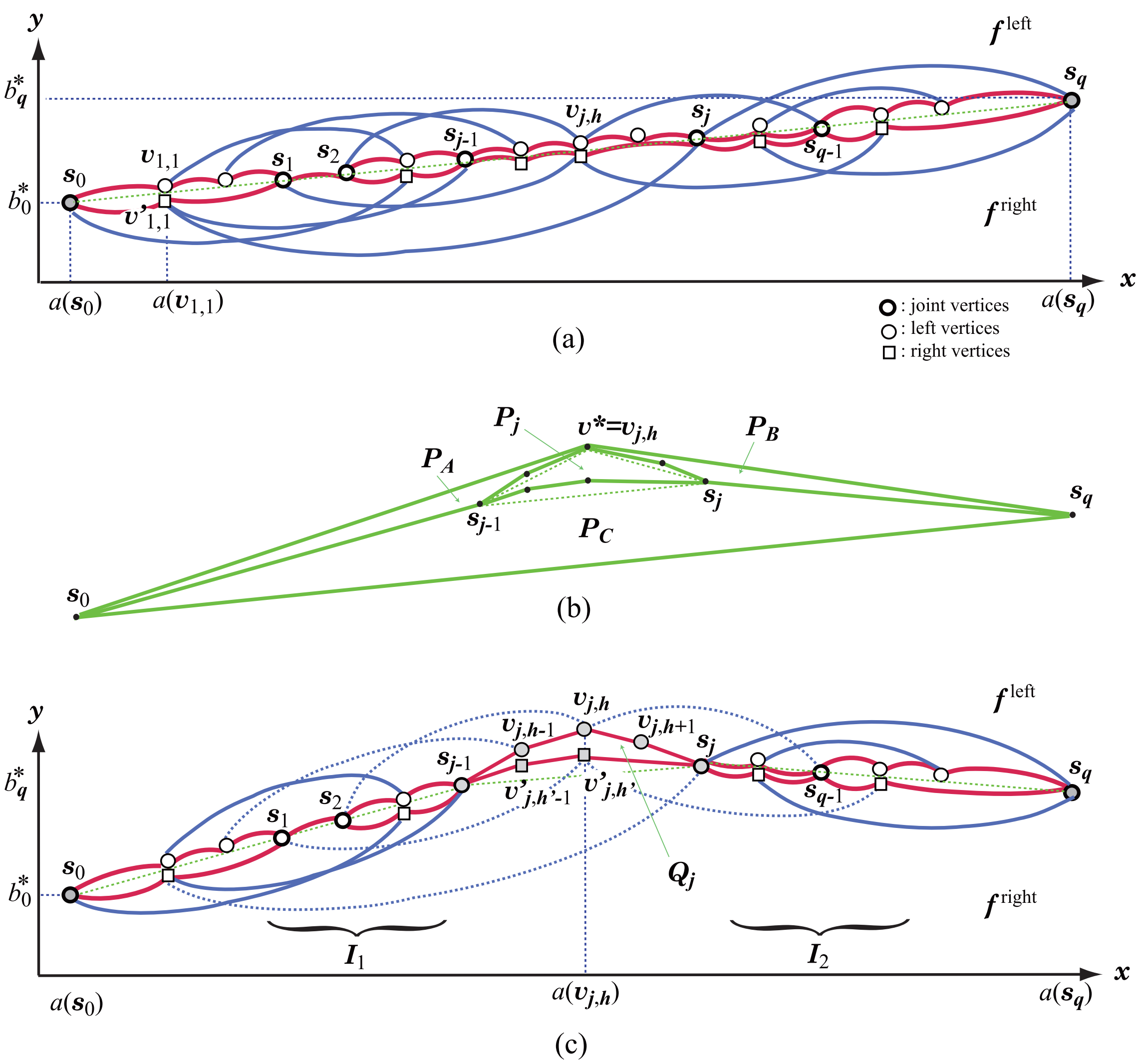

Figure 20: **(a)** A drawing of a cactus instance, where the positions of s_0 and s_q are permanent while those of the other vertices are temporarily placed on segment $L[(a(s_0), b_0^*), (a(s_q), b_q^*)]$ joining the terminals s_0 and s_q; **(b)** Relationship among polygons P_A, P_B, P_C and P_j; and **(c)** Two instances I_1 and I_2 in Case 3, which are generated by drawing the vertices in a left type cycle Q_j as a pseudo-convex polygon with permanent positions.

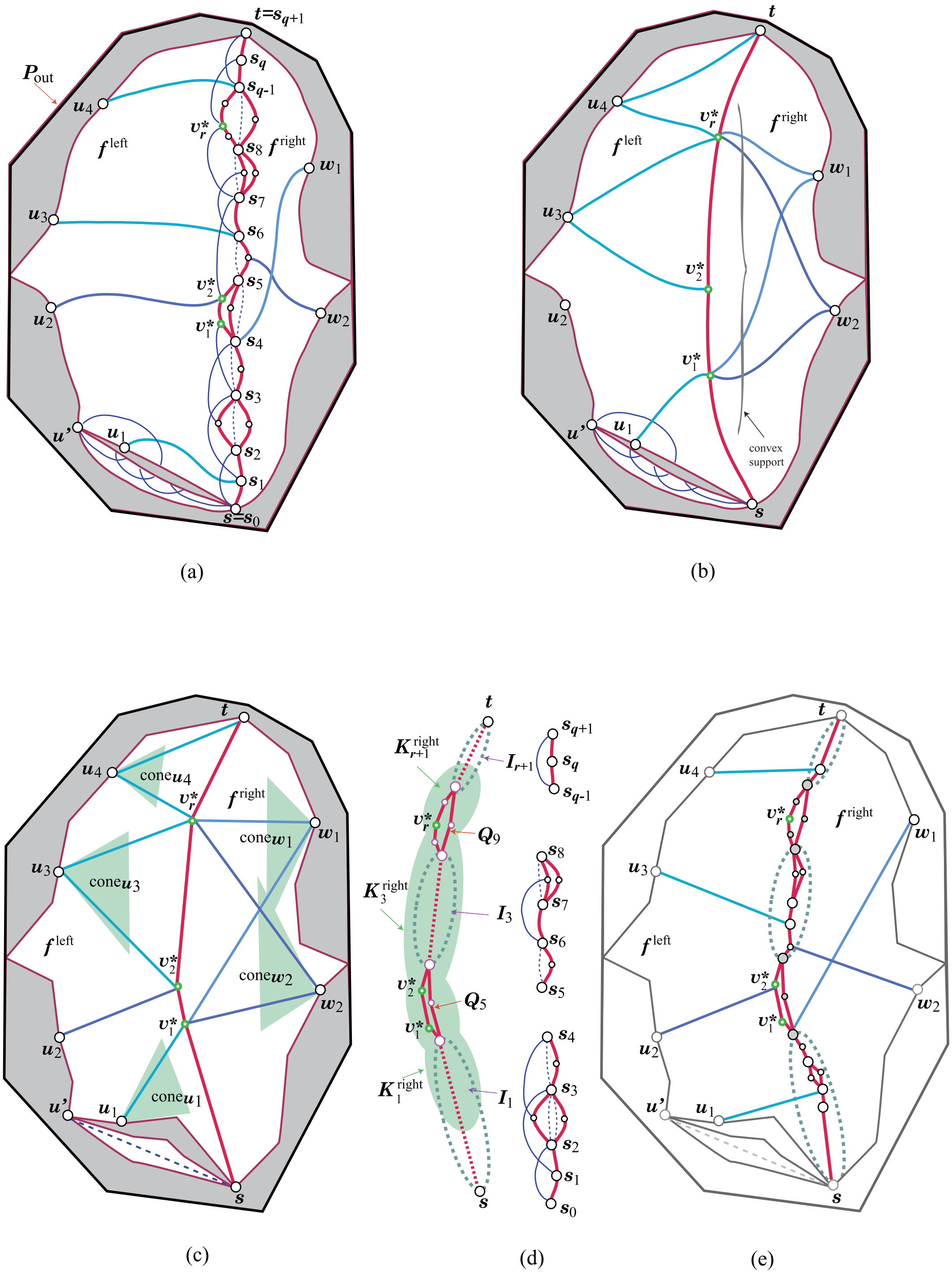

Figure 21: Illustration for reducing an S-node ν: **(a)** An S-node ν whose child nodes are reduced S- or P-nodes; **(b)** Reducing to an instance I' by replacing $G^{-}(\nu)$ with an s,t-path P passing through the set of left vertices exposed on their sides and introducing edges (called "shifts") between P and $U_1 \cup U_2 \cup \cdots \cup U_{r+1} \cup W$, where edge $u_1 s$ has not been introduced due to an s,u'-chain outside f^{left}; **(c)** An FSL-drawing D' of the reduced instance I', where P forms a convex $(r+1)$-gon due to the convex-support on its right side; **(d)** Fix all vertices $v_1^*, \ldots, v_r^*$ and the cycles Q_j containing them, leaving cactus instances I_1, I_3 and I_{r+1}, which can be solved independently with an adequate $\epsilon > 0$; and **(e)** An FSL-drawing D of the original instance I obtained by combining straight-line drawings of the cactus instances into D'.

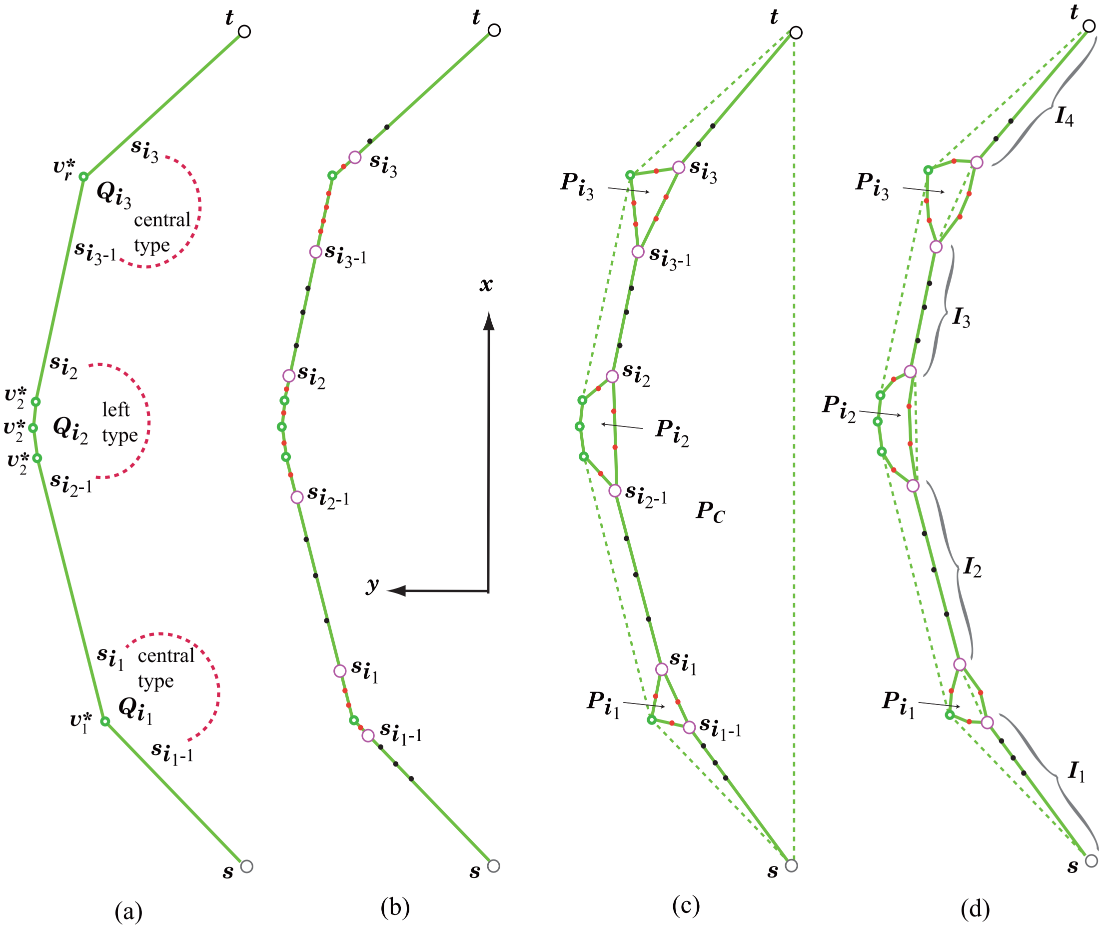

Figure 22: Illustration for constructing an FSL-drawing for I from a drawing D' of the reduced instance I': **(a)** A drawing for the s, t-path P for the reduced S-node, which forms a convex polygon with convex corners of exposed vertices $v_1^*, \ldots, v_r^*$, $v_0^* = s$ and $v_{r+1}^* = t$; **(b)** The initial positions of the vertices in $H = G^-(\nu)$ along guidelines $L[s, v_1^*], \ldots, L[v_r^*, t]$; **(c)** Convex polygons P_j drawn for corner cycles Q_j; and **(d)** Pseudo-polygons converted from the convex polygons in (c), where a cactus instance I_j is left between two corner cycles $Q_{i_{j-1}}$ and Q_{i_j}.

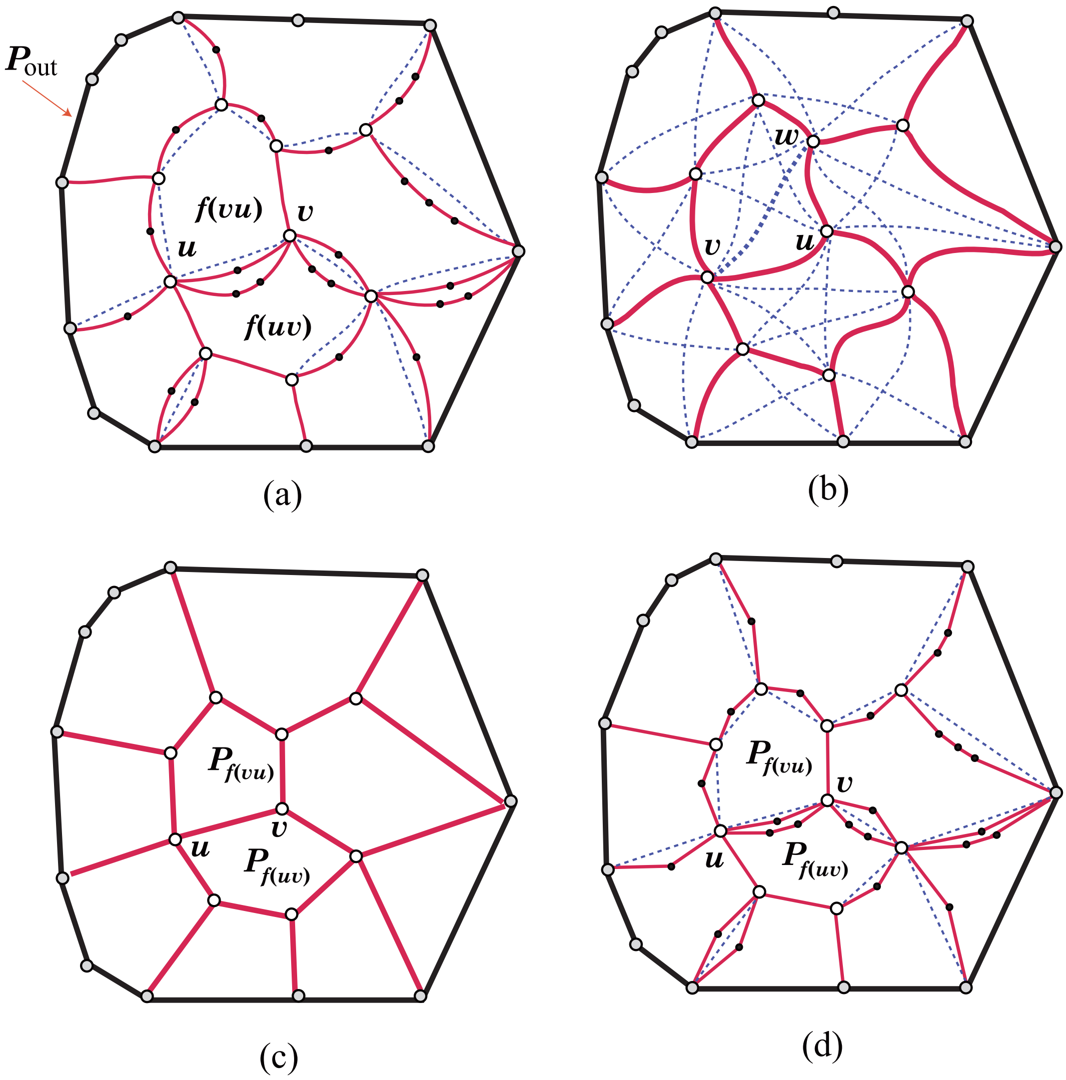

Figure 23: Illustration for reducing the root R-node ν: **(a)** A given instance I where the graph $G^{-}(\nu)$ for the root node is $G(\nu) = G_M$; **(b)** A new instance is obtained by replacing the interior of $G(\nu) = G_M$ with that of skeleton $\mathrm{skn}(\nu)$, and assigning a set of new edges to each inner face in order to draw all inner faces as convex polygons; **(c)** An FSL-drawing D' of the resulting instance I', where all inner faces are drawn as convex polygons; and **(d)** An FSL-drawing D for I is obtained by replacing the virtual edges in D' with required convex/concave links so that each inner face $f \in F_M$ becomes a pseudo-convex polygon.

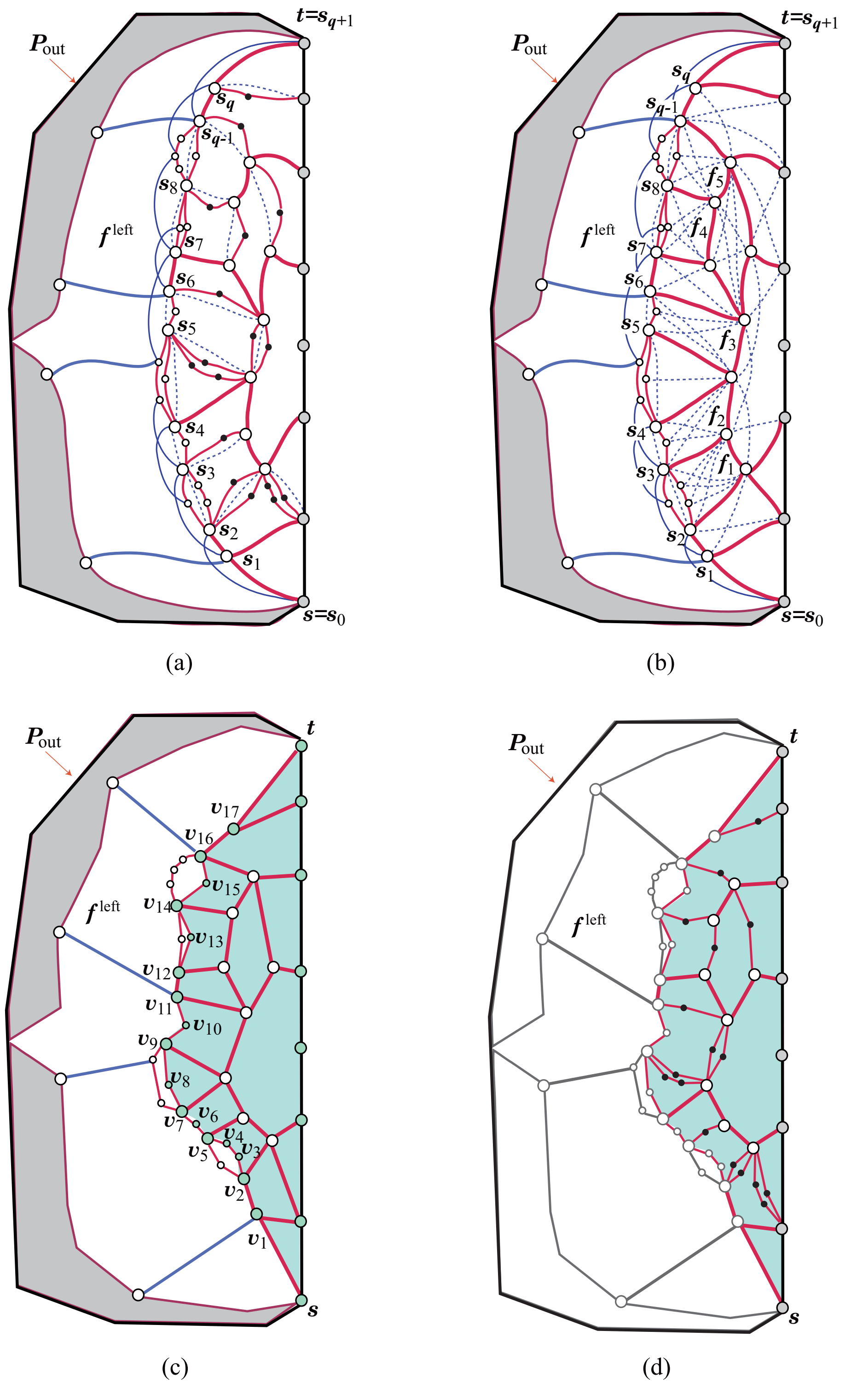

Figure 24: **(a)** The subgraph $H = G^{-}(\nu)$ of G_M for an R-node ν, where the t,s-boundary path $f^{o}_{ts}(H)$ is a subpath along $P_{\rm out}$, where $(s_0 = s, s_1, \ldots, s_q, s_{q+1} = t)$ denotes the s,t-boundary path $f^{o}_{st}(\mathrm{skn}^{-}(\nu))$, the vertices in $\mathrm{skn}^{-}(\nu)$ are depicted with larger circles compared with smaller circles for the vertices in $V^{o}_{st}(H) - V(\mathrm{skn}^{-}(\nu))$ and black circles $V(H) - V^{o}_{st}(H) - V(\mathrm{skn}^{-}(\nu))$; **(b)** The subgraph $G^{-}(\mu)$ for each child S-, P-node μ not along $f^{o}_{st}(\mathrm{skn}^{-}(\nu))$ is replaced with a single edge e_μ, and new edges in E' are assigned within each inner face $f \in F_{\mathrm{skn}^{-}(\nu)}$ so that the polygon P_f drawn for f will be convex or pseudo-convex. In this figure, P_f for faces $f_1, \ldots, f_5$ will be pseudo-convex polygons each of which has one concave link along $f^{o}_{st}(H)$, and P_f for the other inner faces $f \in F_{\mathrm{skn}^{-}(\nu)}$ will be convex; **(c)** An FSL-drawing D' of the reduced instance I', where each inner face f in $\mathrm{skn}^{-}(\nu)$ is drawn as a convex or pseudo-convex polygon P_f; and **(d)** Lemma 17 is applied to the straight-line drawing D_{nu} (enclosed by $(s, v_1, v_2, \ldots, v_{17}, t)$) that consists of these polygons for the inner faces f of $\mathrm{skn}(\nu)$ to obtain an FSL-drawing D for I.

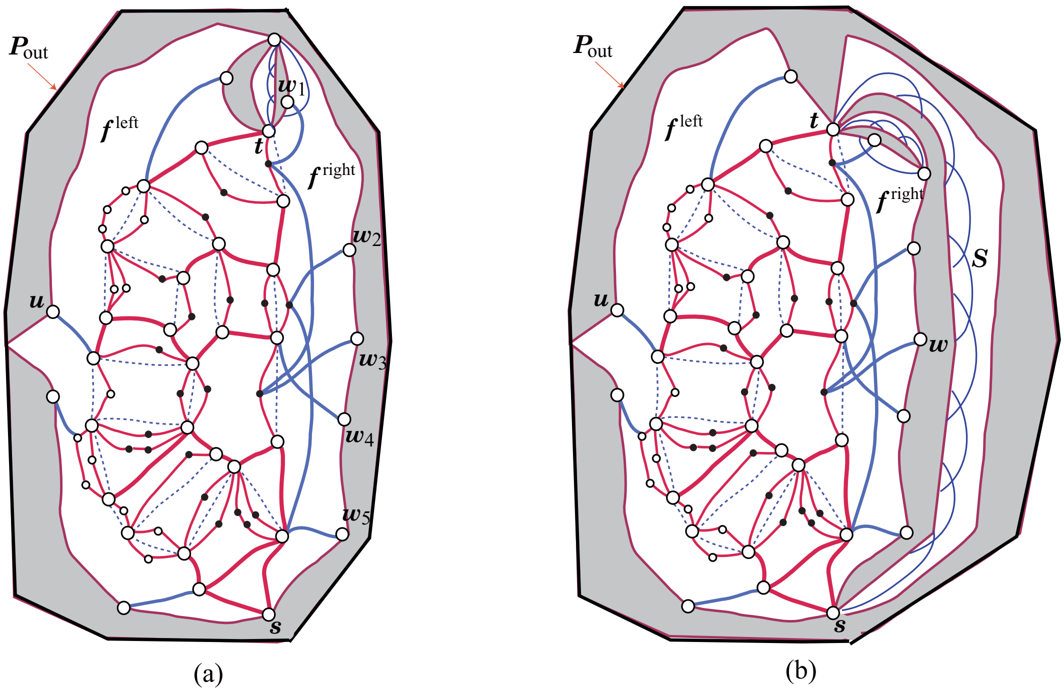

Figure 25: **(a)** The subgraph $H = G^{-}(\nu)$ of an R-node ν such that no side of $f^{o}(H)$ is contained in a subpath of P_{out}, where no t, s-chain surrounds the region f^{right}; and **(b)**The subgraph $H = G^{-}(\nu)$ of an R-node ν in another instance, which has a t, s-chain S surrounds the region f^{right}.

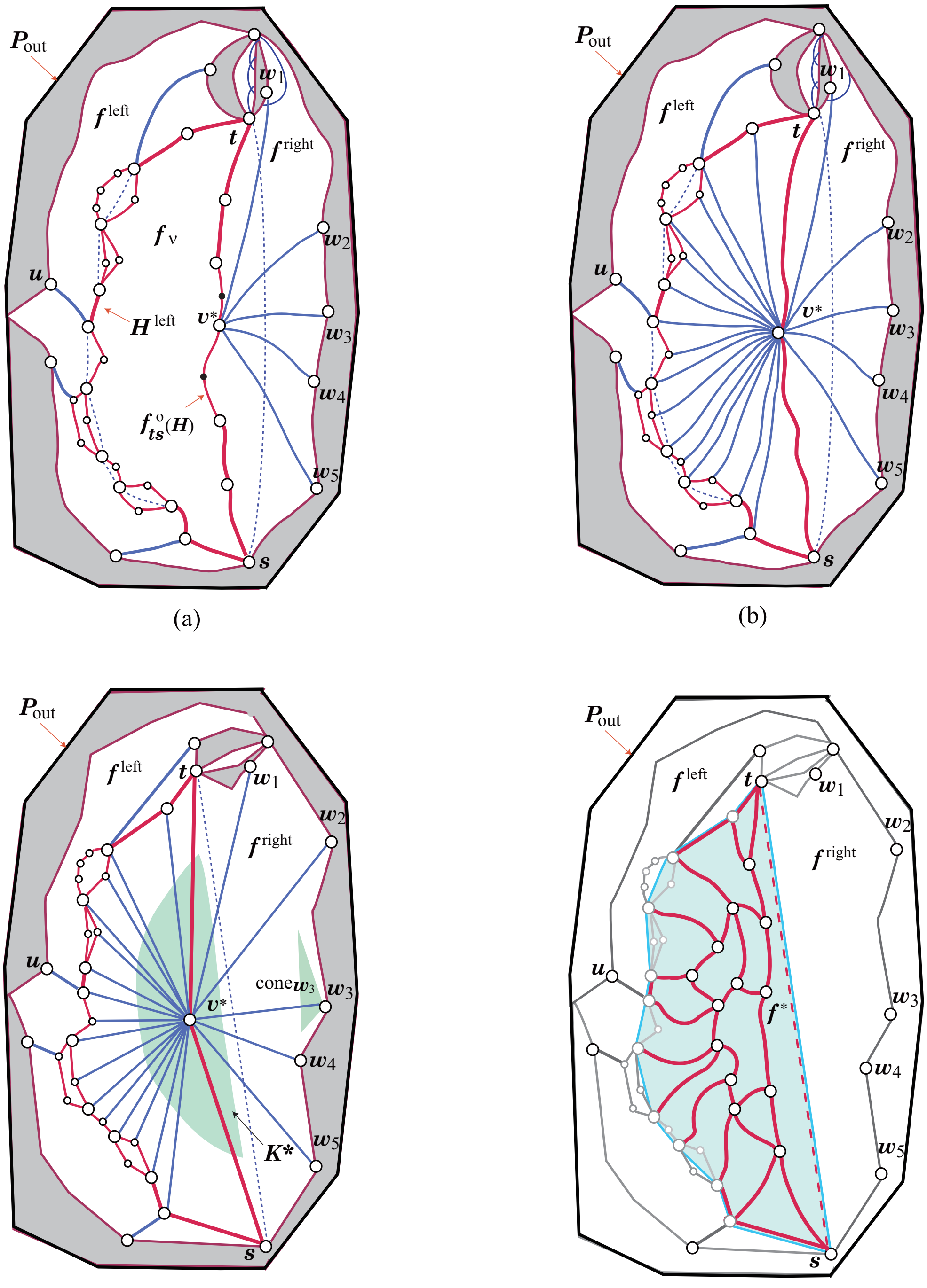

Figure 26: **(a)** The embedding after adding edges v^*w, $w \in W$ and removing the set X of vertices surrounded by $f^o_{ts}(H)$ and H^{left}; **(b)** The embedding for I' after introducing edges v^*v for all vertices v along the right side of H^{left}; **(c)** An FSL-drawing D' for the instance I' in (b); and **(d)** The triconnected plane graph $\text{skn}(\nu)$ with the star-shaped polygon drawn for the outer boundary $f^o(\text{skn}(\nu))$, where $f^o(\text{skn}(\nu))$ is depicted by blue lines.

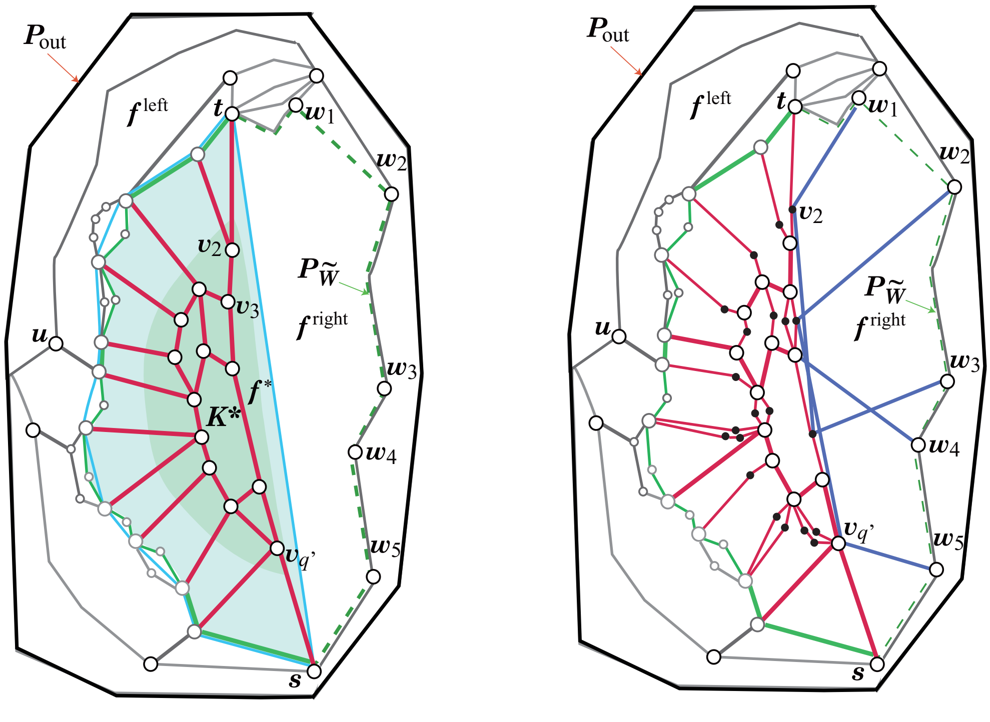

Figure 27: **(a)** An inner convex drawing $D^{\text{convex}}_{\text{skn}(\nu)}$ of $\text{skn}(\nu)$ with boundary $f^o(\text{skn}(\nu))$ (depicted by red and blue lines) such that all the inner vertices are contained in K^* (where $D^{\text{convex}}_{\text{skn}(\nu)}$ and a convex-interior drawing $D_{\text{skn}^+(\nu)}$ are depicted by red and green lines); and **(b)** A straight-line drawing D_ν consisting of polygons $P_{\widetilde{W}}$ and P_f with $f \in F(\text{skn}^-(\nu))$ and $P_{\widetilde{W}}$ such that two vertices $u, v \in V(f)$ are visible as long as they are not on the same link or on the outer boundary of $D_{\text{skn}^+(\nu)}$ (depicted by red and green lines).

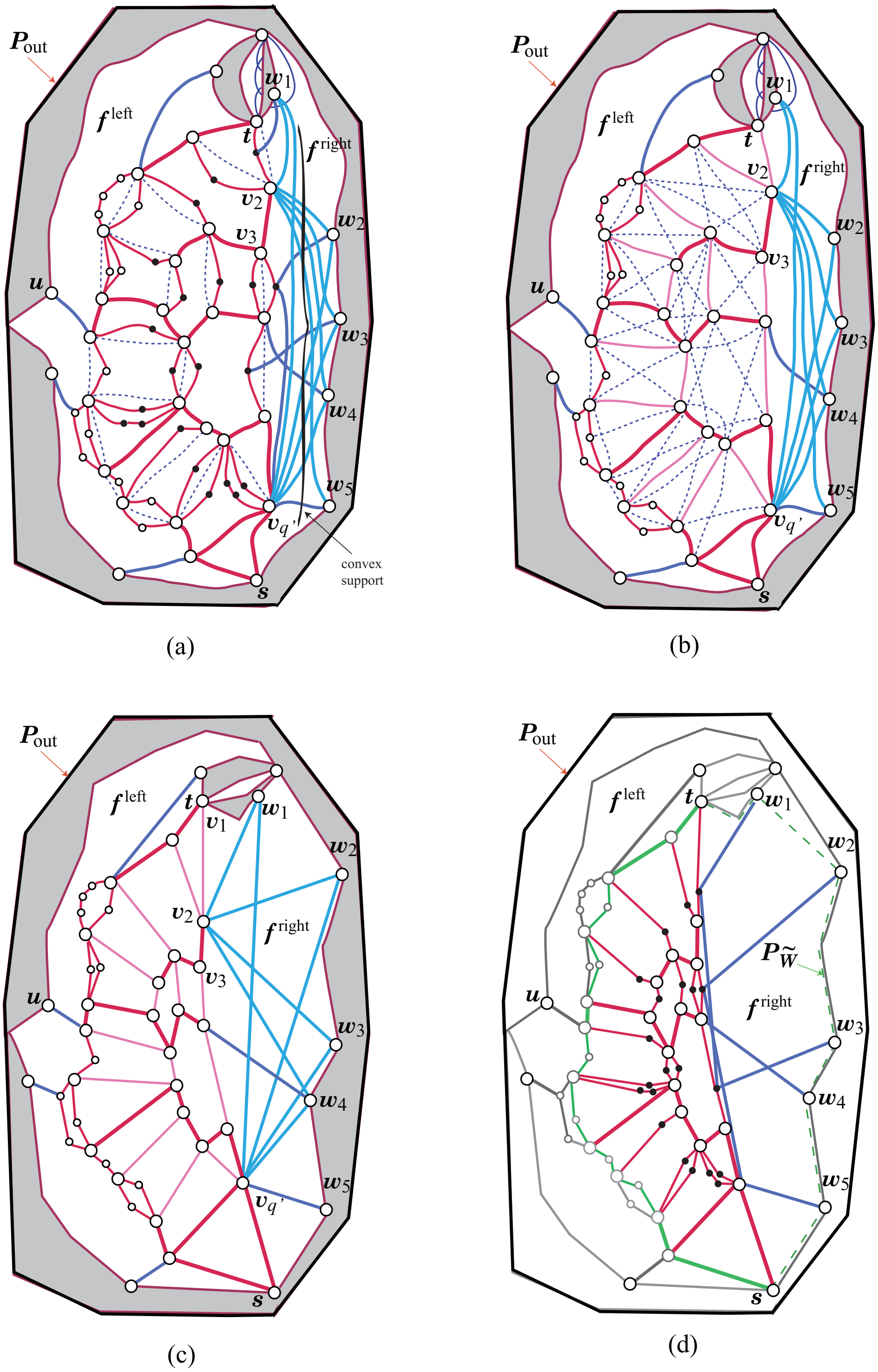

Figure 28: **(a)** The instance obtained after adding new edges $\{wv_2 : w \in W, wv_2 \notin E\} \cup \{wv_{q'} : w \in W, wv_{q'} \notin E\}$ and a convex-support $\{v_j v_{j+2} : 1 \leq j \leq q'-1\} \cup \{tv_{q'}, v_2 s\}$; **(b)** The instance obtained after removing the vertices in $X = V(H) - V(H^{\text{left}}) - V(\text{skn}^-(\nu))$, adding the virtual edges in $E(\text{skn}^-(\nu)) - E(f^o_{st}(\text{skn}^-(\nu)))$ to M', and adding a new edge vw for every adjacent edges $vu, uw \in E(f)$ in a face $f \in F_{\text{skn}^-(\nu)}$ unless v and w are contained in the same path of $G^-(\mu)$ of a child $\mu \in \text{Ch}_{st}(\nu)$; **(c)** An FSL-drawing D' for a reduced instance I'; and **(d)** An FSL-drawing D for the given instance I.